Master Thesis

Investigation of interfacial tension of crude oils by spinning drop technique

Written by:
Ulviyya Movsumova, BSc
m 01135011

Advisor:
Holger Ott,
Univ.-Prof. Dipl.-Phys. Dr.habil.

Leoben, 05.03.2018

EIDESSTATTLICHE ERKLÄRUNG

Ich erkläre an Eides statt, dass ich die vorliegende Diplomarbeit selbständig und ohne fremde Hilfe verfasst, andere als die angegebenen Quellen und Hilfsmittel nicht benutzt und die den benutzten Quellen wörtlich und inhaltlich entnommenen Stellen als solche erkenntlich gemacht habe.

AFFIDAVIT

I hereby declare that the content of this work is my own composition and has not been submitted previously for any higher degree. All extracts have been distinguished using quoted references and all information sources have been acknowledged.

Danksagung/ Acknowledgement

I want to express profound gratitude to my advisor Dr. Holger Ott for his support and encouragement throughout the duration of the project.

I am also thankful for all the equipment and technical support provided by the Chair of Reservoir Engineering at the Montanuniversity of Leoben. Thanks also go to Michael Koopmans for his help and patience.

Finally, I must express my very profound gratitude to my family and to my friends for providing me with unfailing support and continuous encouragement throughout my study and through the process of writing this thesis. This accomplishment would not have been possible without them.

Kurzfassung

In dieser Arbeit werden Ergebnisse experimenteller Untersuchungen an drei Rohölen vorgestellt. Das Spinning-Drop-Video-Tensiometer (Dataphysics SVT 20N) wurde verwendet, um die Grenzflächenspannung (IFT) zwischen Rohöl und destilliertem Wasser zu messen.

Zusätzliche Vorversuche wurden durchgeführt, um die Grenzflächenspannung an der Dekan-Wasser-Phasengrenzfläche zu bestimmen, um einen konstanten Referenz-IFT-Wert für das System zu ermitteln. Der durchschnittliche IFT-Wert von Decan, bestimmt durch dieses Gerät, beträgt 38 mN/m.

Die höchste Grenzflächenspannung wurde für "Rohöl B" beobachtet. Der Durchschnittswert beträgt 12,4 mN/m. Das "Rohöl C" zeichnete sich durch die Grenzflächenspannung von 6-7 mN / m aus. Die niedrigste IFT von 0,8-1,2 mN/m wurde für zähflüssigste "Crude A" erhalten.

Bei allen untersuchten Rohölen nahm die Grenzflächenspannung mit der Zeit ab. Es wurde gefunden, dass das dynamische IFT-Verhalten von der Art des Rohöls und der Viskosität abhängt. Die untersuchten Ölproben zeigen unterschiedliche IFT-Reduktionsraten.

Die Ziele dieser Arbeit waren, Standard-IFT-Messungen durchzuführen und die Methodik für weitere Untersuchungen zu entwickeln.

Teststudien wurden durchgeführt, um den Einfluss der Temperatur und des rheologischem Verhalten von Ölen zu verstehen. Oszillationstests für "Rohöl A" zeigten, dass die beobachteten Schwankungen in der IFT-Kurve einen künstlichen Ursprung haben und mit der Bewegung des Tropfens in Zusammenhang stehen.

Darüber hinaus wurde eine Methodik zur Vorbereitung von Ölproben und Instrumenten für IFT-Messung entwickelt.

Die erhaltenen Ergebnisse sind nützlich für das Verständnis des Grenzflächenspannung-Verhaltens von Ölen und können für weitere Studien verwendet können.

Abstract

Results of experimental investigations on three crude oils are presented in this thesis. A Spinning drop video tensiometer (Dataphysics SVT 20N) was used to measure interfacial tension (IFT) between crude oil and distilled water.

Additional preliminary experiments were performed to determine the IFT at the interface between decane and aqueous phase to establish a constant reference IFT value for the system. The average IFT value of decane measured by the instrument is of 38 mN/m.

The highest interfacial tension was observed for the „Crude oil B". The average value is 12.4 mN/m. The "Crude oil C" is characterized by the IFT of 6-7 mN/m. The lowest IFT of 0.8-1.2 mN/m was obtained for the "Crude oil A".

For all examined crude oils, the IFT decreased in function of time. It was found that the dynamic IFT behaviour depends on the type of crude oil and viscosity. Oil samples studied have different IFT reduction rates.

The objectives of this thesis were to perform standard IFT measurements and develop the methodology for further investigations.

Test studies were performed to understand the effect of temperature and rheological behaviour of oils. Oscillatory tests for the „Crude oil A" showed that the observed fluctuations (jumps) in the IFT curve are of an artificial origin and are related to the movement of the drop.

In addition, a methodology for the preparation of oil samples and instruments for the IFT measurements was developed.

The obtained results are useful for understanding the IFT behaviour of oils and can be applied for further investigations.

List of Tables

List of Figures

Abbreviations

EOR	Enhanced Oil Recovery
SDT	Spinning Drop Tensiometry
SVT	Spinning Drop Video Tensiometer
FEC	Fast Exchange Capillary
IKA	Basic Magnetic Stirrer
CSW	*Cayias,* Schechter and Wade *method*
LY	Laplace-Young method
VG	Vonnegut method
CPU	*Central Processing Unit*
API °	American Petroleum Institute Gravity
TAN	Total Acid Number

Symbols

σ	mN/m	Interfacial Tension
σ^d	mN/m	Dispersion Force
σ^p	mN/m	Polar Interaction
W	J/m^2	Work
ϕ	-	Constant Characteristic of System
r_0	m	Drop Radius
d	m	Diameter
E	J	Total Energy
Eg	mN/m	Dilational Elasticity
E_M	mN/m	Marangoni Elasticity
G	mN/m	Gibbs Surface Elasticity
K	m^2/N	Compressibility
ω	s^{-1}	Angular Frequency of Rotation
$\Delta\rho$	kg/m^3	Density Difference
ρH	kg/m^3	Density of Heavy Phase
ρL	kg/m^3	Density of Light Phase
μ	cp	Viscosity
a	m	Radius at cap
α	-	Shape Parameter
V	m^3	Volume
l	M	Length of droplet
L	m	Length of capillary tube
A	m^2	Area
I	$kg \cdot m^2$	Moment of Inertia

Table of content

Page

1 Introduction

The primary recovery phase based on the natural potential of reservoir covers about 10-20% of the entire oil field [1], [2]. The final oil production using secondary recovery methods reaches 20-40%. Therefore, methods aimed to reduce the residual oil reserves, especially in complex conditions of low permeability, heterogeneity, flooded and carbonate reservoirs, are becoming increasingly important. The average final oil recovery of reservoirs by enhanced oil recovery technique for different countries and regions is from 10 to 15% [1].

Tertiary methods of oil recovery are methods to not only artificially maintain reservoir pressure, but also to change the properties of displacing agents and/or the properties of oil contained in the formation. Thus, an increase in the degree of oil recovery from the reservoir is provided. Modern technologies of enhanced oil recovery based on chemical methods are widely used and effective [1], [2], [3].

Residual oil reserves in the developed oil and gas fields are the main objects of application of chemical recovery [3], [4], [5].

Recently, microemulsions have been widely applied in the tertiary oil recovery processes, in which chemicals are used. This is one of the promising methods due to ability of microemulsions to absorb large volumes of water or a hydrocarbon fluid, and also solubilise impurities and contaminants in microdroplets [5], [6]. Interfacial properties among oil, water, and solid rock must be taken into account at this technique.

Microemusion is formed as an interphase layer, the so-called “middle phase”, with low interfacial tension between oil and water [5], [6], [7]. In particular, this occurs when using surfactants that pass from the aqueous phase to the capillary and film-retained oil after injection into the formation. The use of microemulsion increases the mobility of oil, facilitates its separation from rocks, and accelerates the oil drop coalescence [8], [9].

The phase behavior of microemulsion is complex and dependent on a number of parameters, including the types and concentrations of the surfactants, hydrocarbons, and brine; temperature and to a lesser degree, pressure [10]. The composition of microemulsion basically determines the parameters characterizing its rheological properties. Increasing the efficiency of microemulsion application in heterogeneous reservoirs requires the necessary viscoelastic and relaxation properties [11].

Phase behavior of a microemulsion system and the interfacial tension between the phases are interdependent. Changes in surfactant and brine concentration as well as changes in temperature and pressure lead to variations in interfacial tension.

Numerous studies showed that for the most complete displacement of oil with water and for acceleration of the displacement process it is expedient to reduce the interfacial tension at the boundary of the liquids. A low value of interfacial tension does not guarantee a high degree of oil displacement from the porous medium. Experimental studies showed that the movement of residual oil behind the displacement front is possible only at very low interfacial tension (less than 10^{-3} mN/m) [1], [12]. Therefore, in order to achieve an almost complete displacement of oil, it is necessary to reduce the interfacial tension at the boundary of the displaced and displacing phases by several thousand times [4].

In the processes of oil displacement, the interfacial tension between oil and water, as well as between oil and a porous medium, is of great importance.
Various methods are used for measuring interfacial tension between immiscible fluid phases. The measurements of low interfacial tension are difficult to perform by conventional methods. In most of cases, microemulsion studies include experiments under static condition. However, in order to get a holistic approach to oil mobilization, it is recommended to take into account the dynamics of the reservoir.
The commonly used methods for measuring ultra-low IFT are based on the analysis of the drop shape. In particular, two such techniques are considered the most promising. These are the spinning drop technique (SDT) and pendant drop analysis. Pendant drop method is used to determine the interfacial tension based on geometric analysis of the interface of the drop and is performed on a drop of liquid surrounded by the other phase. A typical crude oil/brine interfacial tension is around 20-30 mN/m. But it is still difficult to measure the tension that is less than 10^{-2}mN/m. Spinning drop method is a good fit for measuring the ultra-low tension system. A distinction of the spinning drop technique is that, instead of gravity, a known centrifugal force is applied for drop deformation. The interfacial tension between liquids is estimated from the shape of axisymmetric menisci [4].
The main purpose of this thesis was to develop an improved basic understanding of mechanism of ultralow interfacial tensions in oil-water system.
This thesis includes studies on the characterization, interfacial activity and rheology of crude oil samples obtained from production sites. The results of studies were analysed to understand the behaviour of oil phase in water. Interfacial tension readings were obtained for crude oil samples using a Spinning Drop Tensiometer from Dataphysics.
The main objective with this thesis is to study possible dependencies of oil droplet formation on different parameters. Data on the droplet size and interfacial tension from comparable experiments at ambient conditions on available oil samples were documented and analysed. The recorded results of interfacial tension and phase behaviour as a result of changing the parameters of the system were summarized.
First of all, attention is focused on achieving a low interfacial tension at various different rotational speeds. The effect of different speeds of the rotation and the volume of oil droplets on the interfacial tension is examined. Test studies were performed to understand the effect of temperature and viscoelastic properties in order to develop a methodology for further study of given oil samples.
In the thesis theoretical considerations related to the spinning drop technique and the principle of the spinning drop tensiometer are described. The experiments were also carried out with decane to establish a constant reference IFT value for the system before starting experiments with crude oil samples and understand the procedure of measurements themselves. In addition, a methodology was developed for the preparation of crude oil samples and instruments for interfacial tension measurements.
Part of this work is devoted to the study of how ultralow interfacial tensions arise in the oil-water system.
Moreover, experiments were performed with aim of determining if the oil type and the oil droplet of different dosages affect IFT values and the time of drop formation.

Extensive studies were conducted to determine the range of applicability and to identify possible experimental difficulties. Repeated tests were carried out to check the consistency of the results.
This thesis will address understanding microemulsions in general and can be used to design the next phase of further study.

2 Literature review

2.1 Interfacial tension in optimization of chemical flooding

Chemical flooding is one of the most promising areas of enhanced oil recovery.
During chemical flood, the chemical solutions are pumped through injection wells for increasing amount of crude oil that remains trapped in reservoirs after primary and secondary recovery. To mobilize and recover oil, waterflood reservoirs are often exposed to solvent, surfactant and polymer chemical flooding [13]. Polymers and surfactants alter or improve the properties of reservoir fluids to make them more conducive to extraction.
All the above-mentioned physicochemical methods of oil recovery, based on an increase in the oil displacement coefficient, have been developed on the principle of reducing the interfacial tension, increasing the wettability of the reservoir with water [1], [14]. Interfacial tension must be reduced from 10-30 mN//m in a typical water flood to 10^{-3} mN/m before a residual oil saturation reduction. It should be noted that enhanced oil recovery methods based only on the principle of reducing interfacial tension have the limited possibilities.
In recent decades, the need for cheap and affordable chemical reagents and methods for improving oil production is becoming increasingly important. Experimental procedures should be aimed at improving the chemical composition of floods and the proper planning of the process of injecting chemical materials.
One of the main problems limiting the effectiveness of flooding process, in particular the effectiveness of the surfactant and polymer flooding, is the difficulty in predicting changes in interfacial tension in reservoir conditions.
The effective interfacial tension is controlled by many factors and reservoir parameters. First of all, interfacial tension depends on the temperature, composition, and pressure. The types and concentrations of the surfactants, salinity of brines can also play a significant role. The influence of these factors and their combinations on the decrease in interfacial tension should be studied in the course of experiments.
The spinning drop tensiometry along with other methods has become widely used to optimize the chemical composition of flooding systems.
In many emulsion and microemulsion systems, the interfacial tension between the oil-rich phase and the aqueous solution is very low, that leads to significant difficulties in applied experimental methodologies. The main purpose of this thesis is to develop an improved basic understanding of the interfacial tension mechanism in the crude oil - water system. The obtained research results can be used in future experiments for the oil-surfactant-brine system.

2.2 Microemulsions

During chemical flooding it is essential that the complex system forms microemulsion with the residual oil. Danielsson et al. (1981) gave the definition of a microemulsion as a thermodynamically stable liquid mixture [5], [6].The main components are oil, water and surfactant. The formation of microemulsion occurs spontaneously under certain conditions and the composition of microemulsion influences its stability.

Depending on the emulsification process, multiple emulsions can be formed. The basic types are direct (oil dispersed in water) and reversed (water dispersed in oil) microemulsions [10].
Interfacial tensions and adsorption densities of the surfactants are essential quantities required for the understanding of microemulsions, their stability and phase equilibria. Microemulsions are characterized by a low interfacial free energy that it is exceeded by the negative free energy term arising from the entropy of dispersion [10]. Thus, the overall free energy of a microemulsion formation is negative and thermodynamically stable.
Microemulsion formation is generally favored when the volume fraction of the dispersed component is quite low. Diameter of small droplets of a dispersed phase is 10-100 nm. The continuous phase of microemulsion in most of cases is water [7].
The small size of droplets contributes to the microemusion stability. In some cases, one of the factors affected the stability of the dispersion is viscosity of the system. However, most microemulsions are of a relatively low viscosity. Thus, the influence of this factor can be neglected [15].
The stability of microemulsions is strongly related to the low interfacial tensions (typically $<10^{-5}$mN/m).

2.3 Interfacial tension theory

The first interfacial theory, explaining the mechanism of microemulsion formation, was developed by Hoar and Schulman (1942) [16]. According to this theory, very low interfacial tension leads to a spontaneous increase in the interfacial area involved in the formation of microemulsion.
The basic concept of interfacial theory is as follows: when two immiscible liquids are in contact with each other, the molecules at the interface of these liquids experience unbalanced forces of attraction. These forces give rise to interfacial tension [15]. Surface tension is defined to a single liquid surface, whereas the interfacial tension is defined to the interface of two immiscible liquids.
The interfacial tension σ_{AB} between two liquids A and B is equal to the difference between the respective interface tensions [15].

$$\sigma_{AB} = /\sigma_A - \sigma_B/ \qquad (1)$$

σ_A interfacial tension of Liquid A [mN/m]
σ_B interfacial tension of Liquid B [mN/m]
σ_{AB} interfacial tension between two liquids A and B [mN/m]

If the suspended droplets in a liquid, with which they are immiscible, are in equilibrium, they spontaneously assume a spherical form.

The effect of surface/interfacial tension on the interface area between liquids may be defined either through force or through energy.
According to Girifalco and Good (1957), the molecules in the interfacial region are at a higher potential than those in the corresponding bulk [15].Three sets of forces must be considered when liquid A is in contact with liquid B. These are the forces acting between molecules in liquid A and in liquid B plus those which act across the interface between molecules of liquids A and B [15].
These forces were expressed in terms of the surface tensions of the two liquids. The work of adhesionW_{12}^{ad} was then given by

$$W_{12}^{ad} = \phi\ (W_{11}^{coh} W_{22}^{coh})^{\frac{1}{2}} \quad (2)$$

where

$$W_{11}^{ad} = 2\sigma_1 + W_{22}^{coh} = 2\sigma_2 \quad (3)$$

and

$$W_{12}^{ad} = \sigma_1 + \sigma_2 - \sigma_{12} \quad (4)$$

W^{ad} work of adhesion [J/m^2]
W^{coh} work of cohesion [J/m^2]
σ_1 interfacial tension of Liquid 1 [mN/m]
σ_2 interfacial tension of Liquid 2 [mN/m]
ϕ constant characteristic of the system [-]

Hence,

$$\sigma_{12} = r_1 + r_2 - 2\phi(\sigma_1\sigma_2)^{\frac{1}{2}} \quad (5)$$

r_1 radius of interface for Liquid 1 [m]
r_2 radius of interface for Liquid 2 [m]

Moreover, the contributions made by different types of intermolecular interaction are additive and could be assessed separately.

The interfacial tension of a liquid would consist of two components, σ^d, due to dispersion forces and σ^p due to polar interactions. The interfacial tension between liquids is then given by

$$\sigma_{12} = \sigma_1 + \sigma_2 - 2(\sigma_1^d \sigma_2^d)^{\frac{1}{2}} \quad (6)$$

σ_1 interfacial tension of Liquid 1 [mN/m]
σ_2 interfacial tension of Liquid 2 [mN/m]
σ^d interfacial tension due to dispersion forces [mN/m]

2.4 Surface elasticity

The increase in interfacial elasticity along with the reduction in the interfacial tension is the crucial parameter which relates interfacial mechanics to microemulsion stability [17], [40]. The interfacial elasticity describes surface resistance to changes in interfacial area, which, in turn, is accompanied by a subsequent change in interfacial tension [8]. This theory supports the data obtained by me in the course of long-time measurements and dilational rheological experiments. Interfacial tension was measured continuously with area changes using a spinning drop instrument adapted to the oscillatory measurements.

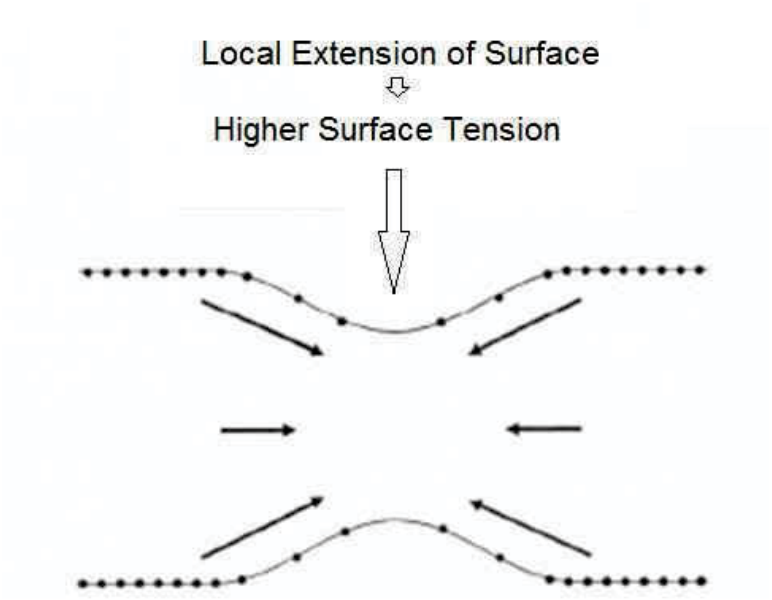

Figure 1: The Gibbs-Marangoni effect [11]

Elasticity arises from the variation of the interfacial tension during deformation of a liquid interface. The surface elasticity is associated to gradients of interfacial tension.

The measurement of dynamic tensions often based on Marangoni elasticity, especially for foam-forming surfactant solutions. Marangoni-Gibbs forces act in opposition to the disturbance [11]. The time-dependent Marangoni elasticity is of particular interest.
When a liquid interface undergoes sudden expansion (Fig.1), the expanded part of the interface has a lower surfactant density compared to unexpanded parts. The cause is in increasing the surface area which corresponds to an increase in interfacial tension. This creates increased resistance to further expansions [11].
Due to the contraction of the surface, liquid flows from the low tension region to high tension region. This is called the Marangoni effect
The Marangoni effect only exists until the surfactant adsorption equilibrium is reestablished in the film, a process that may take place within seconds or over a period of hours.
Surface dilational elasticity, E_G, is given in **eq.7** [18].

$$E_g = -\frac{d\sigma}{dlnA} \tag{7}$$

σ	interfacial tension [mN/m]
dσ	interfacial tension gradient
dlnA	geometric area of the surface [m]
E	viscoelastic modulus [mN/m]

The condition for this equation is that the compressibility of the surface film< K.

$$K = \frac{1}{E_g} \tag{8}$$

E	viscoelastic modulus [mN/m]
K	compressibility [m^2/N]
G	Gibbs elasticity

Surface modulus E is the resistance of the surface to a change in area.
It is should be noted that the equilibrium at the thin interface is difficult to restore after deformation because of the low number of molecules.
Other parameters that affect stability are film thickness and adsorption behavior.

2.5 Surface age

As will be indicated in the following chapters, the measurements showed a decrease in interfacial tension of oils during the first hour of experiments. The interfacial tension of oils reaches a minimum after several hours, and then the value remains constant. This section of the chapter covers the issues related to understanding the factors that affect the changes in

interfacial tension of oils with time, and at what moment the IFT value can be quoted as the true equilibrium value.
The surface age is considered as a time from the instant the interface is formed to the time of the measurement [19].
The well-known fact that the interfacial tension measured on newly formed interfacial surfaces is higher than the equilibrium values has been described in many publications [20], [21], [22]. The lowering of the interfacial tension is consider to be diffusion or/and adsorption controlled. Many authors also consider the factors which affect the rate of interfacial tension depression, such as pH, concentration of solutions, etc.
After the production of interface, the interfacial tension has the same value as the pure liquid(s). The value then reduces until an equilibrium value is reached. When liquids with surface-active substances (surfactants) are used, the time-dependent value is not identical to the equilibrium value.
It is necessary to note that there is difference between static and dynamic measured interfacial tension. In a dynamic tensiometer, the size of the interface changes during the measurement. Thus, spinning drop measurement based on dynamic methods enables the surface age to be specified over a large time range and thus enable fast processes to be simulated. The time-dependent value is referred to as the dynamic tension and is associated with a particular interface age.

2.6 Measurement of interfacial tension

Interfacial tension measurement methods include the capillary rise method, Wilhelmy plate, maximum bubble pressure and drop analysis methods; in particular the spinning drop method. Spinning drop tensiometry is applied for microemulsion studies [12], [16], [17], [25].
Factors effecting interfacial (surface) tension are temperature, solute concentration and intermolecular forces.
In this study the interfacial tension of the oils was measured using a spinning drop tensiometer.

2.6.1 Principle of IFT measurement by spinning drop method

The spinning drop technique has been applied to measure interfacial tensions of and between fluids. It is a good fit for measuring the ultra-low tension system and has previously been well described in the literature [23], [36], [37], [39]. Values of interfacial tension as low as 10^{-6} mNm^{-1} can be measured [38].
The experimental setup includes a unit providing rotation with a constant velocity of the capillary into which liquid (water or solution) is placed and a drop of another liquid of lesser density, e.g. hydrocarbon. Since a droplet liquid is less dense than the bulk liquid, the droplet is located at the center of the capillary during rotation. As the speed of rotation increases, the droplet extends, since the centrifugal force counteracts the interfacial tension. At a sufficiently high frequency of rotation, the drop takes the form of an elongated cylinder (Figure 2). A preliminary study of the component's distribution in a system of two liquids is needed to explain the phenomena of mass transfer across the interface boundary.

At a sufficiently high frequency of rotation, the droplet takes the form of an elongated cylinder.

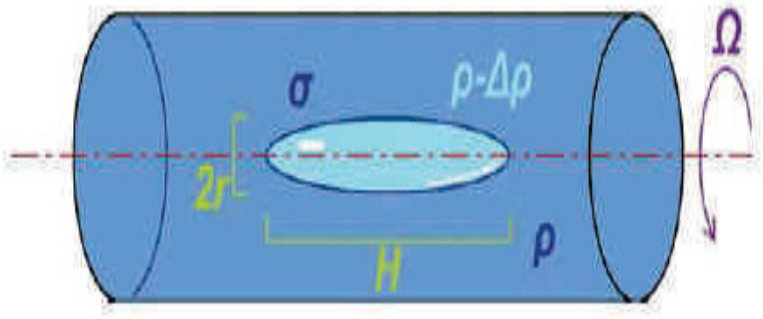

Figure 2: A bubble or a drop suspended in a denser fluid, spinning with angular frequency ω [24]

The total energy of a cylinder with length l and radius r_0 includes potential energy and free surface energy.

The centrifugal force acting on the cylinder is $\omega^2 r^2 \Delta\rho/2$. Integrating for a cylinder of length *l* is $\frac{\pi\omega^2\Delta\rho l r_0^4}{4}$. On the other hand the interfacial free energy is $2\pi r_0 l\sigma$. The calculation of total energy, E, is carried out by **eq.8**

$$E = \omega^2 \Delta\rho r_0^2 \frac{V}{A} + 2V\frac{\sigma}{r_0} \quad (9)$$

E total energy [J]
V volume of cylinder [m^3]
A area [m^2]
$\Delta\rho$ density difference [kg/m^3]
σ interfacial tension [mN/m]
r_0 drop radius in the central cylindrical region [m]
ω angular frequency [rad/s]

Since $V = \pi r_0^2 l$ and $\frac{dE}{dr_0} = 0$.

$$\sigma = \frac{\omega^2 \Delta\rho r_0^2}{A} \quad (10)$$

σ interfacial tension [mN/m]
A area [m^2]
$\Delta\rho$ density difference [kg/m^3]
r_0 drop radius in the central cylindrical region [m]
ω angular frequency [rad/s]
l length [m]

Vonnegut (1942) [4, p.268] was the first who showed that surface and interfacial tensions can be determined from the radius of a long cylindrical fluid drop in a horizontal tube. The equation, known as the Vonnegut equation, is valid for cylindrical rotating drops.
According to J.Bush (2010) [24], for the case when $\Sigma<0$, $\Delta\rho=0$, a spinning drop is stabilized on axis by centrifugal pressures. For high $|\Sigma|$, the droplet is described by a cylinder with spherical caps.

$$\Sigma = \frac{\omega^2 \Delta\rho {r_0}^3}{8\sigma} = \frac{centrifugal\ pressure}{curvature} \qquad (11)$$

Σ centrifugal pressure/drop curvature ratio [-]
$\Delta\rho$ density difference [kg/m^3]
σ interfacial tension [mN/m]
r_o drop radius [m]
ω angular frequency [rad/s]

Drop energy:

$$E = \frac{1}{2}\, l\omega^2 + 2\pi r_0 L\sigma \qquad (12)$$

Rotational K.E. *Surface energy*

Where

E total energy [J]
$\Delta\rho$ density difference [kg/m^3]
σ interfacial tension [mN/m]
r_0 drop radius [m]
l drop length [m]

L length of capillary tube [m]
ω angular frequency [rad/s]
K.E. kinetic energy

Volume $V = \pi r_0{}^2 L$ and moment of inertia $I = \frac{\Delta m r_0{}^2}{2} = \Delta\rho\frac{\pi}{2} L r_0{}^4$.Then the energy per unit drop volume is calculated by **eq.12**.

$$\frac{E}{V} = \frac{1}{4}\Delta\rho\omega^2 r_0{}^2 + \frac{2\sigma}{r_0} \quad (13)$$

E total energy [J]
V volume [m^3]
A area [m^2]
$\Delta\rho$ density difference [kg/m^3]
σ interfacial tension [mN/m]
r_0 drop radius [m]
l length [m]
ω angular frequency [1/s]
I moment of inertia [$kg \cdot m^2$]
m mass [kg]

Minimizing with respect to r_0:

$$\frac{d}{dr_0}\left(\frac{E}{V}\right) = \frac{1}{2}\Delta\rho\omega^2 r_0 - \frac{2\sigma}{r_0{}^2} = \mathbf{0} \quad (14)$$

Where $r_0 = \left(\frac{4\sigma}{\Delta\rho\omega^2}\right)^{1/3}$.

Vonnegut formula: $\sigma = \frac{1}{4\pi^{3/2}}\Delta\rho\omega^2\left(\frac{V}{l}\right)^{3/2}$ allows inference of σfrom l, useful technique for small σ. Radius r_o grows with σ and decreases with ω.
At the length/width ratio of the drop more than 4, the interfacial tension is calculated by **eq.14**

$$\sigma = \frac{r^3\omega^2\Delta\rho}{4} \quad (15)$$

$\Delta\rho$ density difference [kg/m^3]
σ interface tension [mN/m]
r_0 drop radius [m]
ω angular frequency [rad/s]

When the tube rotates with high angular frequency, the drop migrates to the axis of rotation and assumes a cylindrical shape with hemispherical ends. The drop reaches an equilibrium shape which is characteristic of that frequency.
The centrifugal force produces the pressure difference across the interface. When the interfacial tension achieves the balance, the elongation of a droplet ceases.
Rosenthal and Princen et al. [23] presented a complete analysis of the drop shape problem that was used for construction of the spinning tensiometer.

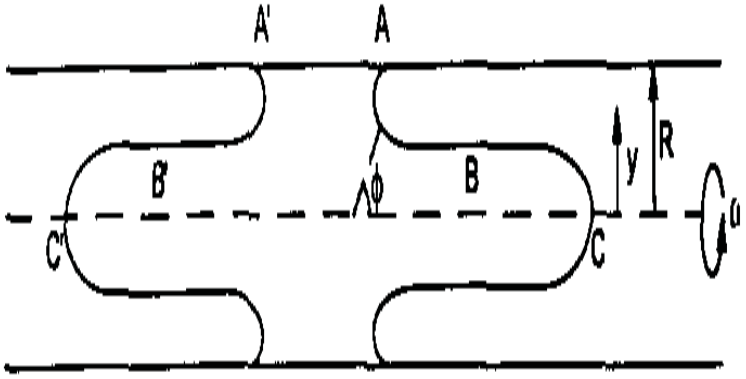

Figure 3: Critical drop shape just prior to release [23, p.242]

The main condition for the drop release (Figure 3), according to Rosenthal et al. [23, p.241], is expressed by **eq.14**.

$$cR^3 > 1 \tag{16}$$

$$c = \frac{\Delta\rho\omega^2}{4\sigma} \tag{17}$$

$\Delta\rho$ density difference [kg/m^3]
σ interfacial tension [mN/m]
r_0 drop radius [m]
ω angular frequency [rad/s]

Difficulties are usually associated with the use a long droplet for measurements, as will be discussed in the following chapters. When smaller droplets used in measurement, droplet length and width, or length and volume are additionally considered. The limiting, cylindrical droplet shape is more often used in practice.

2.6.2 Measurement of interfacial dilational rheology

Spinning drop technique is additionally used as a reliable tool for measuring interfacial rheology. When harmonic oscillations compress and expand the interfacial layer, relaxation processes begin to occur. As a consequence, the interfacial tension starts to vary accordingly. This method is used to characterize the elastic properties of the interfacial layer and viscous properties, which were described in the Section 2.4. Oscillation experiments in this study were performed for available oil samples.

3 Experimental

3.1 Materials

Three samples of crude oils obtained from wells were used for experimental measurements by a spinning drop method. Some physical and compositional properties of oil samples are represented in Table 1. Elemental composition (%wt.) of samples and viscosity are unknown.

Table 1: Selected chemical and physical properties of oil samples

Well	Crude oil A	Crude oil B	Crude oil C
Reservoir	I	II	III
TAN [mg KOH / g oil]	1.96	1.56	0.34
Density @20°C [g/cm³]	0.9306	0.9070	0.8711
Density @15°C [g/cm³]	0.9339	0.9104	0.8746
API °	19.88	23.78	30.15

It can be seen that the “Crude oil A” is of the lower API gravity and can be consider as heavy crude oil.
Anhydrous decane C10H22 used was purchased from Sigma-Aldrich with a purity grade of 99 wt%. A molar mass of decane is 142.29 g/mol and a density of 0.73 g/ml at 25°C.
Distilled water was used for experiments to produce accurate results, and as well define a reference.
All measurements were made with respect to the rotation speed n, since this parameter is more suitable for physical calculations. The unit of rotation speed is min-1.

3.2 Equipment

3.2.1 Spinning drop tensiometer

Crude oil/aqueous interfacial tensions were measured using a spinning drop tensiometer designed for operations at elevated temperatures. A SVT 20N spinning drop video tensiometer from Data Physics with a build-in liquid thermal chamber (the measuring cell) was used in the present study (Fig.3,4). A SVT 20Nis combined with SVT 21 for oscillation experiments [25].

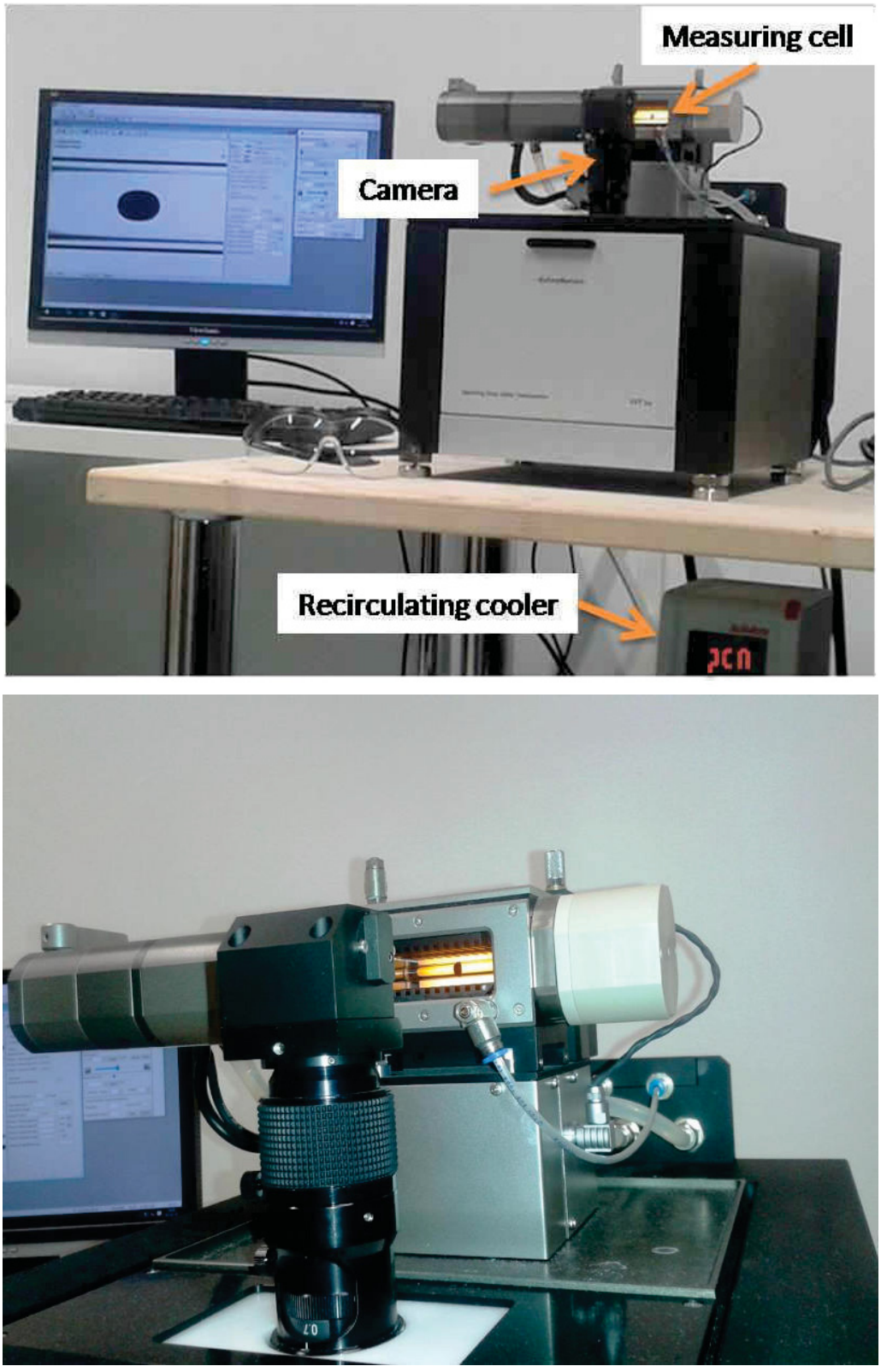

Figure 4: A SVT 20N spinning drop video tensiometer [A]
with a build-in liquid thermal chamber (the measuring cell) [B]

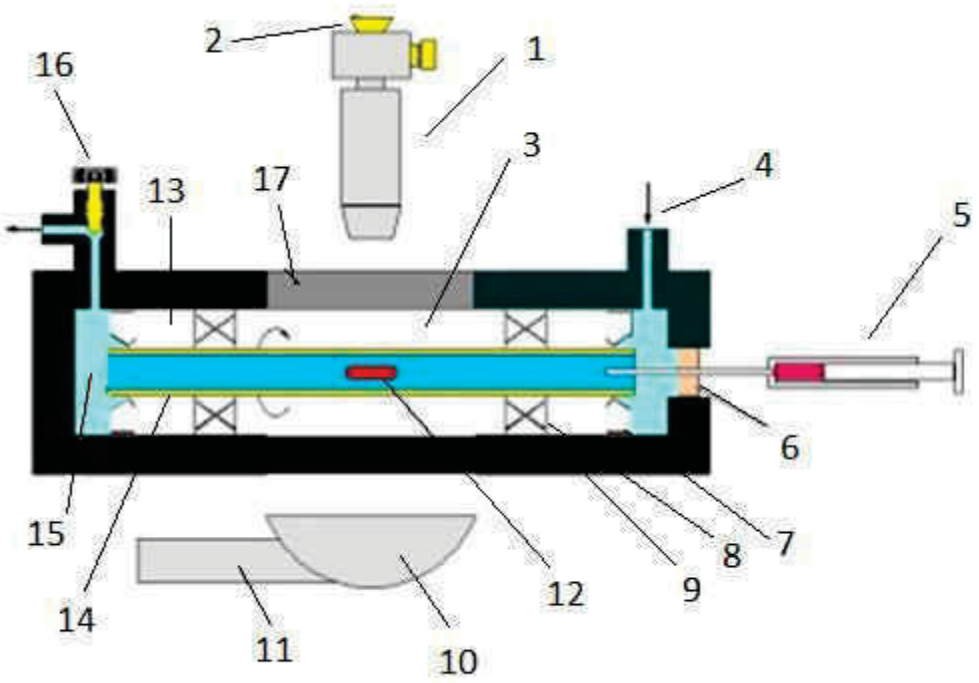

Figure 5: Structural sketch of the liquid thermal chamber (A)
and details of the measuring cell (B) [26, p.894]

(1) camera, (2) ocular, (3) measurement chamber, (4, 16) chamber inlet/outlet for oil (newmodel gas inlet), (5) syringe for dispensing liquid into the capillary,(6) septum, (7, 8, 9) holder for capillary, (10) light source, (11) illumination, (12) inner phase of measurement, (13) chamber for capillary, (14) capillary, (15) heavy phase, (17) windows

The principle of the method of tensiometer is to spin a horizontally mounted glass capillary tube filled with the denser (distilled water) phase containing a small decane/oil drop (volume ≈0.02–10μL) about its longitudinal axis, and measuring the dimensions of the drop. The rotation speed and temperature were the physical variables employed in this work. The measurements were carried out with time interval 1-5 sec, 15-60 sec after reaching a stable state.

Interfacial tension measurements at the minimum density difference 0.05 g/cm^3 could be in error by as much as 10% [25], [38]. Exceeding the minimum density difference in my measurements along with the repeatability of measurements with crude oil samples gives reliable results.

3.2.2 The fast exchange capillary tube

The fast exchange capillary FEC 622/400, illustrated in Figure 6, made of borosilicate glass is of 6.22 mm outer diameter and of 4.0 mm inner diameter; length is 120mm. Temperature limit for the capillary tube reaches 90 degree. During experiments the tube is sealed on one

side by a septum of 7 mm diameter. Sealing the tube with a tight-fitting septum provides a necessary tube temperature during the heating cycle.

Figure 6: The fast exchange capillary FEC 622/400 [25]

Figure 7: IKA 3810000 RCT Basic magnetic stirrer

Oil droplets of 2-5 µL were introduced into capillary tube containing the aqueous phase. The main difficulty encountered was the introduction of a suitable droplet into the tube, especially during the analysis of the more viscous “Crude oil A”.
The oil was slightly pre-heated for a short period to 40-45°C to introduce a suitable volume into the tube. The IKA 3810000 RCT Basic magnetic stirrer, depicted in Figure 7, was used for heating of viscous oil. The aqueous phase inside the capillary tube was also heated to the same temperature. The tube and its content were then cooled to ambient temperature 25°C in the tensiometer before commencing the experiment. The same procedure has been reported in many literature publications, especially for measuring the interfacial tension of asphaltenes and heavy crude oils [27], [28], [33].

3.3 Procedure

3.3.1 Fill in liquid with higher density (outer phase)

A 10 ml disposable syringe and a long needle (∅ 0.60; L 80 mm) were used to fill the capillary in liquid with higher density (outer phase). The filling of the capillary tube is carried out bottom-up, so the air can exhaust from the open side until the liquid oozes out the open end (shaping a calotte). To ensure that the tube is absolutely bubble-free, the capillary should be turned several times and even shaken, as the bubbles often get stuck in the ends.

3.3.2 Fill in liquid with lower density (inner phase)

The injection of a drop of the liquid with the lower density (inner phase) into the filled capillary was done by use of the 1 ml disposable dosing syringe and a long needle (∅ 0.60; L 80 mm). To avoid the contact of the wall of the capillary and the injected drop, the capillary was rotated with 100-200 min^{-1} during injection. The higher rotation rates did not lead to desired results. The injection and releasing the drop of suitable volume can be accompanied by very small movements of a needle and syringe.
It is necessary to ensure that there are no air droplets in the tube, especially in the injected crude sample as it can lead to error in interfacial tension measurements.

3.3.3 Temperature

A constant temperature during experiments and cooling of the system/tensiometer are maintained by Julabo Corio CD-200F [Fig.8].
The Recirculating Cooler operates from -20 … +150°C. Most of the experiments in this study were carried out at room temperature of 25±0.5°C. A continuous test was performed to determine the interfacial tension at the interface between decane and aqueous phase at elevated temperatures in the range of 25°C - 60°C.

Figure 8: Julabo Corio CD-200F

3.3.4 Calibration

To calibrate the absolute image size the software needs a reference value. The first method is the calibration of the dosing needle. The calibration was conducted at the start of the each experiment.
The reference value can be produced by the tensiometer itself, if a stable and sharp-contoured drop is available, by moving the camera carriage a defined way to the left (-delta) and to the right (+delta).This method was used during the experiments, since the parameters set at the beginning could be changed due to software failure. Moreover, calibration of the drop image is no longer valid when the zoom or focus settings are changed.

3.3.4.1 Calibration by camera movement

The position of the left or right hand cap of the drop was detected at different camera positions. This option only works in *Cayias*-Schechter-Wade (CSW) and Laplace-Young (LY) mode. The hand cap of the drop must be detectable. In order to estimate the range of the camera movement I gave zoom setting X 100 as vertical scale. The most suitable zoom for my measurements was 0.7, since it was not always easier, especially for the “Crude oil B”, to get the drop of small size. The zoom of 1 and higher can be used at measurements of

smaller size drops. Then drop was marked with calibration box and the new vertical scale was calibrated. When camera movements are too far, the drop moves out of view and that leads to an error in calibration. To avoid such error the stride value in the calibration dialog was reduced to 20-30% and calibration was retried. The most accurate values were obtained by using the entire drop image width for calibration.
The above-mentioned procedure can be applied for any visible object. The illumination values should also be taken into account.

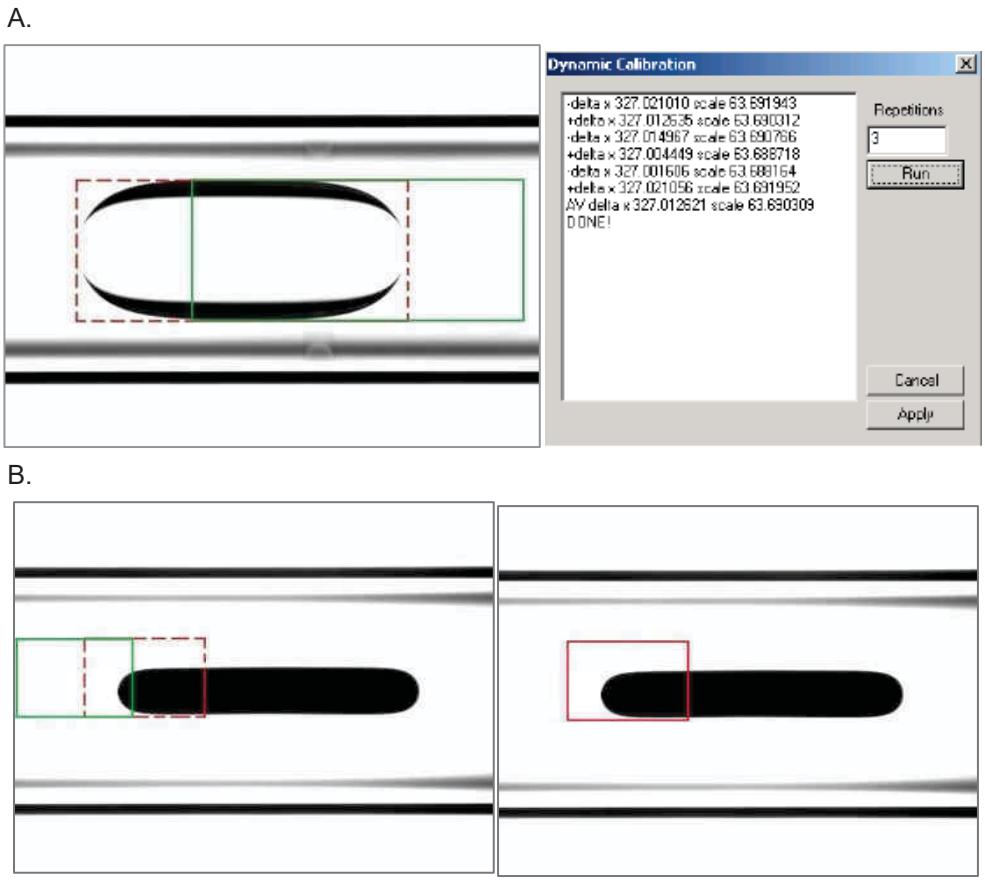

Figure 9: Calibration by camera movement.
A. Decane. Drop calibration by using the entire drop image width;
B. “Crude oil A”. Drop image calibration by using the spherical ends

3.3.4.2 Calibration with reference object

A visible object with a known vertical size is needed to perform this type of calibration. For my measurements, the dosing needle was calibrated, and the size of the object was the diameter of the needle (0.80 mm).The upper and lower edges of the object were detected, and then a vertical scale was calculated [Figure 10]. The position of the needle should be in the middle of the capillary tube. Calibration was carried out by me at the beginning of each experiment. After adjusting the magnification and focus to obtain a sharp image of the needle and the size required for the measurement, a calibrated value was measured. The procedure was repeated several times to get an average calibration value. Changes in the setting

parameters lead to an error in the measurements, so the calibration value for the image size should remain constant during the experiment.
Calibration of the dosing needle was a more appropriate calibration method for measuring more viscous oils (“Crude oil A”), since it was not always easy to achieve a stable drop position in the image window for dynamic calibration. Needle calibration involves difficulties when liquids of lower viscosity (“Crude oil B”) were loaded into the capillary tube of a spinning tensiometer, since a calibration over a long period of time causes water retention inside the syringe and subsequent bubbling during injection.

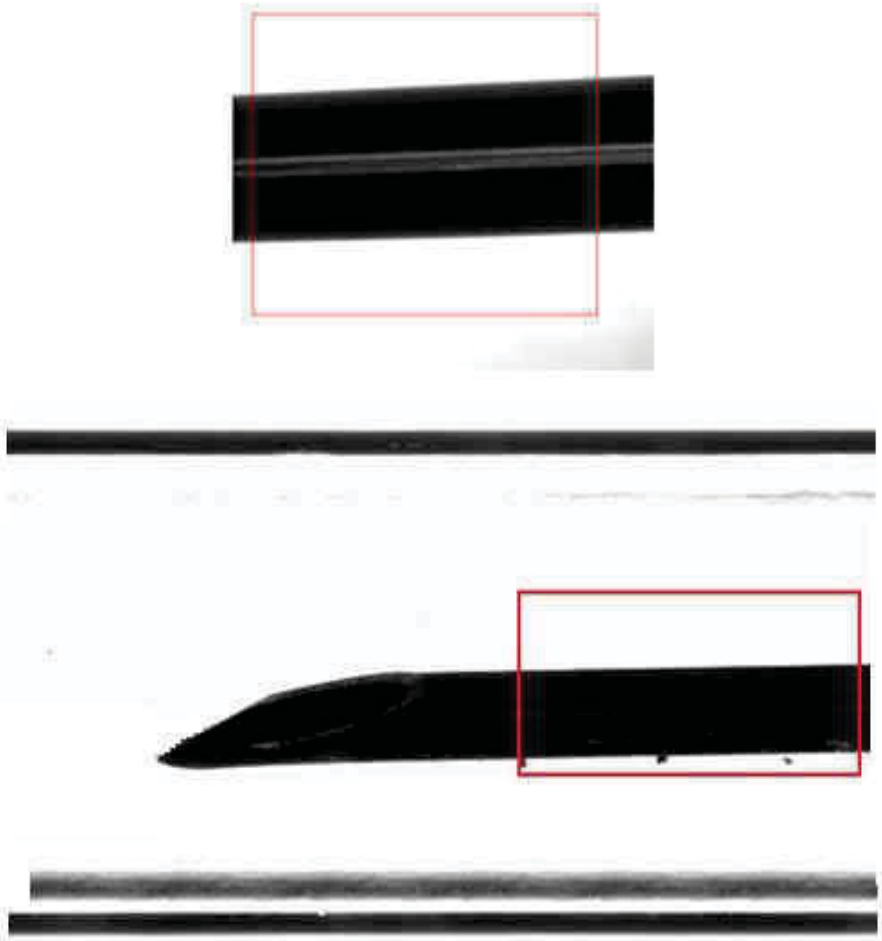

Figure 10: The calibration of the dosing needle

3.3.5 Monitoring

The drop length can be monitored over time to determine its steady state. An example is given in Figure 11. The equilibrium state is reached when the drop length remains unchanged.

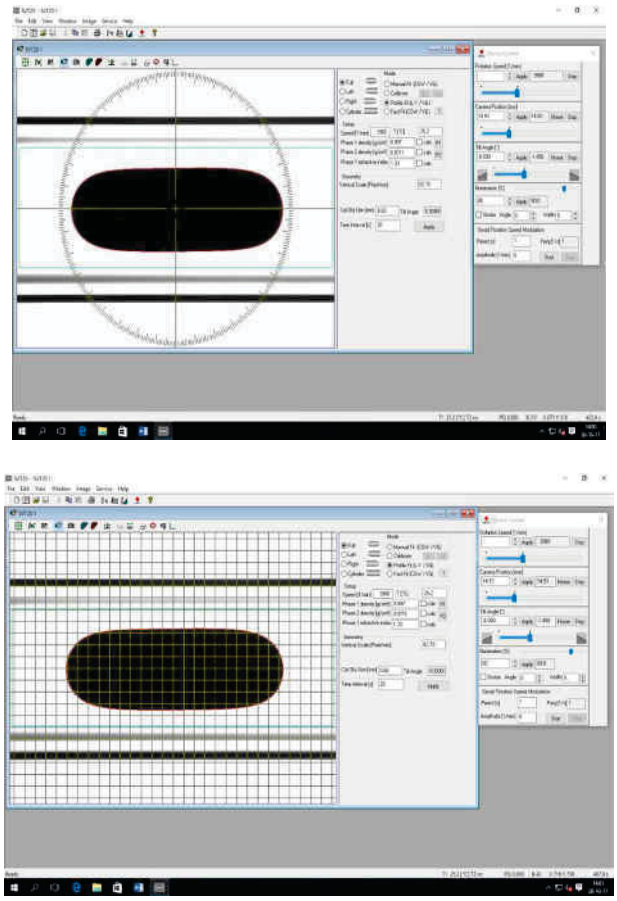

Figure 11: Monitoring of oil droplet

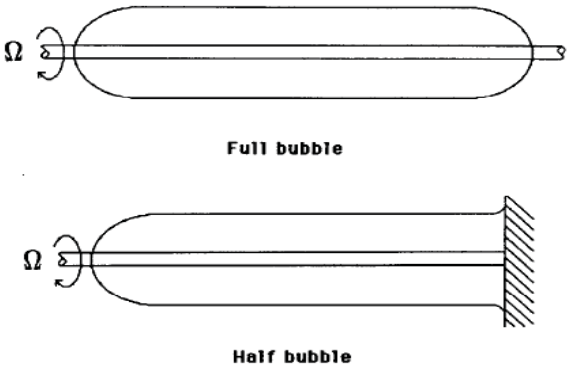

Figure 12: Possible drop configurations [2, p.556]

3.3.6 Cleaning

The preparation of samples and instruments are decisively important for the measuring results. They must be treated always the same way to avoid systematic errors.
Before using the glass capillary for the next experiment, it was cleaned carefully by repeated rinsings with decane and acetone. A method for cleaning a capillary tube must comprise the

step of applying an ultrasonic wave to the capillary tube. The most optimum cleaning procedure includes the following steps:

1. Flush the capillary tube with decane/acetone to dissolve oils and use a cleaning brush. Repeat several times, if necessary. Decane should be used before acetone, since it helps to avoid the formation of particles that can be formed due to the phase behavior. Tetrachloro-ethylene can also be used for cleaning.
2. Fill the capillary, close it with the septa holder and shake.
3. Flush the tube with decane to dissolve possible oil residues, and then flush with acetone.
4. Remove the plastic septum from the septa holder and clean with cotton pads or paper soaked in acetone and/or decane. To easily remove and not damage a septum, blow the septa holder through orifice with air.
5. Fill the capillary tube with propanol. Have it and the septa holder 10-15 min in an ultrasonic bath. Do not use acetone for this procedure as it evaporates very fast. Temperature should be around 60-70°C.
6. Let the tube and the septum holder dry. Blow them with air. Insert the septum into the holder.
7. Wipe the capillary tube from the outside with cotton pad/paper soaked in distilled water to ensure that there is no possible contamination of any chemicals and no liquids get into the tensiometer housing. The tube must be clean, dry and transparent.

Disposable dosing syringes of small diameter were used for injections of oils, as the cleaning of syringes and needles is difficult. Using the glass syringes of small diameter is not suitable, as they are heavy. It creates inconvenience during an injection. Moreover, it is impossible to avoid the formation of bubbles.
The syringes, instruments, glassware and beakers are cleaned with decane and acetone/propanol, and flushed with water.

3.4 Standard measurements

3.4.1 Decane / water system

The main purpose of these measurements was to establish a constant reference IFT value for the system before starting experiments with oil samples and understand the procedure of the measurements itself.
The interfacial tension value for a pair of decane-distilled water has been given in many literature publications. Than et al. (1988) report the interfacial tension of n-decane with water to be 45.7±1.41 mN/m at room temperature of 25°C [12]. They also provide information on interfacial tension measured with sessile drop method. In this case, the value of interfacial tension is 47 mN/m. Experiments conducted by Morrow et al. (1988) for n-decane in double-distilled water also showed an IFT value of about 47 mN/m [29]. Lee (1999) published the IFT value of 51 mN/m [30]. Goebel et al. (1997) gave the value of 53.2 mN/m [16].

In this study, the standard value of decane in distilled water was assumed to be 46 mN/m according to Than et al. [12]. Interfacial tension measurements for each pair of liquids were conducted in three modes: Cayias, Wade and Schechter (CSW mode), Laplace-Young (LY mode) and Vonnegut (VG mode). The difference between them will be described in detail in Paragraph 3.6.

Distilled water used for the measurements was poured from a newly opened vessel. A decane droplet of about 0.02-0.03 ml was injected into the water inside the rotating tube. For every individual rotational speed applied in the experiments, the first condition is to reach equilibrium. The exact equilibrium value was however not very important for the results, but rather a confirmation that the equipment and calculations were calibrated. Droplets were assumed to be in equilibrium state when measured values of interfacial tension remained unchanged for half an hour. All experiments were performed at room temperature of 25°C.

The first test was conducted at the rotational speed of 3600 min^{-1}, which consider as a minimum rotation speed. The transformation of droplet during one hour is shown in Figure 13.

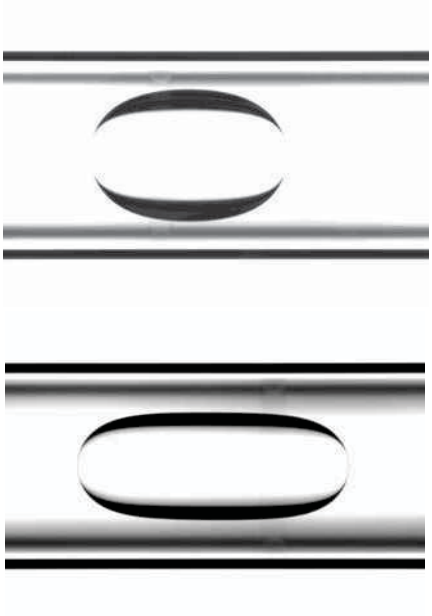

Figure 13: Snapshots of the spinning drop of decane in water
at the beginning of the experiment and after 1 hour.
Rotation speed- 3600 min^{-1}

As can be seen from Figure 14, the interfacial tension IFT CWS and LY are characterized by almost identical values, while there is a larger discrepancy between these values and IFT VG values. The interfacial tension calculated according to Cayias-Schechter-Wade (CWS) approach is always the highest value among the results obtained by other calculation methods. The average IFT CWS value of decane measured by the instrument is about 53.9 mN/m at 25°C, which is close to literature values of 46-53.2 mN/m [12], [16], [29]. The mean of IFT LY and IFT VG values are 46.3 and 29 mN/m, respectively.

It was found that the interfacial tension value is sensitive to the measured surface area of the droplet. Figure 15 shows that the interfacial tension increases with decreasing of the volume of the droplet. Since measurements were mainly made on the left spherical end of the droplet due to the large volume of the droplet, it caused a discrepancy between the interfacial tension values measured by the three different approaches. Moreover, the interfacial tension, measured by the Laplace-Young approach, varies over a larger range than the other two interfacial tension distributions.

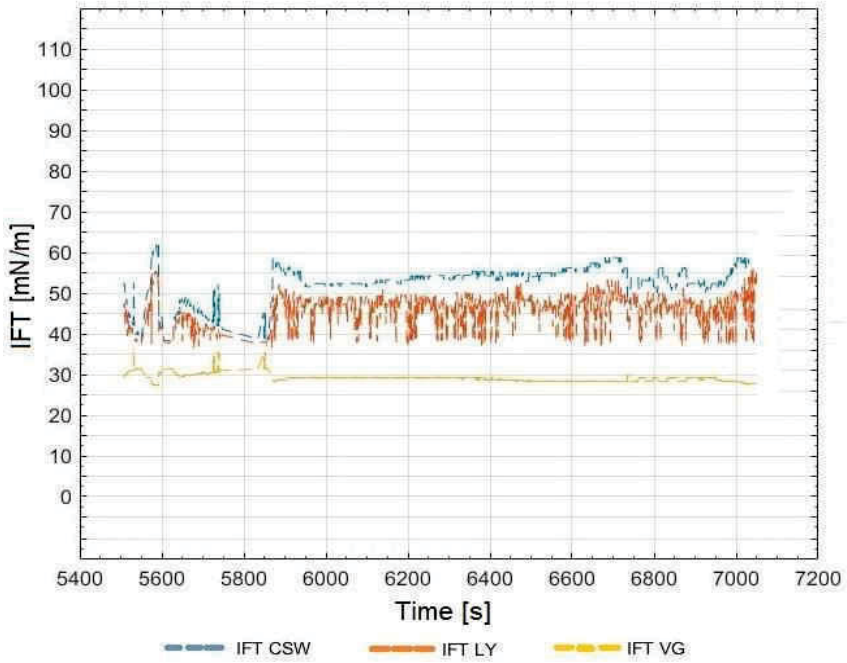

Figure 14: IFT measurement of decane-water with a rotation speed of 3600 min^{-1}.
Measurements on the left spherical end of a droplet

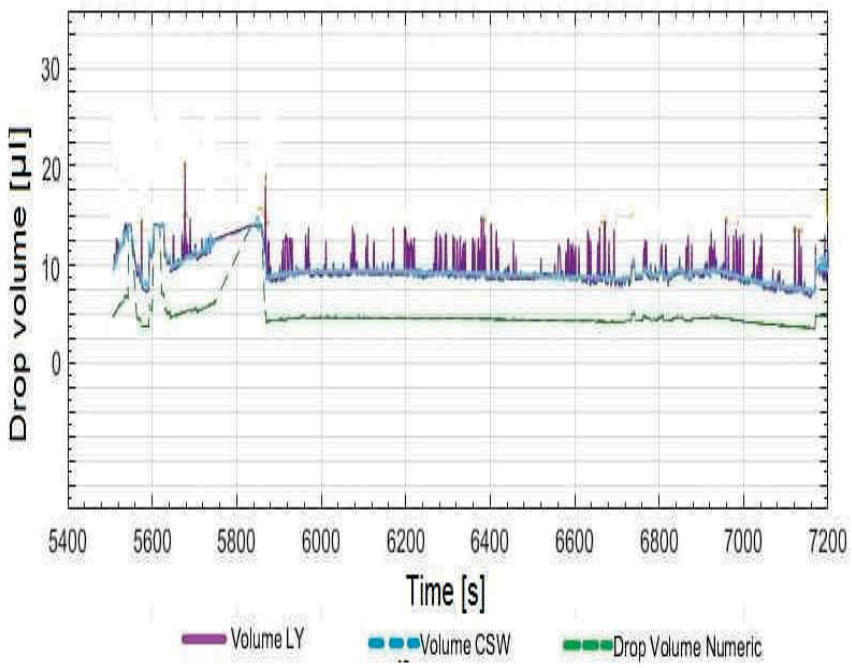

Figure 15: Drop volume measurement of decane at a rotational speed of 3600 min^{-1}.
Measurements on the left spherical end of a droplet

A wide range of obtained values for three interfacial tension modes indicate that the system was probably not at equilibrium when the first measurement was taken in 1.5 hours. And one more reason, that influences the values of interfacial tension with respect to the drop formation time, may be that the selected speed is too low. That is why I repeated the measurements at a higher rotation speed (n). The tests were carried out both with a certain constant rotation speed (n=const), and with a sequential increase in the speed of rotation.
A series of measurements performed with a higher rotational speed of the capillary tube showed a not-so-large discrepancy in the interfacial tension values determined by three methods. The obtained results are depicted in Figure 16. The average of the IFT is 45.5 mN/m.

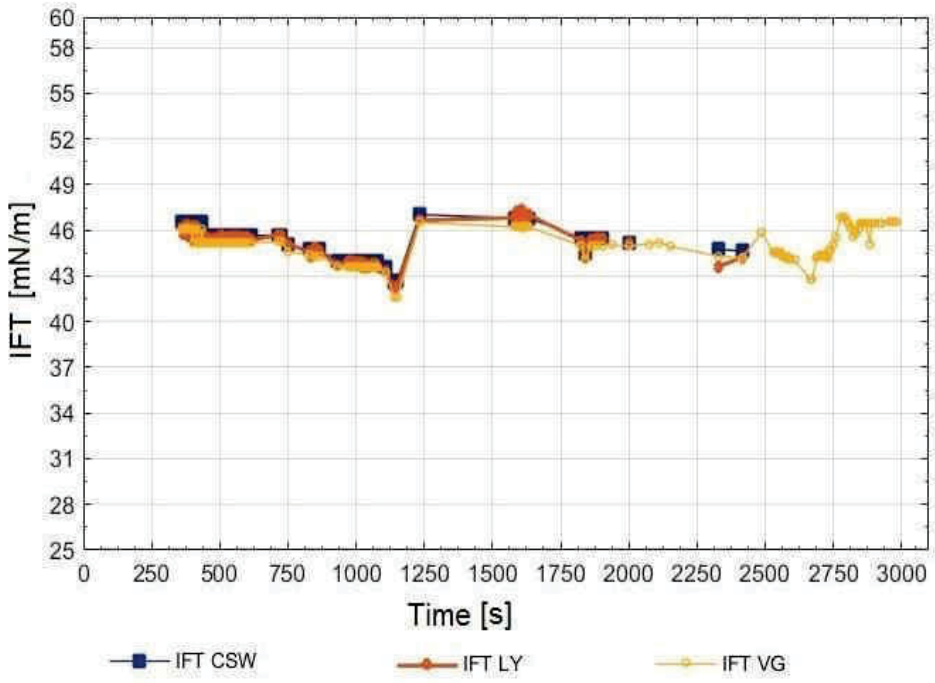

Figure 16: IFT measurement of decane-water at various rotation speeds

From these preliminary tests I realized that the decisive factors that can affect interfacial tension values and the time of drop formation are the dosage of the oil droplet and the chosen rotation speed of measurements.
To understand an effect of the volume of the droplet, I conducted a new series of tests and tried to inject a droplet as little as possible to get more accurate measurements. I injected the decane drop of less than 0.02 ml into the capillary tube. It should be noted, that too small droplets disappear during rotation.
For comparison, the measurements were repeated at different speeds. Figure 17 shows snapshots of a decane droplet in distilled water at various rotational speeds in 30 minutes after the start of rotation.

Figure 17: Snapshots of the spinning drop of decane in water
at the rotation speeds of 3600 min^{-1}, 4500 $min^{-1}$and 6800 min^{-1}

An example of these measurements is shown in Figure 18. The test was carried out at the rotation speed (n) of 5200 min^{-1} on a droplet of a full shape. It can be observed from the figure, that the calculated values of interfacial tension are relatively similar for all three measurement methods and do not show such a large discrepancy, as in the previous experiments. The interfacial tension reached 36-38.5 mN/m.
The measurements performed at higher speeds showed similar values for interfacial tension.

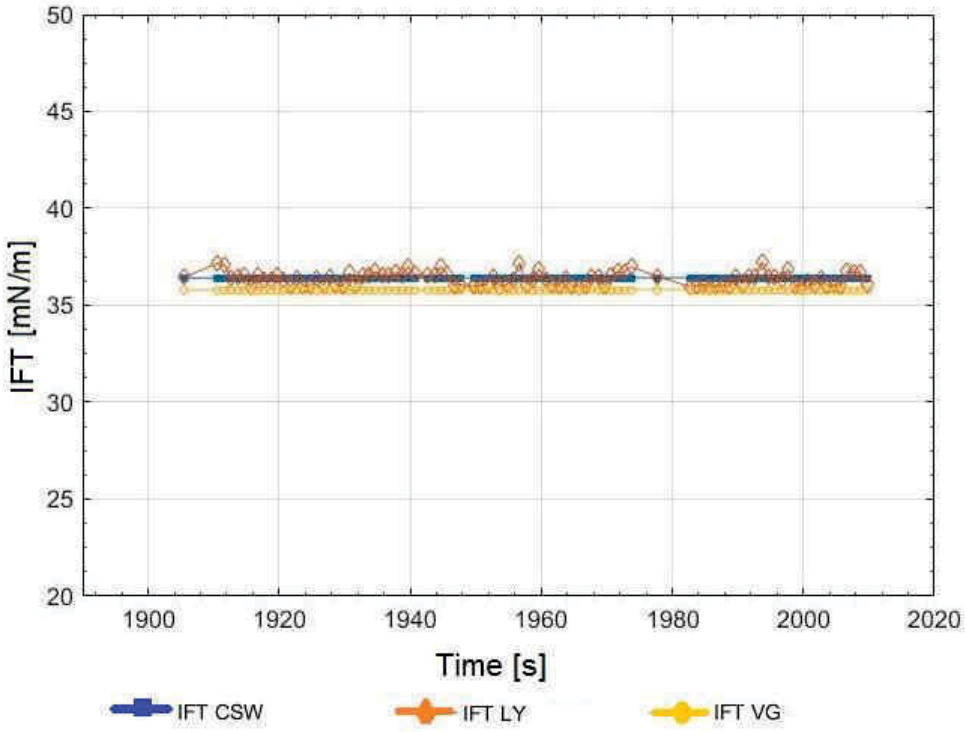

Figure 18: IFT measurement of decane-water with a rotational speed of 5200 min^{-1}.
Measurements on a droplet of a full shape

After a series of tests it became obvious that the selected drop type affects the value of interfacial tension. To get the most accurate and correct results, it is important to always use full drop type, whenever possible.

It can be observed from Figures 19, 20 that interfacial tension values are relatively higher for measurements performed at the spherical ends of the droplet due to a difference in calculation.

In addition, it should be noted that it is very difficult to maintain a more or less constant volume of droplet ends during time measurement, because the drop constantly changes and moves. In this case, I had to manually adjust the frame over the ends of the droplet and fit the ellipse inside the frame to the drop. The constant drop volume for measurements at such procedure is hardly to reach. As a consequence, this leads to fluctuations in the values of interfacial tension. An example of such an error is depicted in Figure 21. Due to the drop elongation, the area marked by the measurement box increases, and as a consequence, the IFTCSW value (blue circles) decreases. On the contrary, interfacial tension, measured by Vonnegut method, is increasing.

Moreover, the selection of the measurement mode determines the availability of the method for calculations. For a droplet with a cylindrical shape with no ends, the calculation of the interfacial tension values can be done only according to the Vonnegut method. This method was applied when the left and right ends of a droplet were invisible, and also for comparing interfacial tension values.

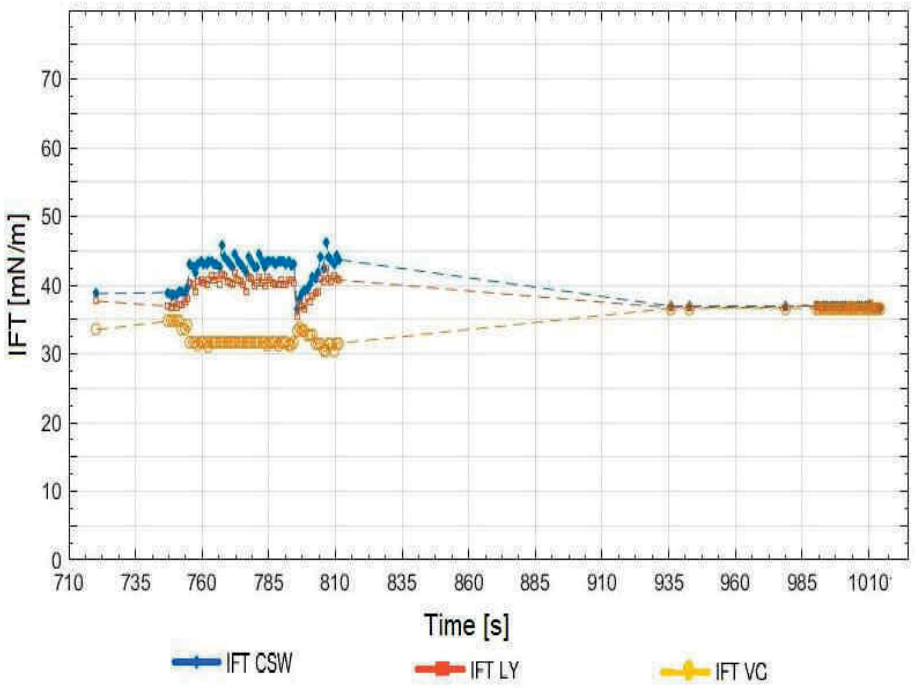

Figure 19: IFT measurement of decane-water with a rotational speed of 5200 min^{-1}. Measurements at the right end and on a full-shape drop

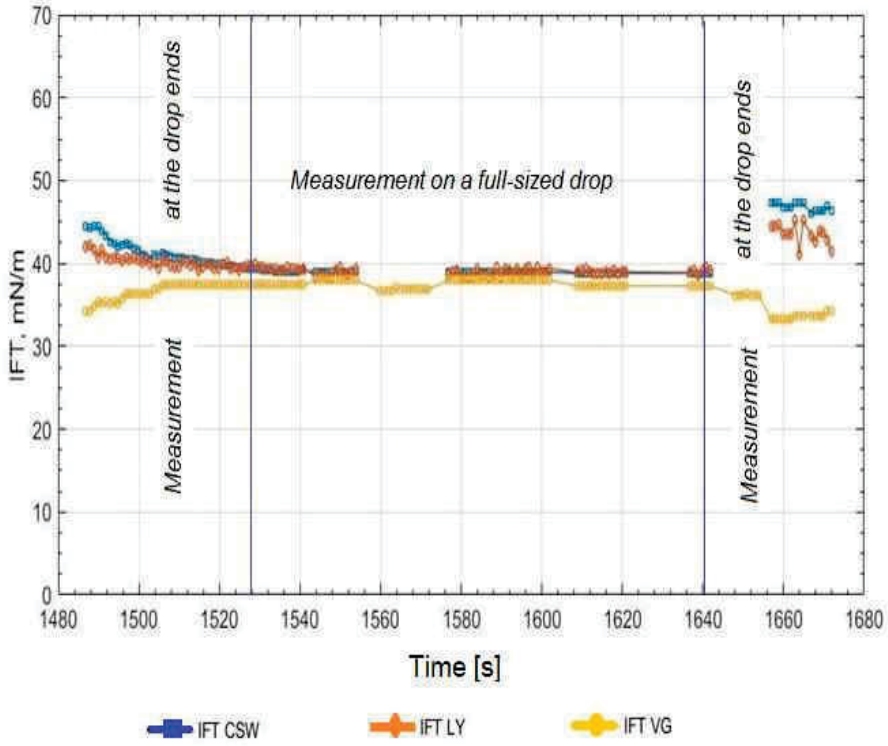

Figure 20: IFT measurement of decane-water with a rotation speed of 5200 min^{-1}. Measurements at the spherical ends and on a full-shape drop

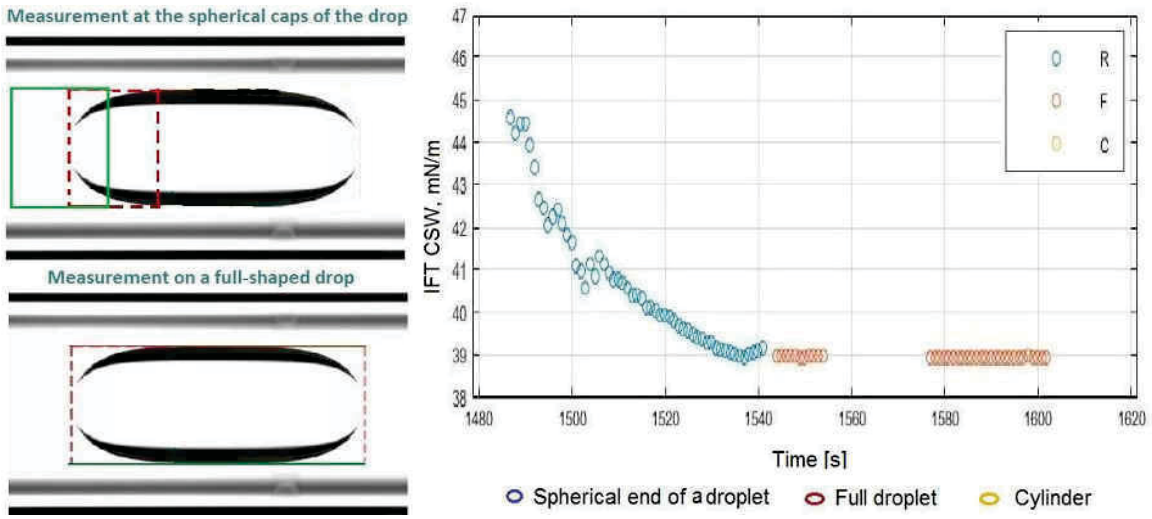

Figure 21: Discrepancy in the IFT CWS measured
on a full-shape droplet and at the spherical ends. Rotational speed- 6700 min^{-1}

Table 2 gives the values of the interfacial tension at room temperature for decane-distilled water system. Measurement was performed on a full-size droplet and at the spherical ends of the droplet.

Table 2: IFT of decane-distilled water, measured on the full-shape droplet and at the spherical ends

Drop Shape	**Drop Volume, μl**						**Measured IFT, mN/m**						**Std. IFT value, mN/m**
	Mean			Std. Dev.			Mean			Std. Dev.			
	CSW	LY	VG	CSW	LY	VG	CSW	LY	VG	CSW	LY	VG	
Full drop	27.79	28.02	27.91	0.06	0.14	0.03	38.96	38.85	37.99	0.007	0.40	0.001	46 [15]
Drop end	20.26	20.10	9.98	3.46	3.74	1.86	40.7	40.01	36.85	1.59	0.72	0.94	

The interfacial tension values measured on a full-shaped droplet are lower than those given in the literature [12], [16], [29]. The maximum standard deviation is 0.4 mN/m for interfacial tension calculated by Laplace-Young method. A set of data from repeated measurements can be said to be precise, since the values are close to each other. However, the absolute value is lower than those given in literature. Therefore, the measurement cannot be considered accurate. Comparison with the values of other published works is even worse.

For measurement conducted at the spherical ends of a droplet, the agreement of my data with the standard value is better. The variation is in an acceptable range for each set of data. The interfacial tension value determined by Vonnegut approach is lower than interfacial tension values measured by LY and CSW methods. The standard deviation is 0.72 mN/m for interfacial tension calculated by Laplace-Young, the maximum standard deviation of 1.59 mN/m is noted for interfacial tension measured by Cayias-Schechter-Wade(CSW) approach. This corresponds to changes in the volume of the droplet. The standard deviation of this parameter is higher than the measured values for interfacial tension measured on the full-shaped droplet. And the average interfacial tension calculated by Vonnegut method differs significantly from the mean interfacial tension values for Cayias and Laplace-Young approaches [31].

The observed discrepancy in the data measured at the ends of the droplet could arise from a systematic error in determining the length and radius of curvature. An example of a variation of interfacial tension with a change in the drop volume (manually selected) is given in Figure 21.

The difference in interfacial tension between the measured and actual values in both sets of data can be explained by impurity of liquids, in particular distilled water. I did not take any additional steps, except a general preparation of the sample for measurement, to ensure the purity of the liquids. The cleaning procedure is described in detail in Section 3.3.6.The purity decane-water system can be achieved by using doubly distilled water or heavy water for the experiments. Such a practice is mentioned in many publications [32]. Goebel et al. (1997) reported a facile method to increase the purity of the decane used for measurement [16]. This method is based on the removal of the surface active solutes.

In addition, a purity grade of 99 wt.% for decane purchased from Sigma-Aldrich is not optimal for the reference experiment and this can also lead to a measurement error.

On the other hand, instrument calibration often addresses a systematic error. But, since the calibration was performed strictly according to the rules and was repeated during the measurements, I eliminate the significant influence of this factor. The most probable cause of errors can be in the process itself.

3.4.2 Effect of temperature

The interfacial tension behaviour between a crude oil and an aqueous surfactant phase as a function of temperature has been studied by many authors [28], [32], [33], [34]. In my study, tthese experiments were done to understand the technique of the forthcoming measurements of oil samples. I performed interfacial tension measurements at temperatures of 25°C - 60°C. The decane and water densities during the measurement were determined by using automatic calculation. The tests were made at the constant rotational speed of 4900 min^{-1}.

It should be pointed out that experiments with brines, surfactants reported in many publications show the decreasing in interfacial tension of decane-water system [35] with an increase in temperature. I can expect to see the similar trend in decane-distilled water system.

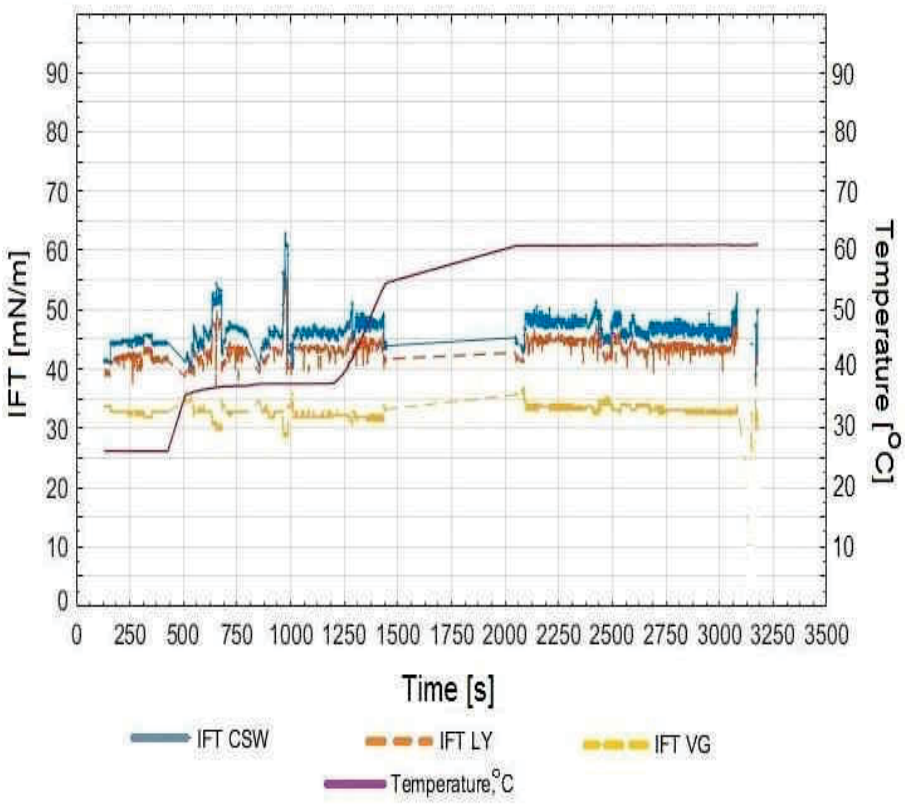

Figure 22: IFT measurement for decane-water at elevated temperatures

As seen in Figure 22, the lowest interfacial tension of 33 mN/m was calculated by using the Vonnegut method. This value is lower than the average IFT value obtained at room temperature of 25°C. But, I obtained higher interfacial tension values calculated by Cayias-Schechter-Wade and Laplace-Young methods. Interfacial tension varies between 45 and 47 mN/m. Therefore, this test requires to be repeated.

3.5 Measurement errors/Problems

1) The measurement of interfacial tension with spinning drop tensiometers is frequently made ambiguous by the appearance of small air bubbles. Careful loading procedures can supress this problem. Air bubbles which do not touch the oil bubble can be ignored if they are small in size.

Air bubles can also appear during heating cycles and during decreasing in the rotational speed, particularly if a tight-fitting septum does not provide a necessary tube sealing during the experiments.

Figures 23 and 24 illustrate the typical mistakes during experiments.

Small air bubbles which enter into the liquid bubble of low density, whose interfacial tension is the point at issue, can frustrate the measument. In my experiments, it often led to a decrease in interfacial tension. Air bubbles can form at high rotation speeds. But they do not cause a change in interfacial tension, since high rotation speed prevents the coalescence of bubbles.

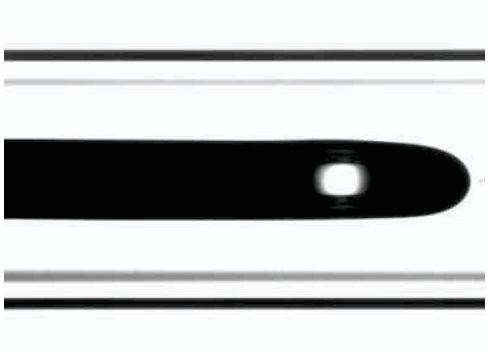

Figure 23: Air bubble in the oil bubble

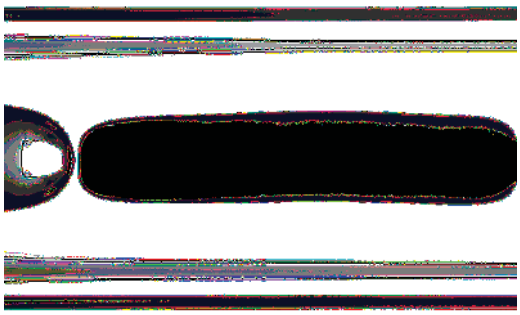

Figure 24: Air and oil bubbles

To discard air bubbles and prevent them touching the oil bubble during experiments, the most optimum procedure is to change the tilt angle. The increase in the rotational speed is associated with a change in interfacial tension value and requires the additional time to reach equilibrium. Therefore this technique is undesirable during the constant-speed measurements.

When air bubbles nevertheless occurred, I got rid of them by quick decreasing and increasing of the rotational speed ($\pm$500 min^{-1}) as in case with satellite droplets. This procedure is more suitable at single IFT measurements.

In case if it was impossible to avoid combining air and oil bubbles, measurements can be done at another spherical end or in the bubble cylindrical part. This method can be used only when the drop is long enough and it is guaranteed that the presence of air bubble does not lead to errors in the calculations.

2) The position of the rotating bubble is very sensitive to gravity. The rotating tube should be leveled to avoid the bubble drift. Vibration and heating can cause the similar effect. Vibration was also noted at the camera movements, especially during oscillating experiments.

To suppress gravity, it is necessary change the tilt deviation between camera and measuring system or to increase the rotational speed (n), but evidently this will not ensure a good result. As was mentioned, the droplet should not be extremely long due to possible fluid dynamical complications.

3) Another issue is the spin up time. Since the droplet during measurements is not centrally located and rigidly secured in the rotating cylinder, time needed for establishing equilibrium interfaces is slow. It depends on viscosity of fluids, drop size, gravity, slow response for the establishing equilibrium interface.
4) In some experiments, the obtained oil bubble was characterized by a rippled surface even at high rotational speed. An example is given in Figure 25.
Such effect was observed, in particularly, for viscous “Crude oil A”. The droplet was too long and had various thicknesses. This resulted in wide scattering of IFT values.
Therefore, it is very important to follow the prescribed procedure and try to get as little droplet as possible.

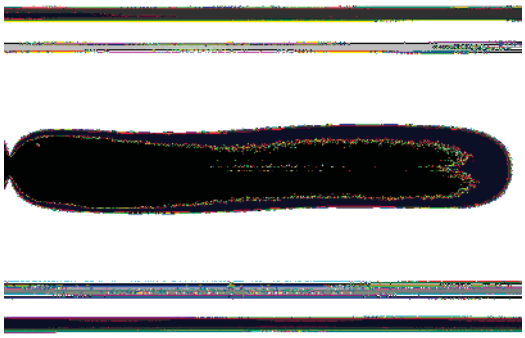

Figure 25: A rotating bubble of oil in distilled water

As already mentioned in the previous chapter, the state of equilibrium is associated with the steady rigid body rotation. The constant diameter of the drop and the optimum rotational speed can be obtained at the equilibrium state and the interfacial tension can be accurately computed.
It is useful to know the types of errors that may occur. We may recognize them and avoid the situation that leads to error. Thus, we reduce as many sources of error as possible.

3.6 SVT measurements

In these measurements, the interfacial tension of oils was calculated using three different approaches: Cayias, Schechter and Wade (CSW), Laplace-Young (LY), and Vonnegut (VG) [23], [36]. A brief description of each method is given in the following sections. Data for the “Crude oil-A” is given as an example for analysis of how different parameters change over time.

3.6.1 Young-Laplace method

The Young-Laplace approach is based on calculating the curvature of the droplet shape. Therefore, this method is the more accurate than Vonnegut's approach. Analysis of the shape of the droplets makes it possible to determine the droplet diameter or curvature.
Princen and others [36] proposed a solution of differential equations that serve to describe and represent the rotating droplet. The method is based on the evaluation of elliptic integrals. The obtained profile data are compared with the theoretical results. This procedure requires a high CPU usage. The results however are quite accurate.
The interfacial tension is given by

$$\sigma = \frac{\Delta d \omega^2 a^3}{2\alpha} \tag{18}$$

σ interfacial tension [mN/m]
d drop diameter [m]
ω angular frequency [rad/s]
a radius at cap [m]
α shape parameter [-]

The shape parameter and the radius at the caps are calculated by a fitting procedure. The rotation speed and the densities must be provided.

3.6.2 Cayias,Schechter and Wade approach - Width and Diameter

Cayias,Schechter and Wade method is based on the use of the width and diameter of a spinning drop. By means of these two parameters the entire shape of the measured droplet is determined. The basis for calculations proposed by Cayiaset al. is the same theory ofPrincen that was used in Laplace-Young fit. The inability to measure the shape factor αin this method reduces the accuracy of measurements in comparison with the more perfect Laplace-Young approach. Interfacial tension is given by the same formula

$$\sigma = \frac{\Delta d \omega^2 a^3}{2\alpha} \tag{19}$$

σ interfacial tension [mN/m]
d drop diameter [m]

ω angular frequency [rad/s]
a radius at cap [m]
α shape parameter [-]

An iterative procedure is used to estimate the shape parameterα and radius parameter at the spherical caps. In this approach, only the maximum elongation of droplets in the horizontal and vertical direction is used for calculations. Most of the profile data is negligible and not taken into account. This distinguishes this method from Laplace-Young approach.

3.6.3 Vonnegut's approximation – Diameter

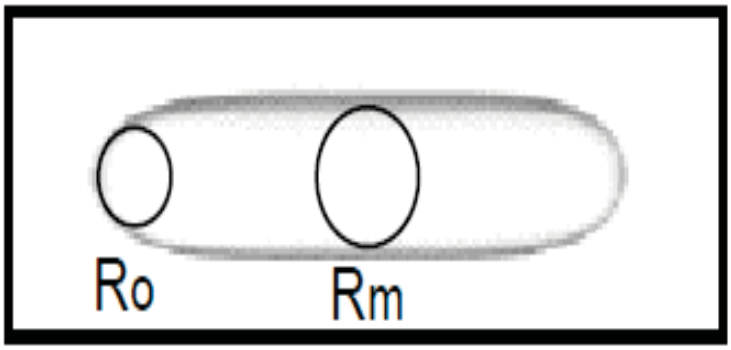

Figure 26: "Cylindrical" elongated drop curvature radii
in Vonnegut's approximation case [37, p.3]

In Vonnegut (VG) the limit is controlled by the ratio of the width to the diameter. For the ratio greater than 4, the droplet is assumed to be of cylindrical shape with spherical ends.
The interfacial tension is given by empirical formula

$$\sigma = \frac{\Delta d \varpi^2 y_0^3}{4} \qquad (20)$$

σ interfacial tension [mN/m]
d drop diameter [m]
ω angular frequency[rad/s]

3.6.4 Relationship between parameters calculated by different IFT approaches for "Crude oil A"

Here, I show the relationship between parameters calculated by different approaches. As an example, "Crude oil A" oil was taken. The measurement was performed on a full-sized droplet at a rotational speed (n) of 4100 min^{-1}. The volume of the droplet is about 6.7 μl.

The droplet had a smooth spherical shape and, thus, the condition of a fixed curvature of the droplet was satisfied, as required by Laplace-Young approach. In the previous section it was shown that a droplet can have a ripple surface. This effect was frequently observed in the measurement of the“Crude oil A”. In this situation, the liquid interface is not flat and has an anisotropic curvature. It becomes obvious that it is no longer possible for such droplet to satisfy a uniform contact angle along the contact line.

Figure 27 shows the interfacial tension distribution and the radius of curvature on a flat interface of a full-sized droplet. The distribution function shows a characteristic decrease in interfacial tension over time, which corresponds to a decrease in the drop curvature radius.

As the curvature radius at apex Laplace-Young curve decreases, fluctuations in the volume of the droplet increase. It can be clearly seen in Figure 28. The observed changes can be ascribed to the elongation of the droplet.

The interfacial tension decreases from 3.6 mN/m to 0.9 mN/m, whereas the curvature radius decreases from 0.69 mm to 0.43 mm in 6000 seconds. As mentioned above, most of the profile data is used for calculation at the Laplace-Young fit.

Figure 29 illustrates the changes in curvature radius versus surface area of the droplet for the“Crude oil-1”. In contrast to the interfacial tension, the distribution of the surface area strongly corresponds to the interfacial tension distribution in accordance with theoretical predictions.

In this experiment, the surface area changes from 18 mm^2 to 23.9 mm^2; the variation in the values of the surface area in time increases slightly. The range of the curvature radius is 0.3 mm. The corresponding change in interfacial tension is 3 mN/m.

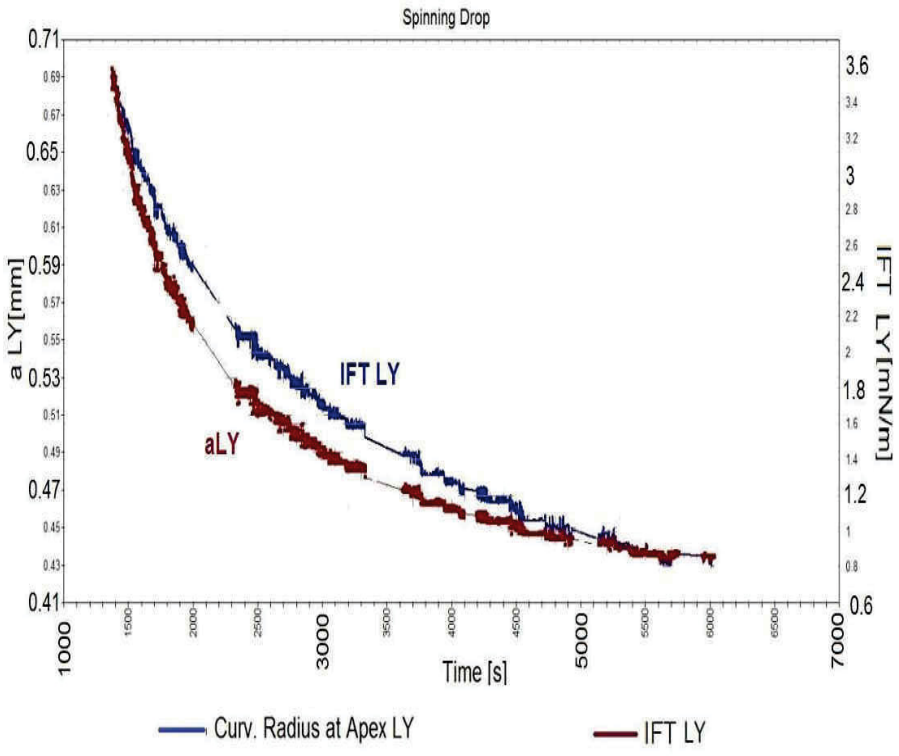

Figure 27: IFT LY and curvature radius LY versus time for “Crude oil A”

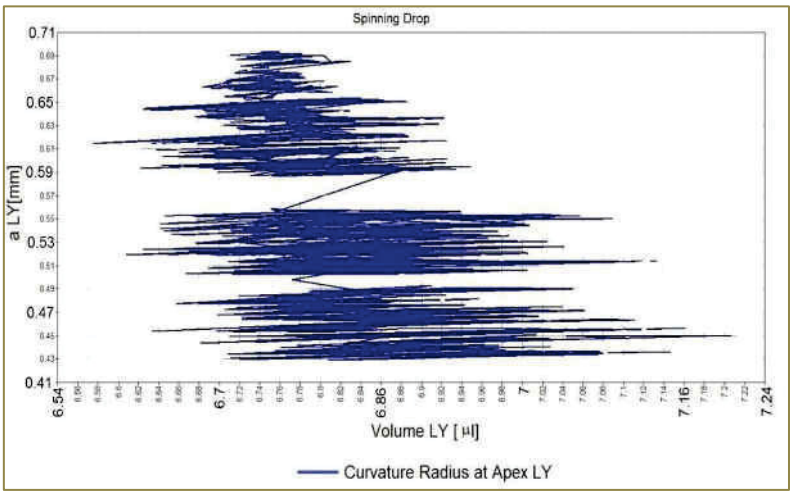

Figure 28: Curvature radius LY versus volume LY of droplet for “Crude oil A”

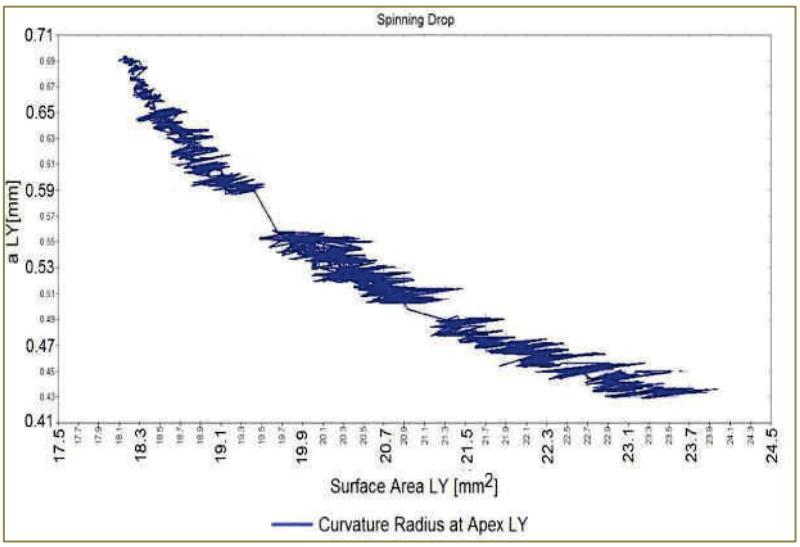

Figure 29: Curvature radius versus surface area of droplet for “Crude oil A”

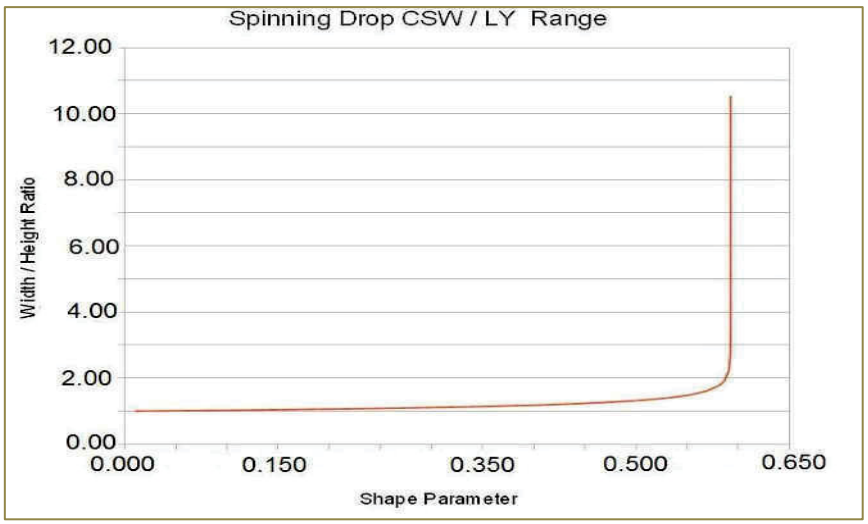

Figure 30: Shape parameter of droplet versus Width/Height Ratio [38]

Another important parameter for spinning drop measurement is the shape parameter, which is calculated by a fitting procedure.

As known from theoretical findings, the shape parameter ranges from 0 to 16/27. Towards 0 the interfacial tension rises to infinity. At a width to height ratio of 4 the shape parameter differs from 16/27 by less than 0.0000001. As can be seen from Figure 30, above this ratio the shape of the drop cannot be numerically estimated with the theoretical expressions

It can be seen in Figure 31 that the shape parameter in the experiment with “Crude oil A” varies from 0.58 to 0.592, reaching a peak in about 2400 sec, and then remains constant. This means that the droplet has reached certain stabilization within 30 minutes.

As shown in Figure 31, the shape parameters, calculated using the Laplace-Young and Cayias-Schechter-Wade approaches (**eq.18**), are identical.

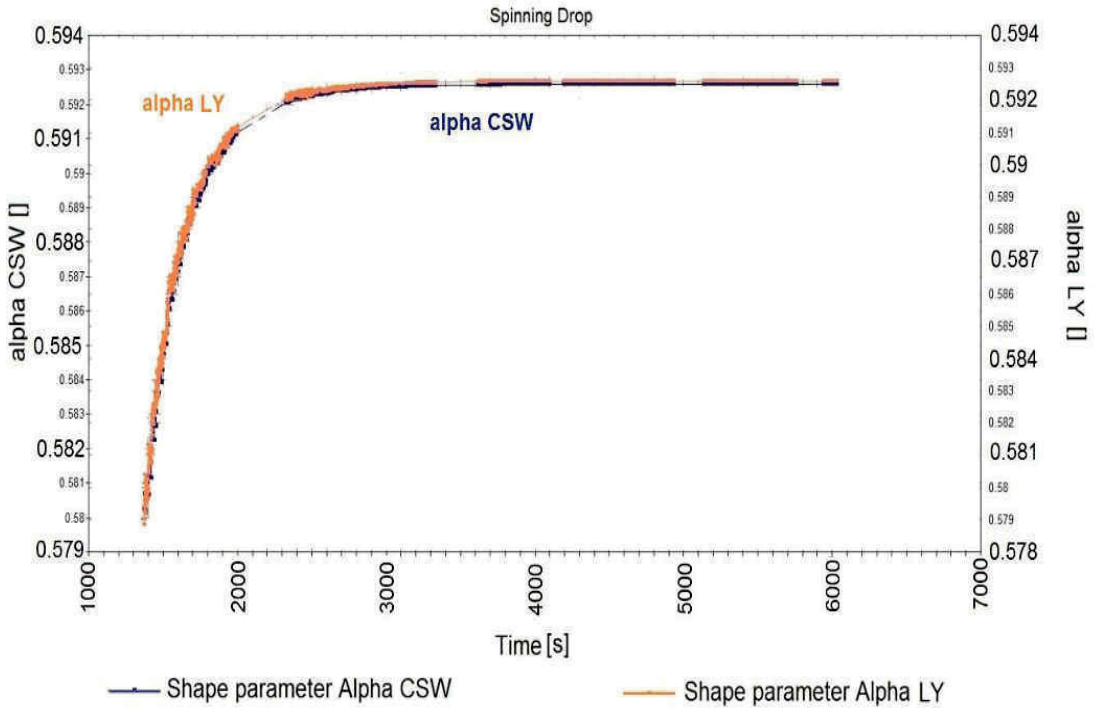

Figure 31: Shape parameters CSW and LY as a function of time. “Crude oil A”

Figure 32 shows that the peak in the shape parameter corresponds to a horizontal drop diameter of 4.2 mm and a vertical diameter of 1.65 mm.

The distribution in the interfacial tension and drop surface area for a full-size droplet is depicted in Figures 33 and 34. The value of interfacial tension at the moment when the shape parameter reaches its maximum is 1.9 mN/m. It is obvious that a decrease in interfacial tension corresponds to the increase of surface area.

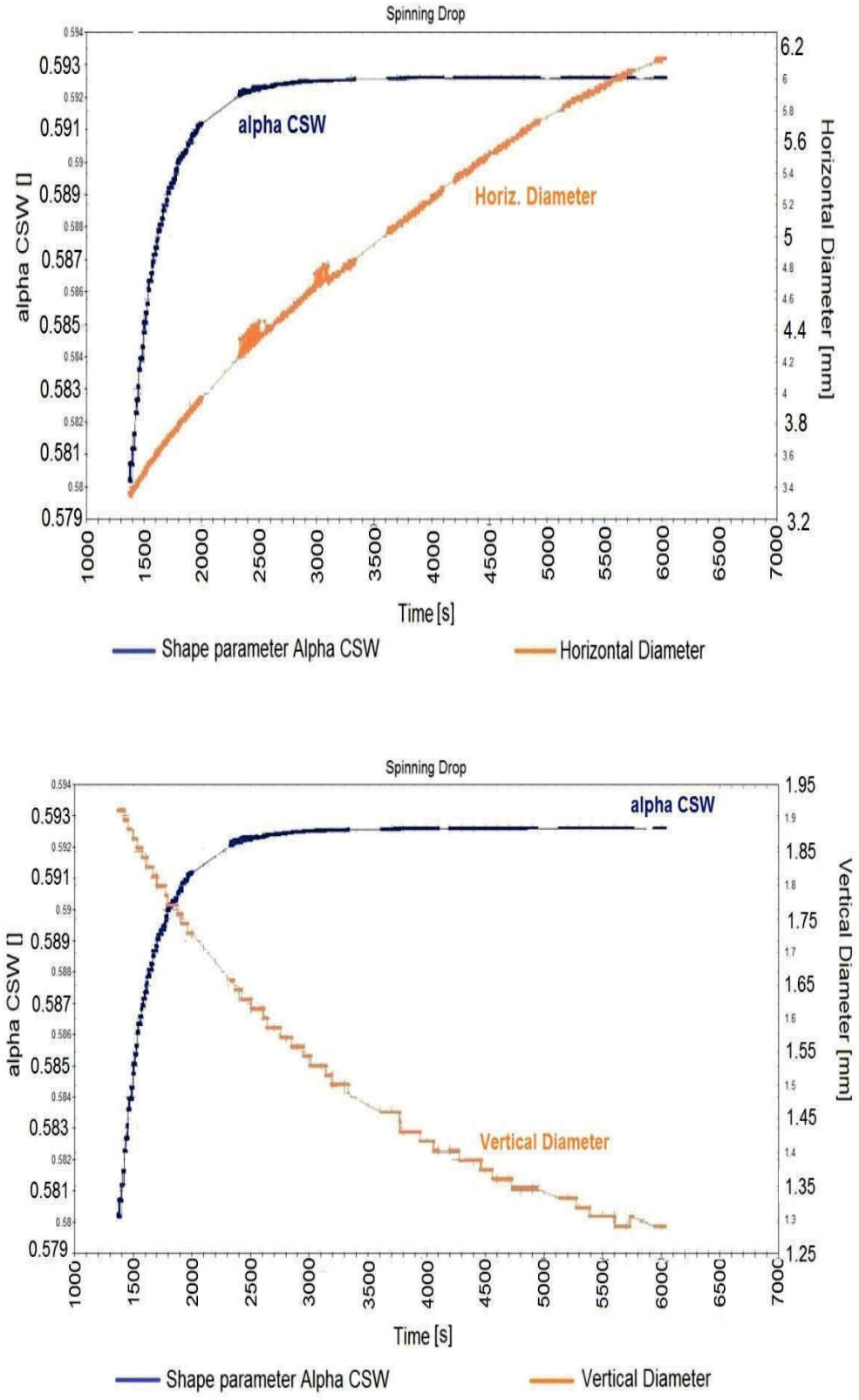

Figure 32: Shape parameter CSW and horizontal/vertical diameters as a function of time. "Crude oil A"

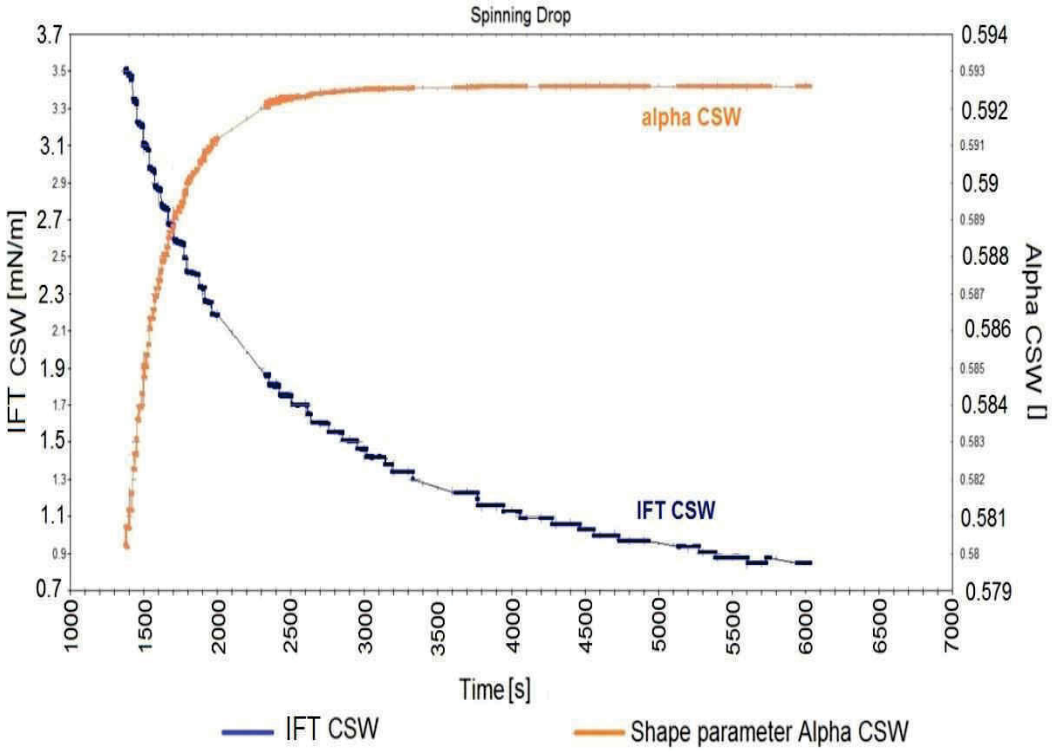

Figure 33: IFT and shape parameter as a function of time. “Crude oil A”

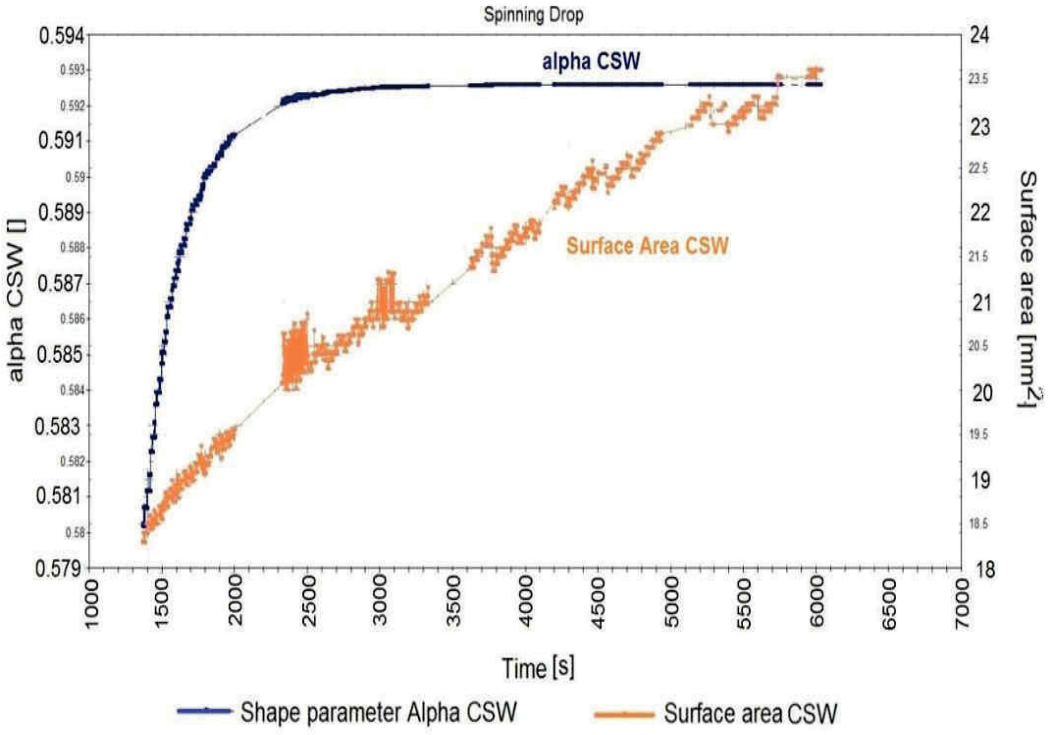

Figure 34: Surface area/shape parameter as a function of time. “Crude oil A”.

4 Oil-water interfacial tension

For all examined oil samples, the droplets had very smooth surfaces and, as predicted by the theory, were elongated along the horizontal axis of rotation with increasing speed of rotation. Due to the lack of data on the chemical composition and properties of the available oil samples, the measurement procedure for each individual oil sample was determined by trial and error. Repeated measurements were conducted at various speeds.

4.1 Crude oil B

I started the experiment by injecting a small drop of oil about 0.01-0.02 ml into the water inside the rotating tube. The temperature was maintained at 25°C, as with standard measurements. Since the sample does not have a high viscosity, this procedure did not cause any special difficulties. Despite the initial ease, it turned out that it is quite difficult to achieve an elongation of the drop to the size required for measurements. An increase in the rotational speed and in pre-run measurement time did not always lead to the desired result. I decided to inject the drop of larger volume.

The first test was carried out at different rotational speeds to understand the behavior of the oil sample and obtain preliminary interfacial tension values. The measurement was started in 1 hour and lasted approximately the same time interval. The test did not show a wide change in interfacial tension with the drop formation time. The average interfacial tension values are about 12-16 mN/m. Measurements were performed with a full-shape droplet. It was noted that interfacial tension slightly increases with a gradual increase in the rotational speed (Figure 35). As can be seen in the figure, the difference between interfacial tension values measured at the low rotational speed of 4400 min^{-1} and the high speed of 6000 min^{-1} is only 2 mN/m.

Measurements at spherical ends and in the cylindrical part of the droplet showed a variance in interfacial tension values. A dominant feature is a variation of the measured volume at the spherical ends of a drop, as was previously noted for the decane-water system. At the high speeds, the droplets inside the capillary tube merged into one single drop and I stopped measurements.

Since I did not have any information about a timescale during which the oil-water system reaches equilibrium, I conducted a long-time measurement. Results are illustrated in Figure 36. The test was carried out with a full-shape droplet at a rotational speed of 5500 min^{-1} to reach the required elongation of the drop. The experiment was carried out over 19.5 hours.

Measurements were started after 25 minutes after beginning the rotation and showed the interfacial tension about 15 mN/m. There is no large discrepancy in interfacial tension values calculated by different methods. A clear decrease in interfacial tension is observed with surface age, interfacial tension reduces from 15 mN/m to 13 mN/m and reached about 12 mN/m in 1.7 hours. Droplet interfacial tension reached an approximately constant value in 4 hours and more than 15 hours remained relatively unchanged. At the end of the test, the interfacial tension value was 11.9 mN/m.

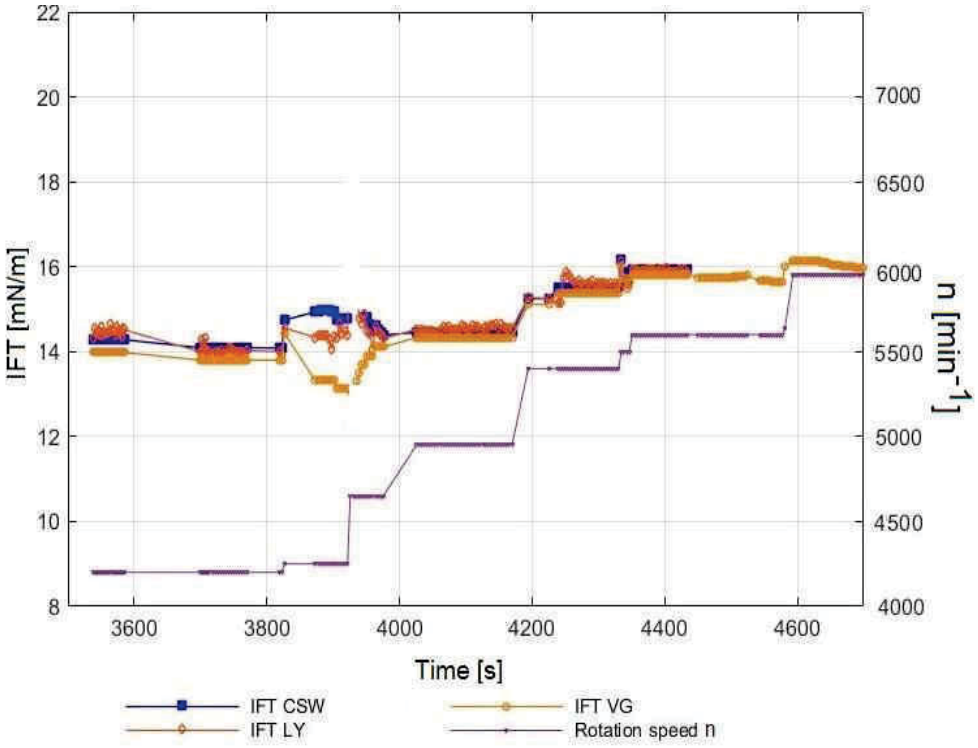

Figure 35: IFT measurement of “Crude oil B”- water
with different rotation speeds

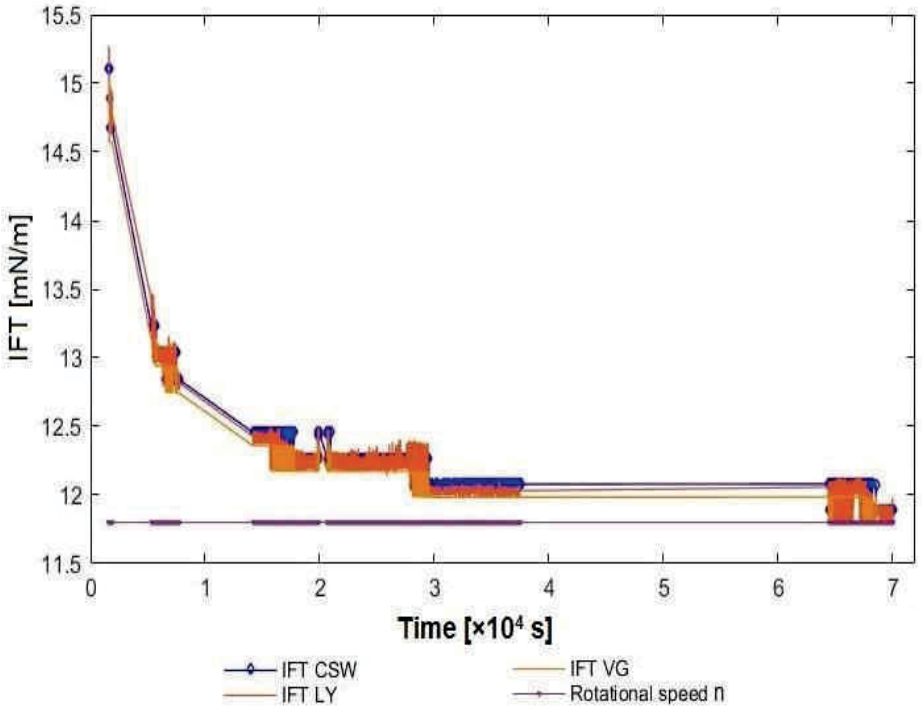

Figure 36: A long-time IFT measurement of “Crude oil B”-water
with a rotational speed of 5500 min^{-1}

As can be seen from Figure 37, fluctuations in the drop volume over time decrease. As can be observed in Figure 38, the surface area increases sharply in the first 500 seconds of an experiment and then the change over time goes much slower.
This can be explained by the quick drop elongation at the moment when we start rotation. The stabilization in the surface area along with the interfacial tension data can be an indicator that the oil drop reached equilibrium.

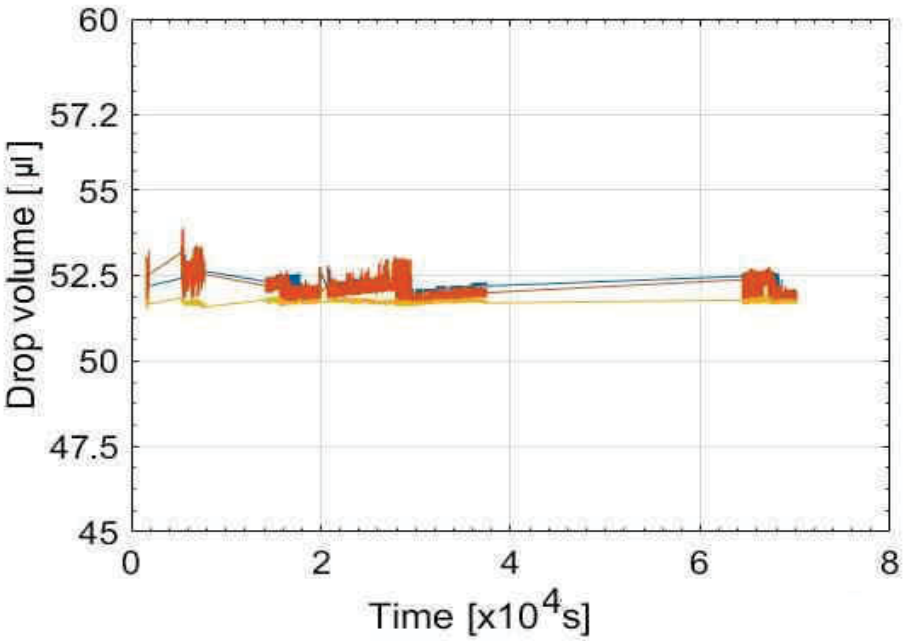

Figure 37: Drop volume vs. time. “Crude oil B”. Rotational speed - 5500 min^{-1}

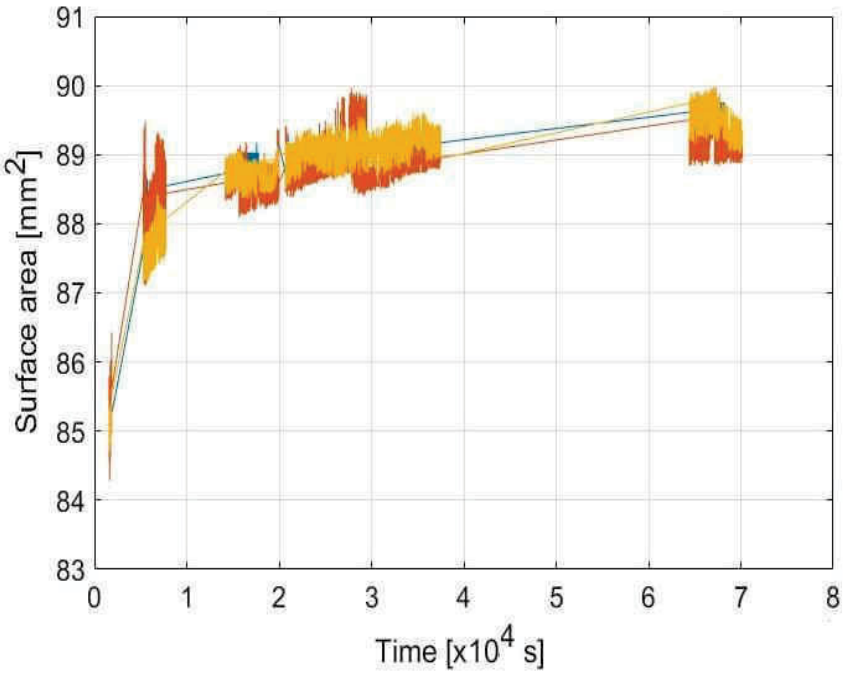

Figure 38: Surface area of the oil drop vs. time. “Crude oil B”. Rotational speed – 5500 min^{-1}

A test measurement with higher speeds and elevated temperatures of 30-38°C was performed to understand the behavior of the “Crude oil B”. The oil droplet of smaller volume was injected in the capillary tube. The drop volume is 20-22 µl, the surface area changes during an experiment between 40 and 48 mm^2. Additionally, I achieved the better elongation of the drop to the size required for measurement. The obtained results showed an increase in the interfacial tension values, as depicted in Figure 39. The comparison with the interfacial tension data, measured in the test carried out with high speeds and room temperature, allows assuming that the observed increase in interfacial tension values to 20-23 mN/m is the response to an increase in temperature. As in the previous test, the similar trend in the interfacial tension distribution was observed. Interfacial tension at time t=500 sec is about 26 mN/m. As the oil droplet elongates, the interfacial tension decreases and drop interfacial tension relaxes to an approximately constant value around 19.5 mN/m in about 2000 sec after starting rotation. Then the interfacial tension has remained stable for long time.

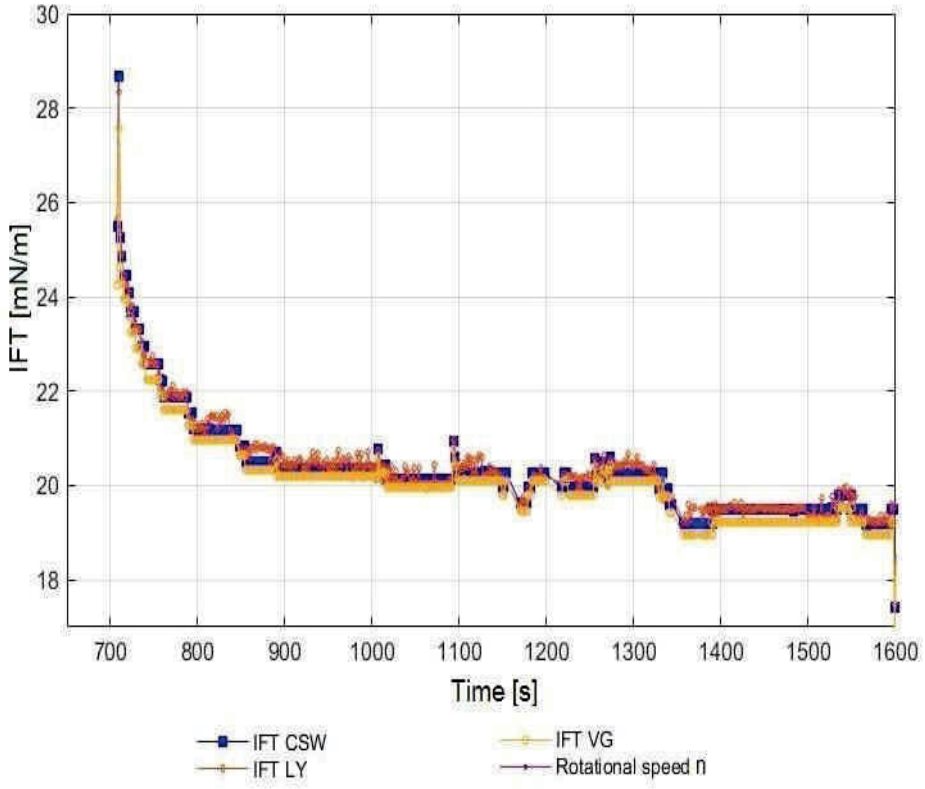

Figure 39: IFT measurement of “Crude oil B”- water at high temperatures

As mentioned in the previous chapters, the required rotational speed for interfacial tension measurements depends on the density difference between the outer and inner phases. The recommended range, mentioned in various publications, varies between 3000 and 6000 min^{-1}. I conducted a series of measurements with different rotational speeds of the capillary tube. The change in interfacial tension with the drop formation time for the “Crude oil B” in distilled water is shown in Figure 40. Measurement, performed at a rotational speed of 4300 min^{-1}, is

given as an example. Test was started after 20 minutes after beginning the rotation. The initial interfacial tension is about 18.5-19.5 mN/m. Measurement was carried out on a full-size drop. A decrease in interfacial tension is observed with surface age, interfacial tension reduces from 19.5mN/m to 16 mN/m in 250 seconds.

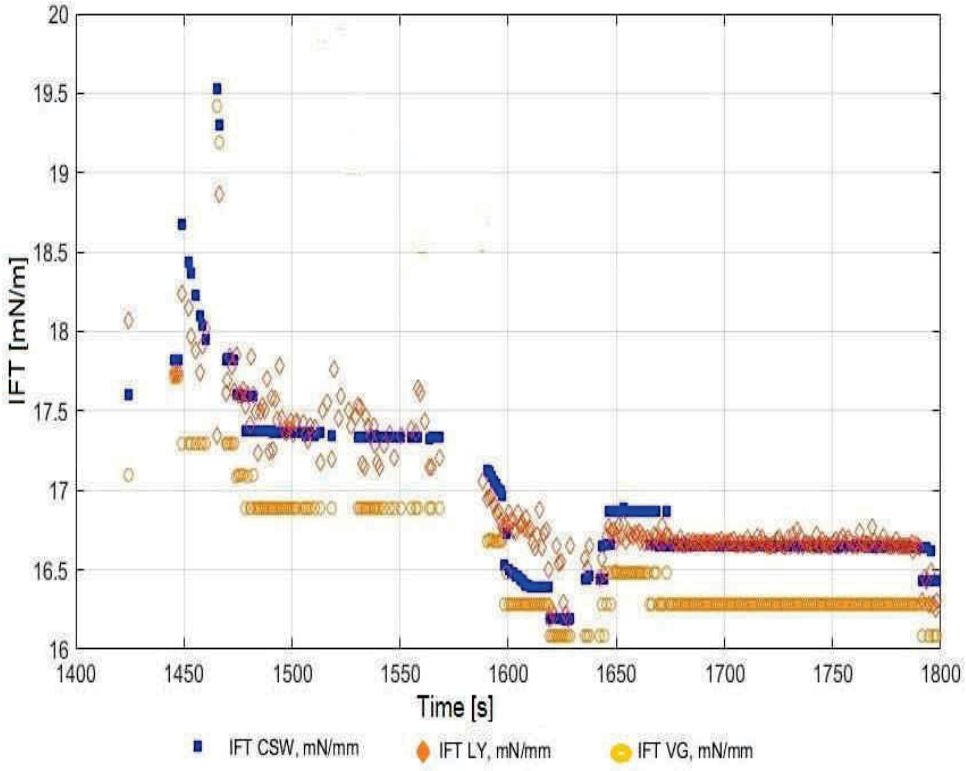

Figure 40: IFT measurement of “Crude oil B”-water with a rotational speed of 4300 min^{-1}

The long-time measurement was carried out with the rotational speed of 5800 min^{-1}. The average IFT CWS value is about 14.4 mN/m. The mean of the IFT LY and IFT VG values are 13.78 and 12.89 mN/m, respectively.

As can be seen in Figure 41, a clear decrease in interfacial tension was observed with surface age. The initial interfacial tension values are 20-23 mN/m. There is large discrepancy in the interfacial tension data in the first 30 minutes. After this point, the variation in the interfacial tension decreases. The oil-water system reaches equilibrium in 1.94 hours. The interfacial tension distribution is nearly linear and remains constant. The interfacial tension reaches 12.5-13 mN/m.

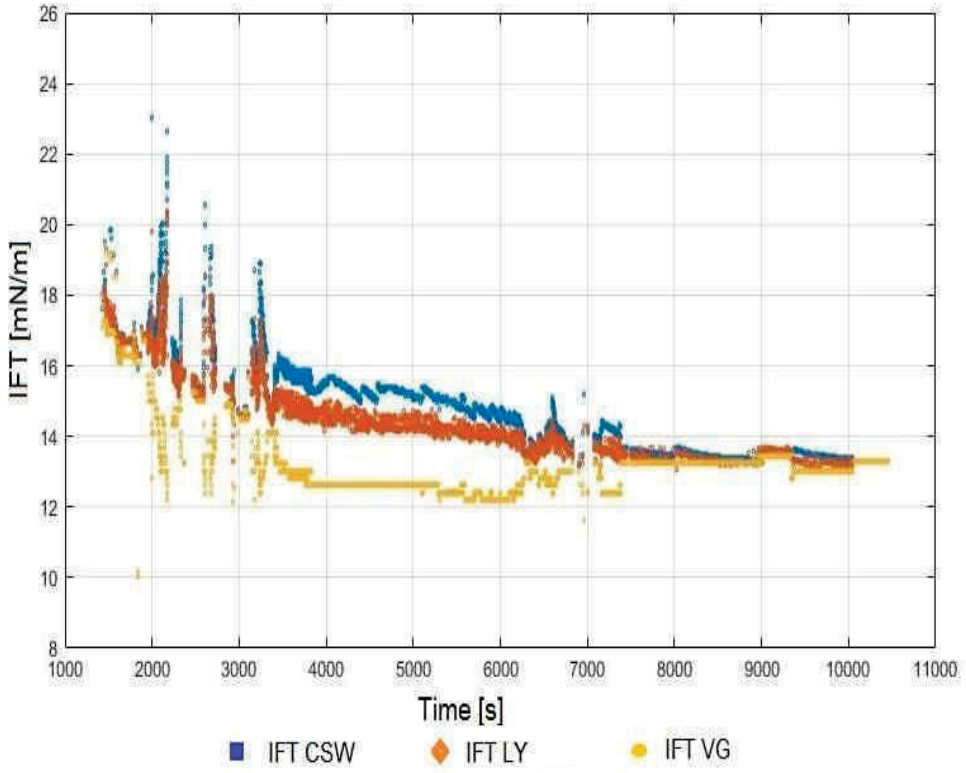

Figure 41: IFT measurement of “Crude oil B”- water with a rotational speed of 5800 min^{-1}

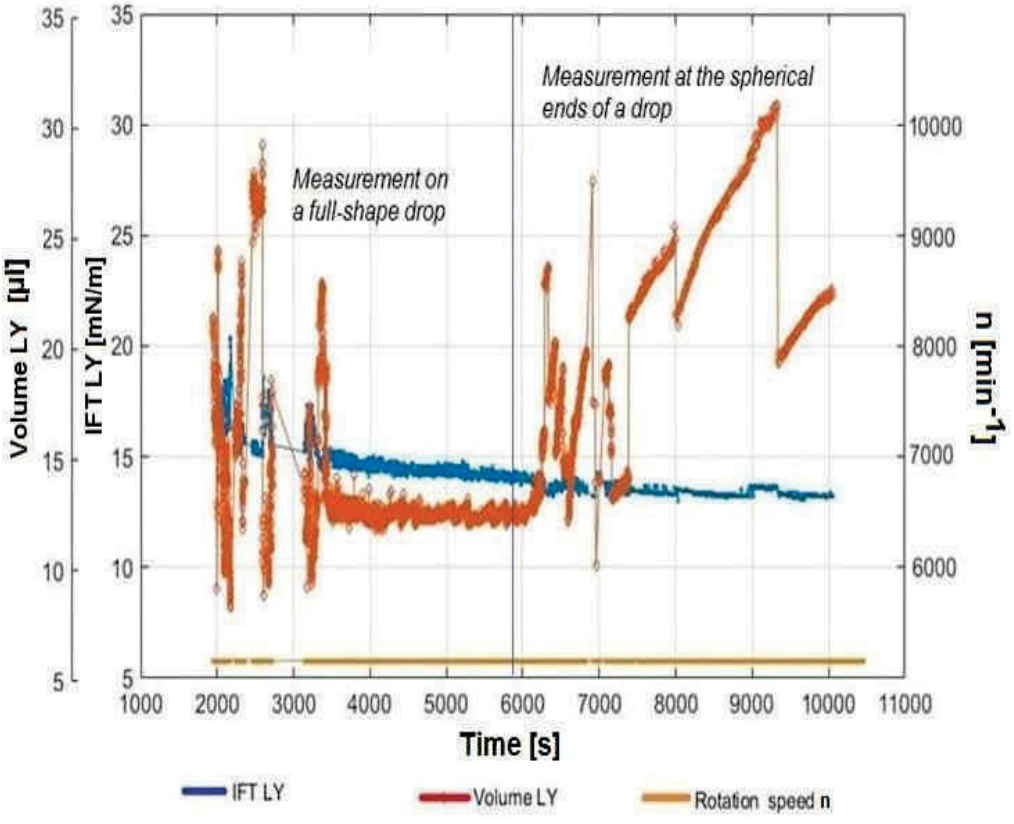

Figure 42: IFT LY, drop volume LY vs. time. “Crude oil B”. Rotational speed - 5800 min^{-1}

Figure 42 illustrates the changes in these parameters over time. It should be noted that the behavior of the interfacial tension is consistent with changes in the volume of droplet. It is most obvious after reaching the time interval of 6000 sec and once again confirms that the equilibrated state was achieved. After the system reached equilibrium, measurements performed both on a full-size droplet and at the ends of drop show the same interfacial tension.

4.2 Crude oil C

As in case of the previous oil sample, systematic trends in the variation of the interfacial tension are observed for “Crude oil C”. Visual analyses and available data on physical properties allowed me to assume that the viscosity of oil is not so high. The injected volume of oil phase varied between 0.2 and 3 ml, since the interfacial tension was initially unknown. Problems that arise during the oil injection were described in the previous chapter.

The primary results were the interfacial tension ranging over 6 and 7.5 mN/m. It is interesting that all the obtained interfacial tension curves followed the same behavior. First, the IFT reduces with starting rotation and then, reaching a certain minimum, begins to increase.

Figure 43 shows the behavior diagram of the IFT of “Crude oil C” in a distilled water system. As can be seen, a well-defined minimum is observed during the first seconds of the experiment.

I conducted long-time measurements at the rotation speed of 4200 min^{-1}. The drop stabilized very quickly during the first 15-30 minutes; sometimes the droplet had a rippled surface. The IFT increased from approximately 4.7 mN/m to 5.5 mN/m for 4 hours.

The first long-term test was continued for 12 hours and the next morning the IFT was also measured. There was a slight increase in the IFT to 7 mN/m, but this can also be explained by the merging of small droplets.

It is should be noted, that standard IFT measurements do not require such a long time. But they were conducted to check whether the IFT will remain constant for such a long period. Perhaps, understanding the IFT behavior would be useful for the subsequent measurements in the surfactant-oil system.

Second test was conducted with a smaller volume of the injected oil drop. The obtained results are presented in Figure 44. The measurements were performed on a full-size droplet. The drop volume was 23.5-24 μl. The surface area is around 50 mm^2. The rotational speed was chosen 3900 min^{-1} to see the changes of the drop more clearly. It was observed that in the first 10 minutes the drop elongated along the horizontal diameter and then contracted at the constant drop volume. This moment corresponds to a minimum in the IFT at the beginning of each experiment.

The obtained data show the same trend as in the previous test. The initial IFT value is 6.9 mN/m. The minimum in the IFT was reached after 30 minutes and was around 5 mN/m. Then the IFT started to rise up and reached a temporary plateau in 50 min from the beginning of the experiment. At this stage the IFT value approaches close to 6.2 mN/m and then remains constant.

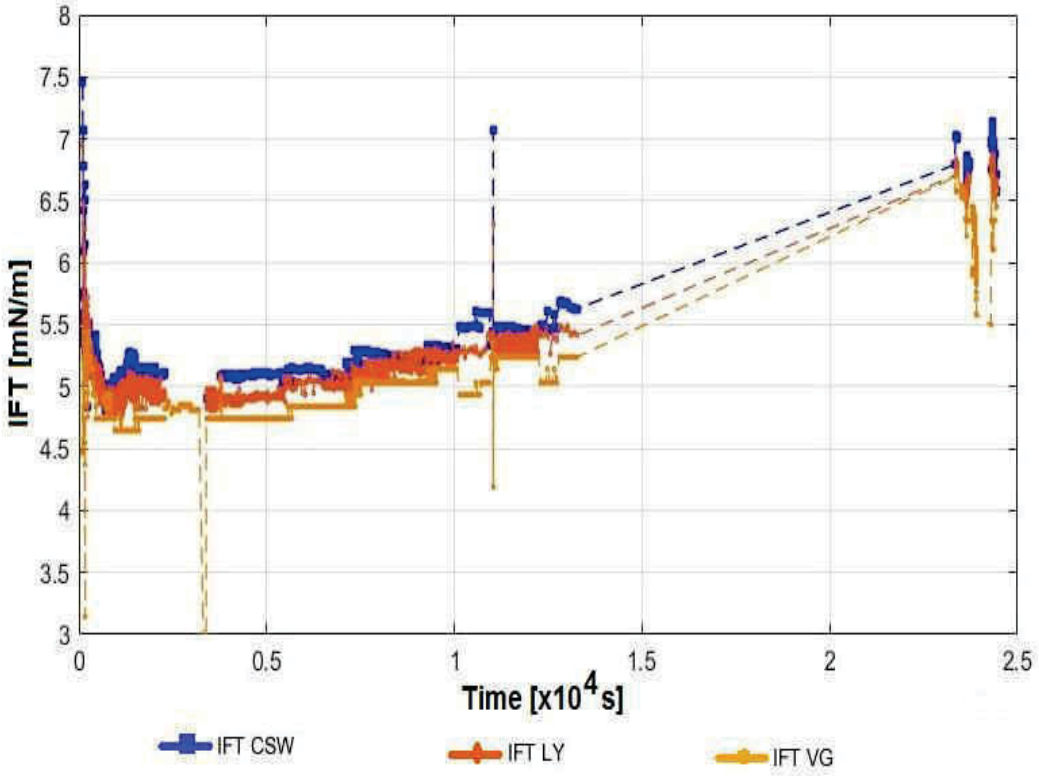

Figure 43: IFT long-time measurement of “Crude oil C”-water with a rotational speed of 4200 min^{-1}. Measurements at spherical ends (L) of a droplet

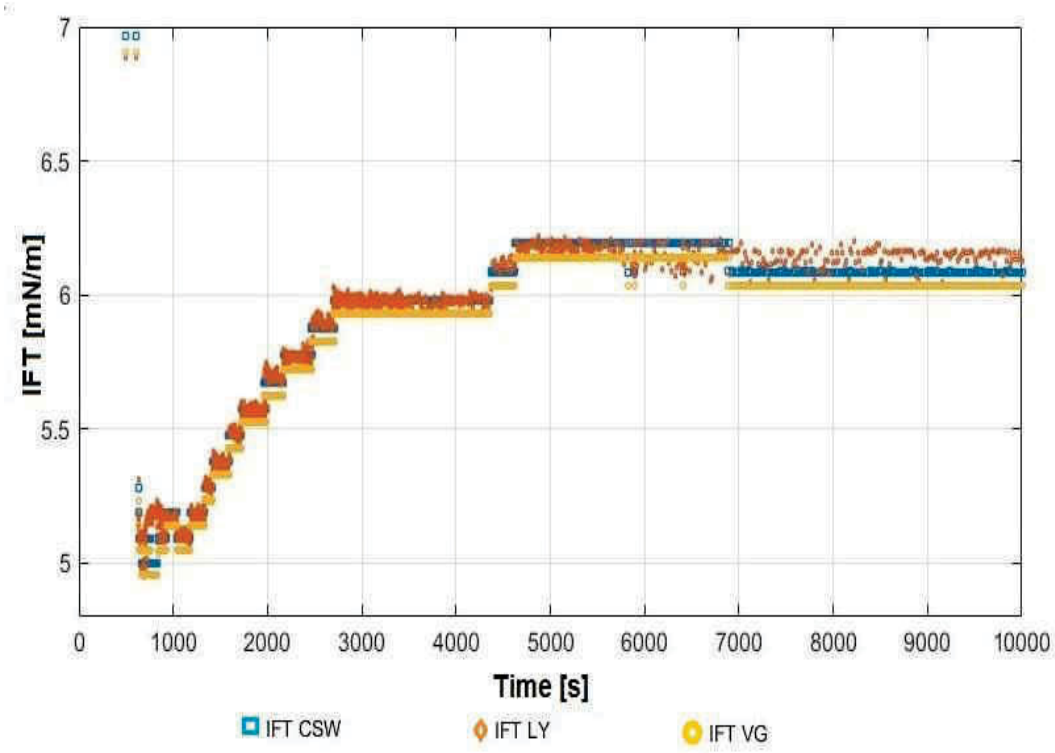

Figure 44: IFT long-time measurement of “Crude oil C”– water with a rotational speed of 3900 min^{-1}

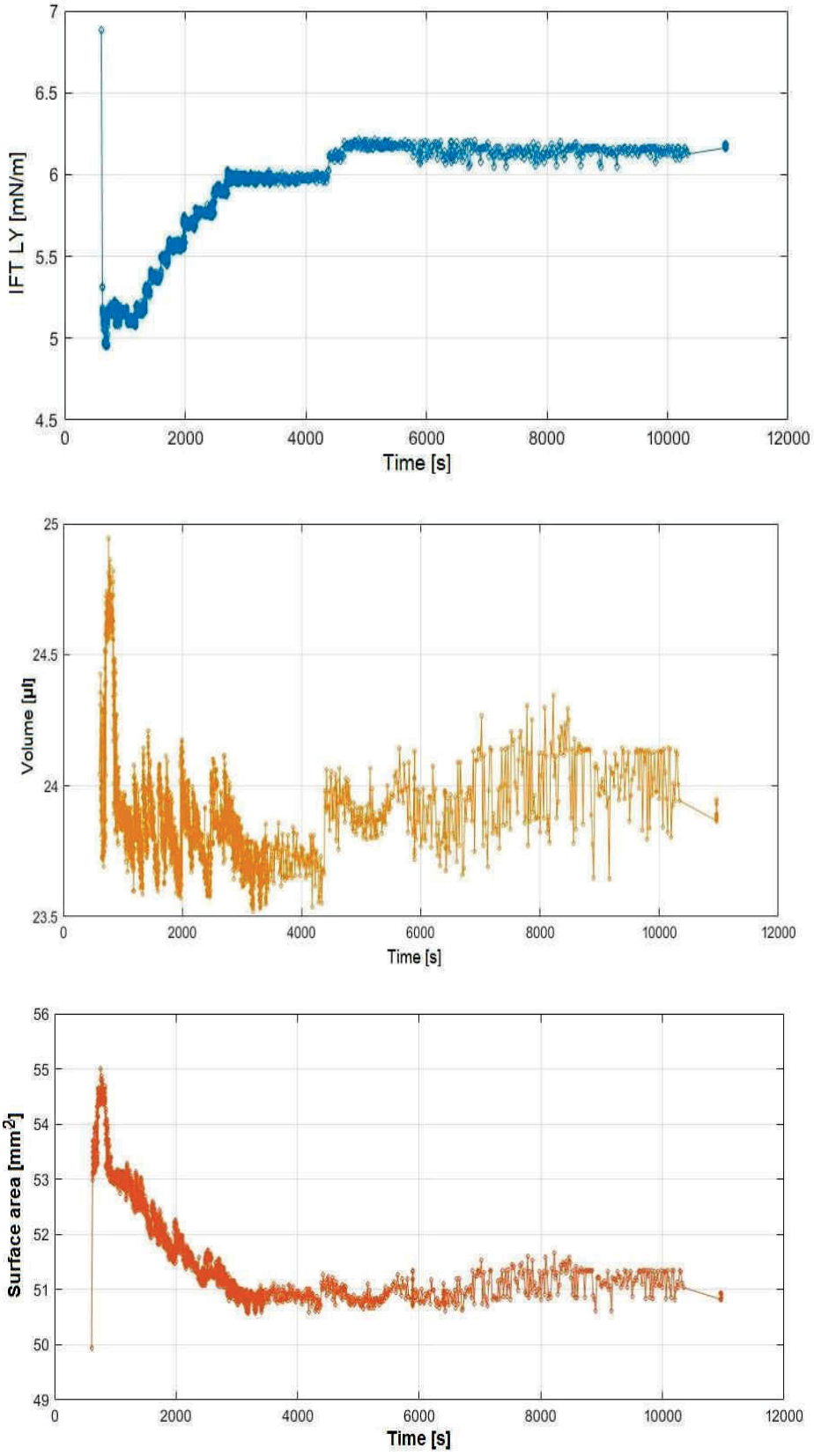

Figure 45: IFT LY, drop volume and surface area versus time.
Long-time measurement of “Crude oil C”- water with a rotational speed of 3900 min^{-1}

The observed interfacial tension distribution can be explained by the changes in the drop volume. As can be seen in Figure 46, it is easy to note that the range of fluctuations of the drop volume is larger for the low interfacial tension values. It corresponds to the minimum peak in the interfacial tension trend. I also assume that it relates to the larger amplitude of the drop motion at the beginning of the test.

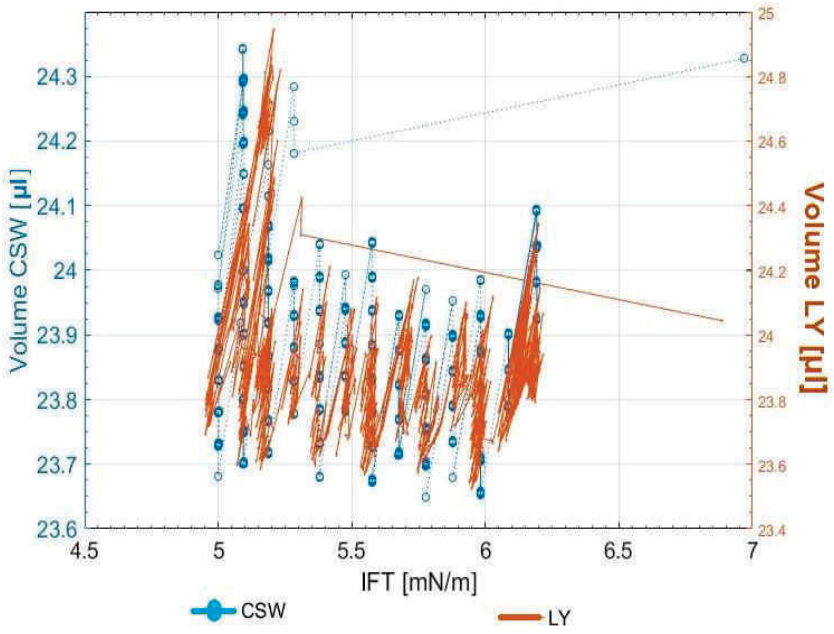

Figure 46: Volume versus IFT. “Crude oil C”

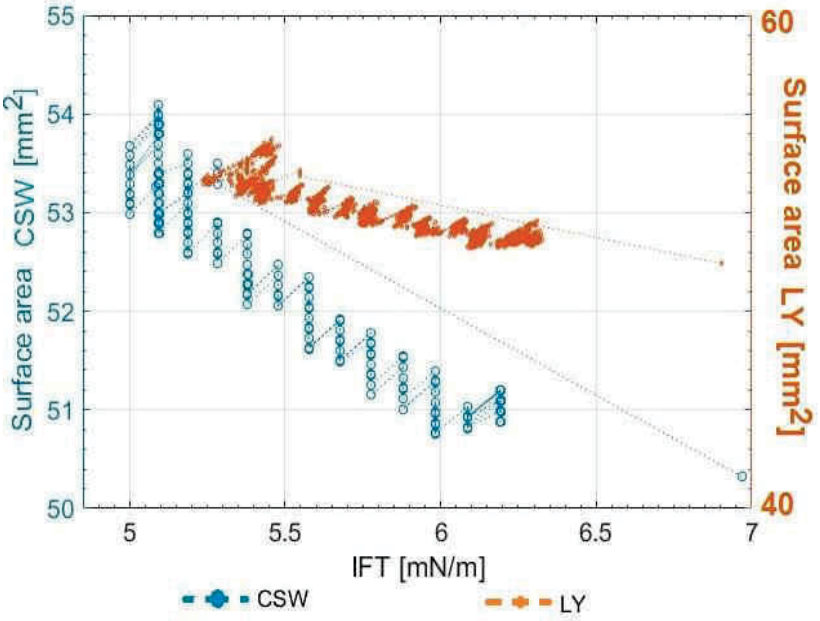

Figure 47: Surface area versus IFT. “Crude oil C”

As illlustrated in Figure 47, the surface area of the measured droplet is reversely proportional to the interfacial tension. A decrease in the interfacial tension is associated rather with the

drop elongation in the first minutes of the experiment, whereas the subsequent contraction of the droplet lead to the increase in the interfacial tension. Therefore, the observed IFT behavior can be explained by physical properties of the “Crude oil C”.

For comparison, I conducted an experiment with a higher speed of rotation. Figure 48 shows that the distribution of interfacial tension is about the same as in the previous test. The interfacila tensionis higher and reaches 6.9 mN/m in 2 hours. So, I came to the conclusion that the speed of rotation of the capillary tube can affect the aging rate of oil droplets and the IFT value.

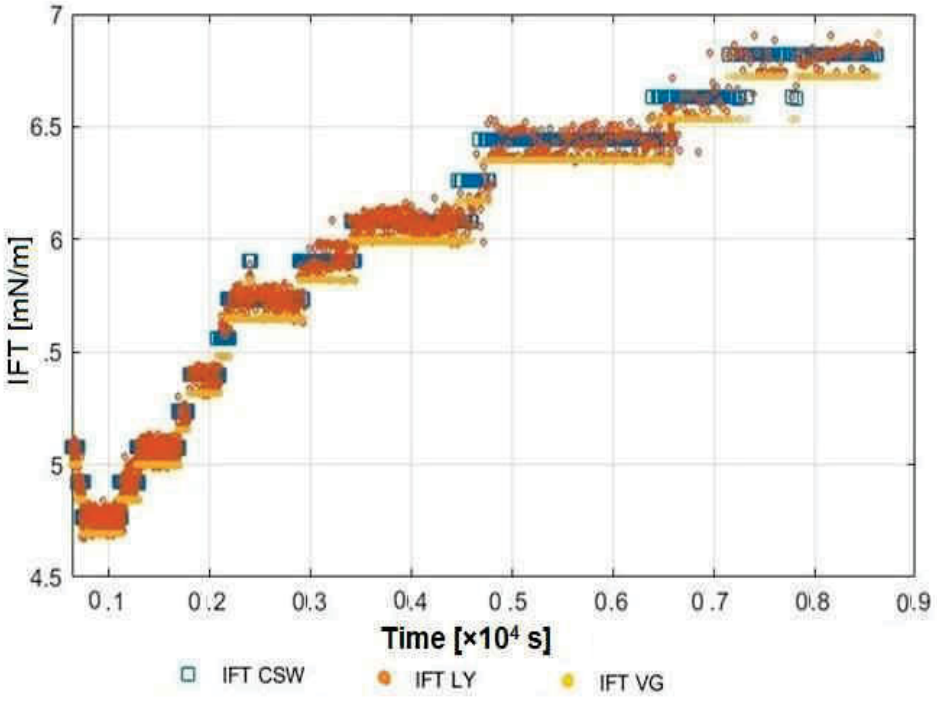

Figure 48: IFT long-term measurement of “Crude oil C”- water with a high rotational speed of 7000 min^{-1}

As can be seen from Graph 50, there is no any clear difference in the interfacial tension values for measurements carried out with various rotational speeds. All experiments were fulfilled on the droplet of the same volume of about 24 μl. The drop volume is iilustrated in Figure 49.

As is known, the oil droplet usually has a longer relaxation at a slower rate [39], [40]. And the interfacial tension is lower. However, as can be seen from Figure 50, the more or less different behavior of the interfacial tension can be observed only at a rotation speed of 3900 min^{-1}. The example depicted in the figure shows the measurements in the first minutes of the experiment.

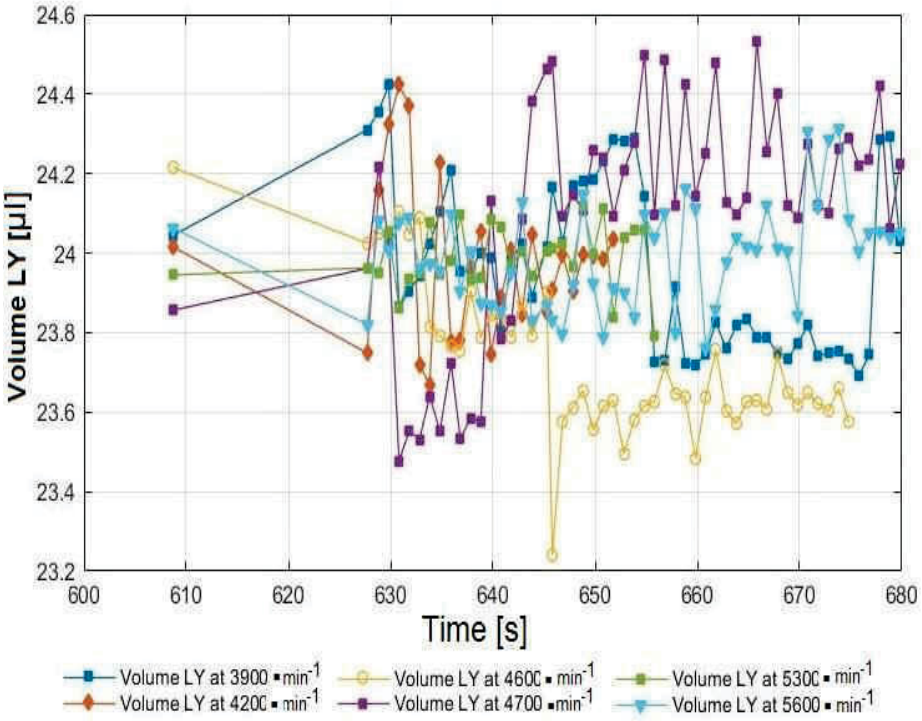

Figure 49: Droplet volume LY vs. time.“Crude oil C”

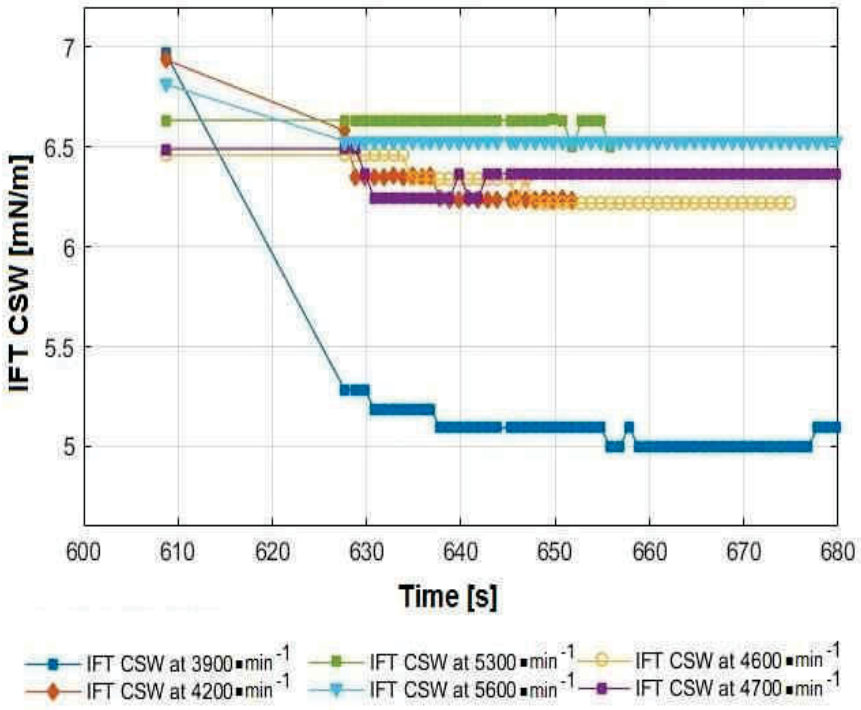

Figure 50: Changes in IFT CSW with time at various speeds. “Crude oil C”

4.3 Crude oil A

4.3.1 IFT measurements at a constant rotational speed

As already mentioned, “Crude oil A” is the most viscous oil among the available three oil samples. According to API gravity which is 19.88 °API, the “Crude oil A” can be classified as heavy oil. And so, the equilibration of the oil-water system may not be reached in a short time. To resolve the problem, different combinations of rotational speeds and drop volumes have been tested in the study. The “Crude oil A” was studied by several series of long-term measurements at a temperature of 25.5°C.

According to Isaac et al. (1988) [32], for heavy oils and tensions below 1 mN/m, speeds below 6,000 rotations per minute are preferable. The lower the tension, the lower the droplet rotation speed is recommended. Measurement at low speed ensures that the length to diameter ratio of about 4is maintained.

The first trial measurement of the “Crude oil A” gave low interfacial tension values about 1.2-1.3 mN/m. Test was performed at the moderate speed of 4000 min^{-1}. The next series of experimental measurements was continued at a low speed of 2300 min^{-1} with a gradual increase in rotation to 3700 min^{-1}.

The results, illustrated in Figure 51, show that interfacial tension between oil and water phases falls down with time. The interval that covers the so-called drop formation time is about 30 minutes. An increase in the rotational speed caused an instant increase in interfacial tension. In addition, it should be noted uneven changes in the distribution of interfacial tension. Measurements were carried out at ends due to the large volume of the droplet. During the experiments the interfacial tension decreases, but does not reach a plateau.

It became clear that a long duration test is needed to determine the time required for equilibrium. A long-time experiment is a more effective way to determine the impact of two or more factors on the interfacial tension, where only one factor is changed over time, while the other factors are kept fixed. This time I injected a droplet of smaller volume of 6 μl. All measurements were performed on a full-size droplet to reduce calculating error. Based on the observations made, I decided to conduct an experiment with a constant rotational speed of 4100 min^{-1}. The changes in interfacial tension were continuously monitored. The recording time interval was 1 second at the beginning of the test and then it was changed to 3-20 seconds after achieving relative stabilization in the interfacial tension. The experiment lasted about 4 days. Interfacial tension kept changing over the entire time of experiment. As can be seen in the graph (Figure 52), this volume takes around 1 hour to reach 1 mN/m. The initial IFT value was 3.5 mN/m.

The total interfacial tension distribution over time is given in Figure 53. Drop formation at t=0. The lowest IFT VG value of 0.59 mN/m was achieved only on the second day after 21 hours. The interfacial tension decrease was already much slower, but after 4 hours the interfacial tension started to rise up again. The IFT VG reached 1.32 mN/m at the end of the fourth day.

The dynamic behavior of the interfacial tension calculated by Cayias-Schechter-Wade (CSW) and Laplace-Young (LY) methods corresponds to the changes in the interfacial tension measured by Vonnegut approach (VG).

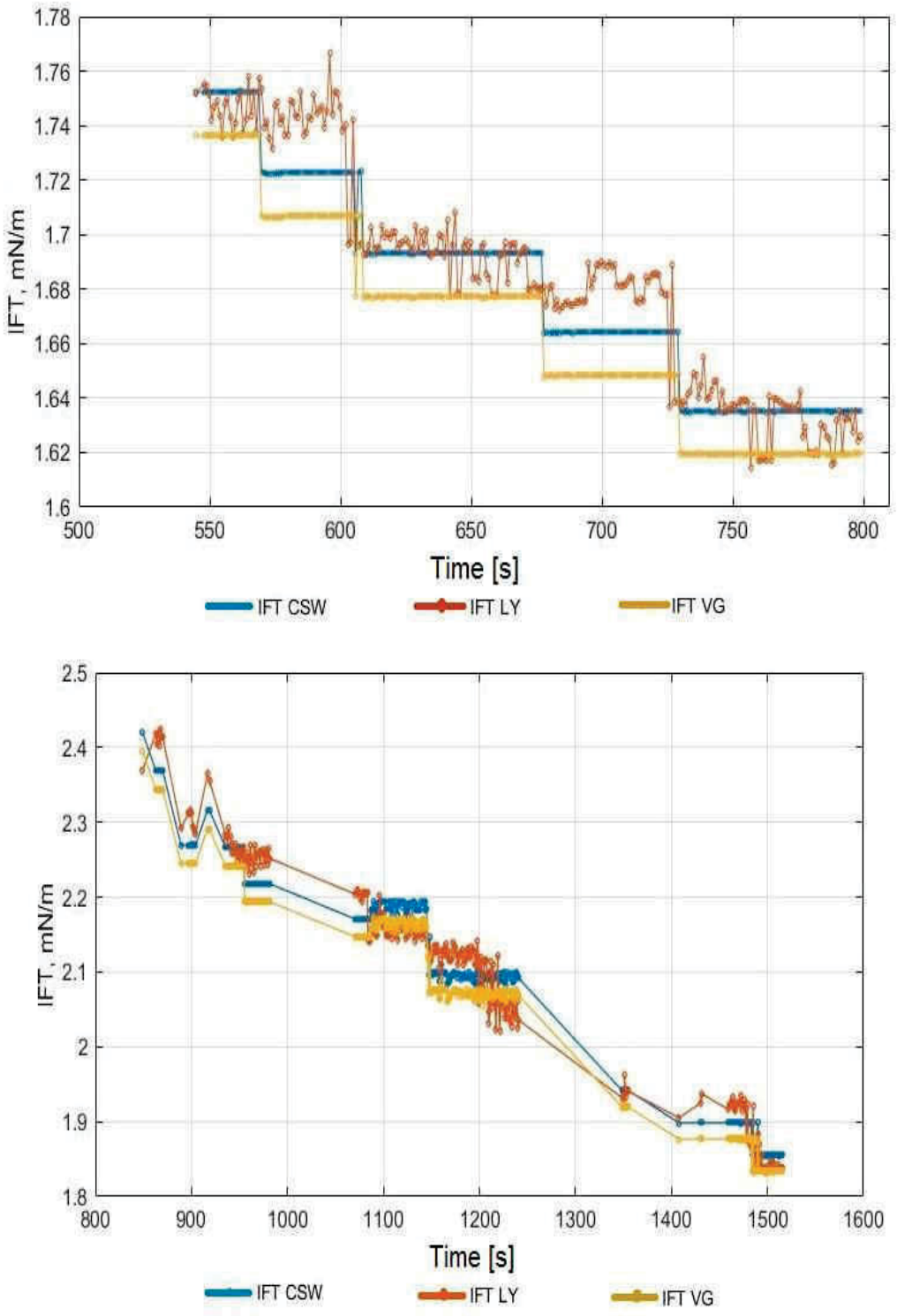

Figure 51: IFT measurement of “Crude oil A”- water
A. with a rotational speed of 2300 min^{-1};
B. with a rotational speed of 3700 min^{-1}

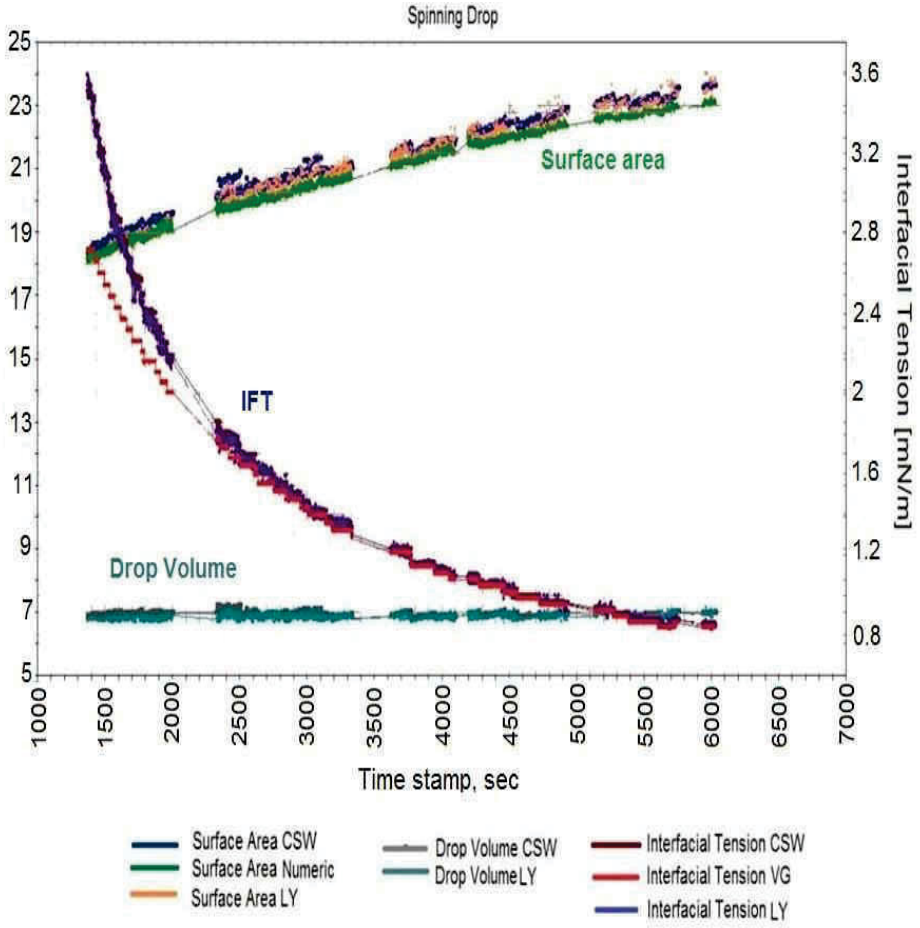

Figure 52: IFT measurement of "Crude oil A"-water with a rotational speed of 4100 min^{-1}

IFT values were summarized and the average "equilibrium" interfacial tension value was calculated for each day of the time measurements. The results are presented in Table 2.
It can be seen that interfacial tension decreased nearly by 50 percent and reached the equilibrium state on the second day.

Table 3: Average "equilibrium" IFTs of the "Crude oil A" oil-water system

Day	Average equilibrium IFT, mN/m		
	CSW	LY	VG
I	1,38	1,37	1,29
II	0,66	0,66	0,65
III	0,673	0,669	0,66
IV	0,957	0,953	0,942

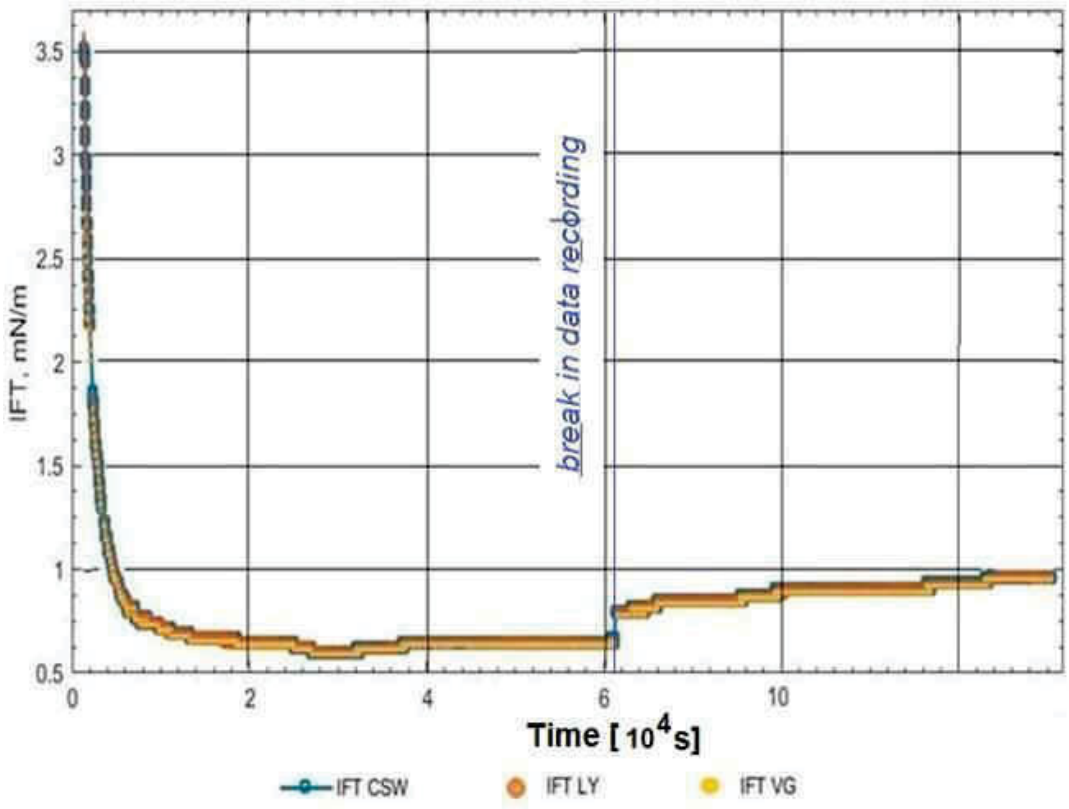

Figure 53: Long-term IFT measurement of “Crude oil A”- water
with a rotational speed of 4100 min^{-1}

It should also be noted that after the third day of measurement, the interfacial tension began to increase. This is clearly seen in Figure 53. At the end of the fourth day, the interfacial tension reached an IFT value of 0.95 mN /m. In general, the interfacial tension decreased by half compared to the initial interfacial tension within 24 hours and remained constant within two days. The interfacial tension value reached 0.66 mN/m.

To reveal changes in other parameters, the results of the performed experiment are plotted as a function of time. Figure 54 shows the droplet volume estimated by Cayias et al. (CSW)approach. As can be seen, changes in the drop volume are more frequent during the first 5.5 hours of the experiment, and then the changes occur slowly. The droplet volume is 6.7-7.2 μl. The variation in the droplet volume decreases to the end of the experiment. The same behavior was observed for IFT measured by Laplace-Young method.

The stepwise change of curves, shown in the figures, had an artificial origin and was caused by the droplet motion in the capillary tube. Thus, we are dealing with inaccuracies in measurements. To avoid a significant difference in the results obtained during the interfacial tension measurements, the mean values and uncertainties should be calculated and taken into account in the further interpretation of the data.

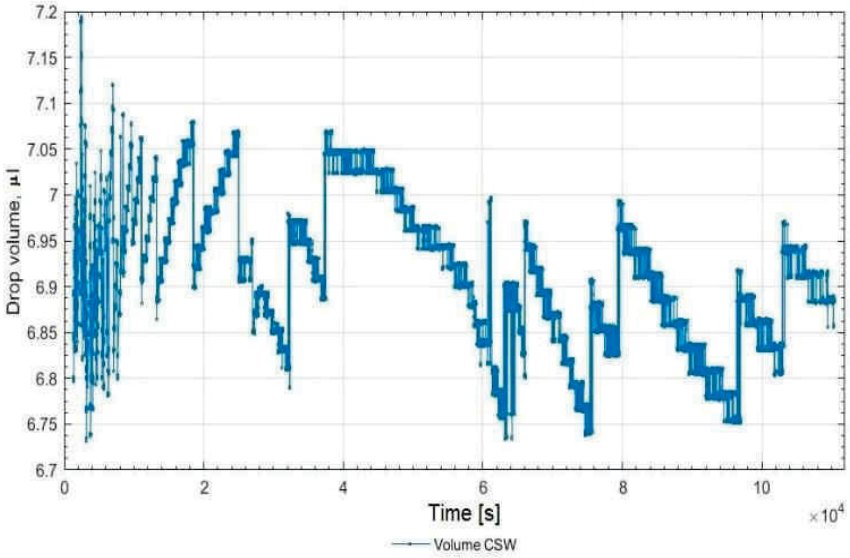

Figure 54: Drop volume measurement over time of “Crude oil A”
with a rotational speed of 4100 min^{-1}

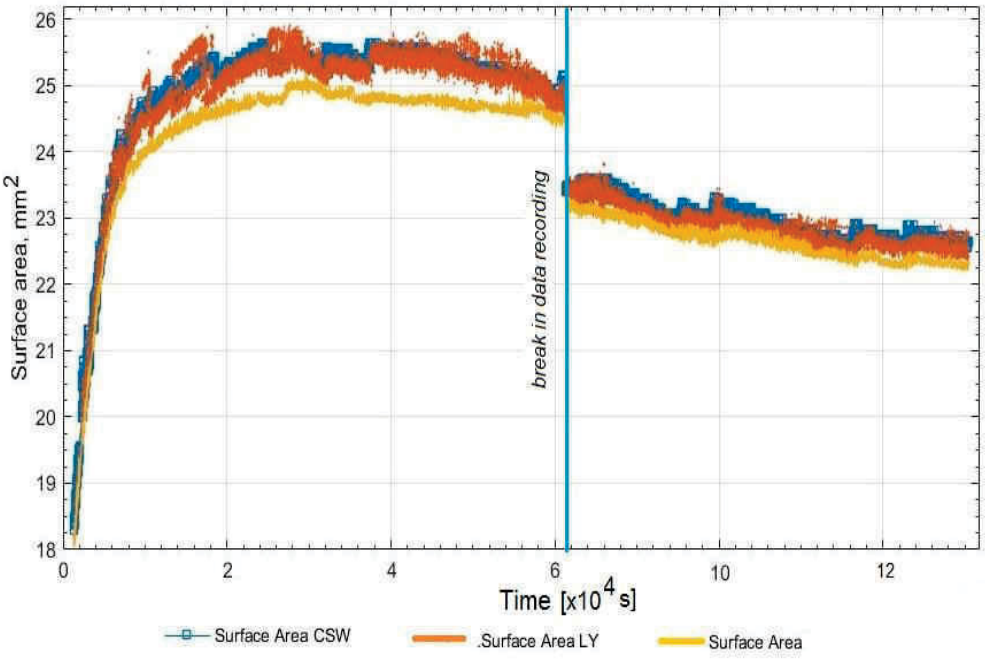

Figure 55: Surface area measurement over time of “Crude oil A”- water
with a rotational speed of 4100 min^{-1}

As illustrated in Figure 55, the dynamics of the droplet was observed by monitoring the variation of the surface area in time. The observed decrease in the interfacial tension of the “Crude oil A”-water system is accompanied by a sharp increase in the surface area during the first hours of the experiment. The surface area changed from 18 mm^2 to 25-26 mm^2. The surface area remains more or less constant for 2 days, and then begins to decrease. It reached 22 mm^2. There is not much difference between the values calculated using the Cayias-Schechter-Wade (CSW) and Laplace-Young (LY) approaches.

The interfacial tension distribution was compared with variations in droplet volume and surface area. As expected, the decrease in interfacial tension is inversely proportional to the surface area of the measured drop, and, as a consequence, to the elongation of the drop. Figure 56 shows the change in the interfacial tension calculated by Cayias-Schechter-Wade and Laplace-Young methods. There is no difference in the calculated values for these two approaches. The data are consistent each other, only a larger variance is observed for the interfacial tension calculated by Laplace-Young approach (LY).

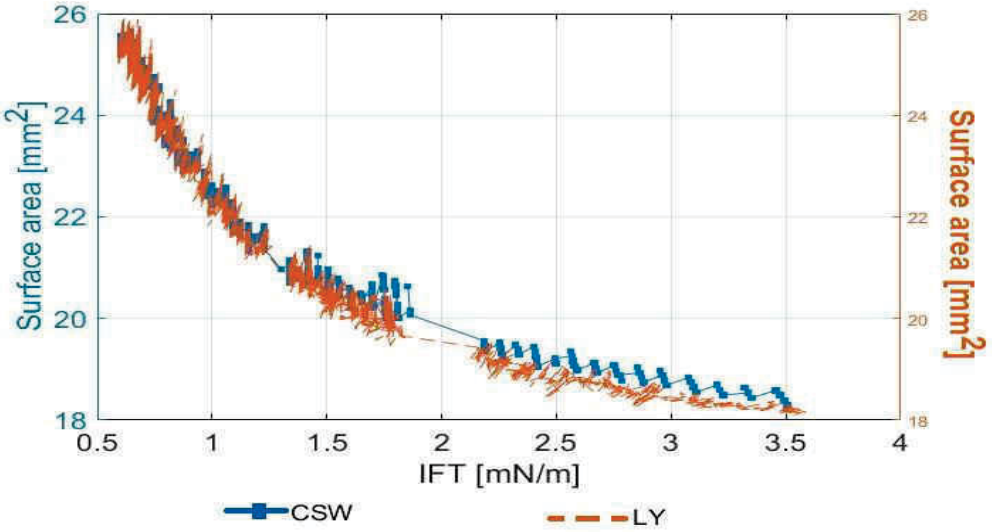

Figure 56: IFT vs. surface area for “Crude oil A”. Rotational speed - 4100 min^{-1}

Comparison of droplet volume and interfacial tension variation showed that a narrower range of volume fluctuations refers to a higher interfacial tension at the start of the test. This can be more clearly observed from the interfacial tension vs. droplet volume distribution calculated using the Laplace-Young approach. The relationship of the interfacial tension versus time is given in Figure 57.

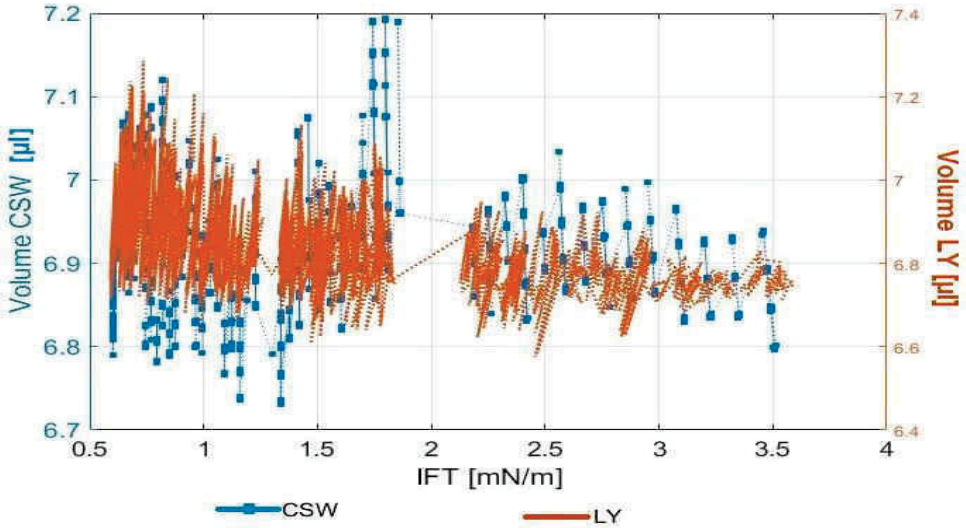

Figure 57: IFT vs. drop volume for “Crude oil A”. Rotational speed - 4100 min^{-1}

The equivalent experiments were carried out with a rotational speed of 5000 min^{-1}. In this case the drop volume was larger than in the previous test. Figure 58 shows the IFT distribution over time.

As can be seen from Figure 58, the IFT dynamic behavior is identical to the earlier obtained results. The interfacial tension initially decreased in function of time and reached a temporary plateau. The first registered IFT value was much higher comparing with the lower-speed measurements. However, the change to the lower and more stable interfacial tension was fast. For example, the IFT VG changed from 6.2-6.39 mN/m to 1.5-1.6 mN/m in 50 minutes (to 4 mN/m in 10 min). The IFT minimum was achieved in 3 hours and was 0.96 mN/m. It should be noted that due to the large droplet volume the measurements were performed first on a full-size droplet and then at the ends of the drop. But this did not lead to a big variance in the IFT values, since the drop reached the equilibrium state.

To have a better understanding of the fluctuation in the initial value of interfacial tension, the test was repeated with a smaller drop at the same rotational speed. It is interesting to note that the initial interfacial tension between oil and water phases had a lower initial interfacial tension value of about 3.6 mN/m. This means that the speed is not the key factor responsible of the magnitude of the starting interfacial tension and the interfacial tension is more dependence on the dosage of the droplet injected.

Another test was conducted with a minimum rotation speed of 3600 min^{-1}. The results obtained are depicted in Figure 57. The first recorded IFT value was 2.53 mN/m (IFT CSW). The drop reached the required size in about 40 minutes. A minimum of 1.05 mN/m in the IFT distribution was achieved on the next day, after 24 hours. The measurements were carried out on a full-size drop. The volume of the droplet was 20 μl.

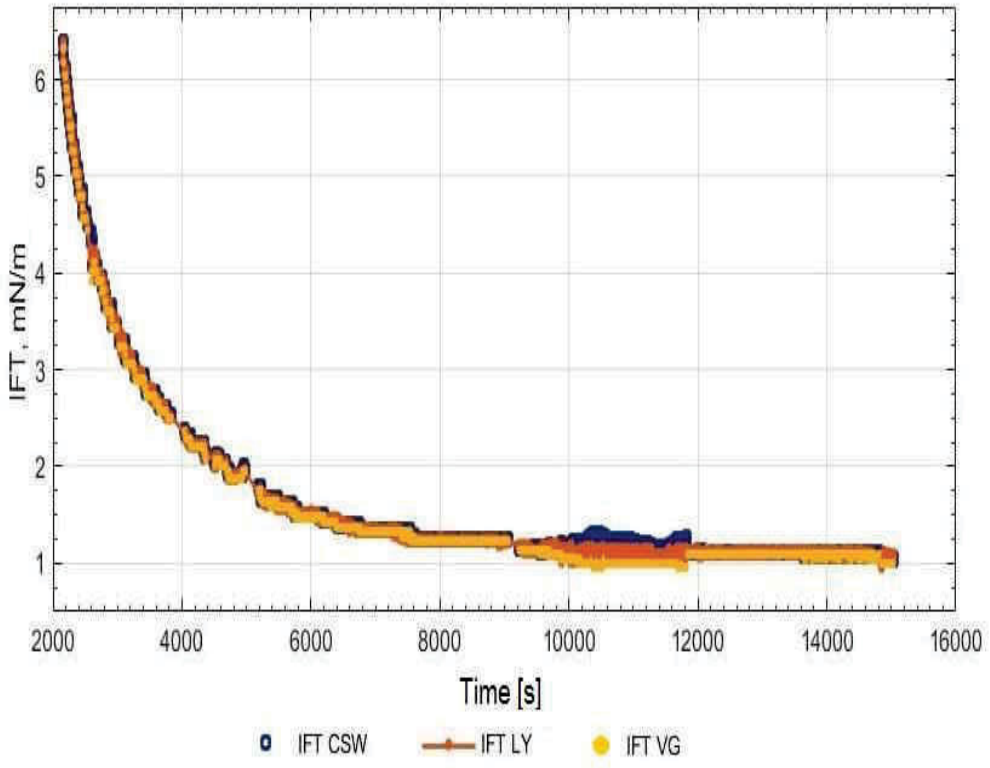

Figure 58: Long-term IFT measurement of “Crude oil A”- water with a rotational speed of 5000 min^{-1}

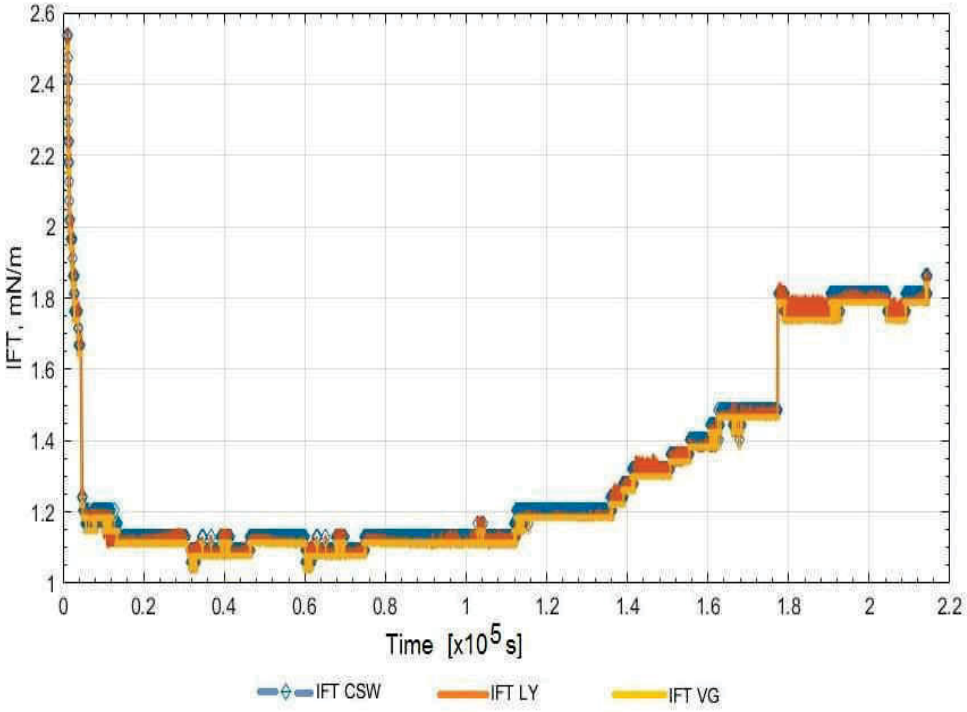

Figure 59: IFT long-time measurement for “Crude oil A”. Rotational speed - 3600 min^{-1}

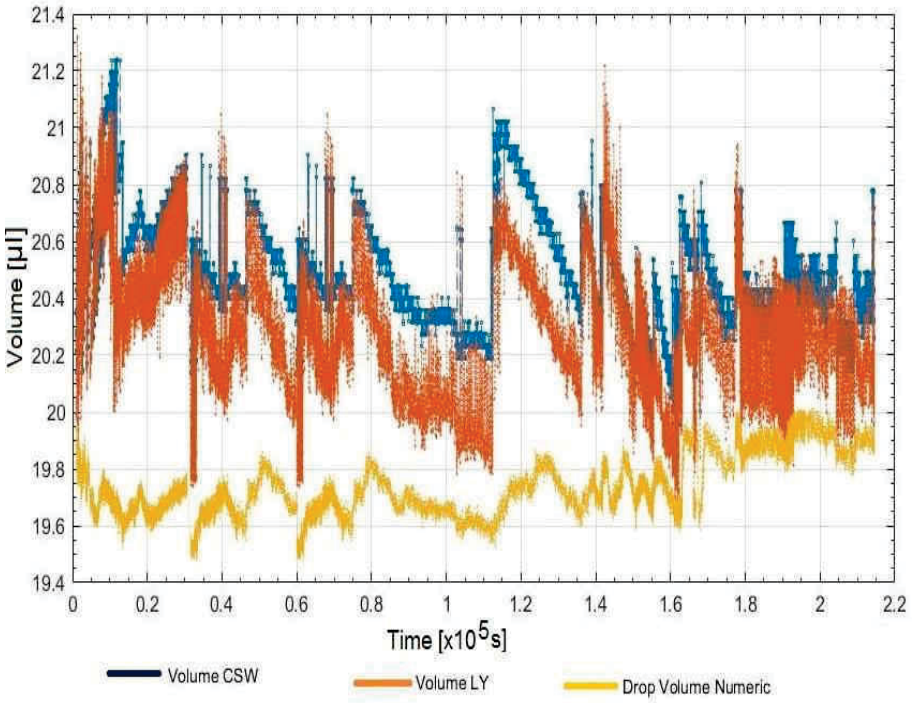

Figure 60: Drop volume long-time measurement for “Crude oil A”.
Rotational speed - 3600 min^{-1}

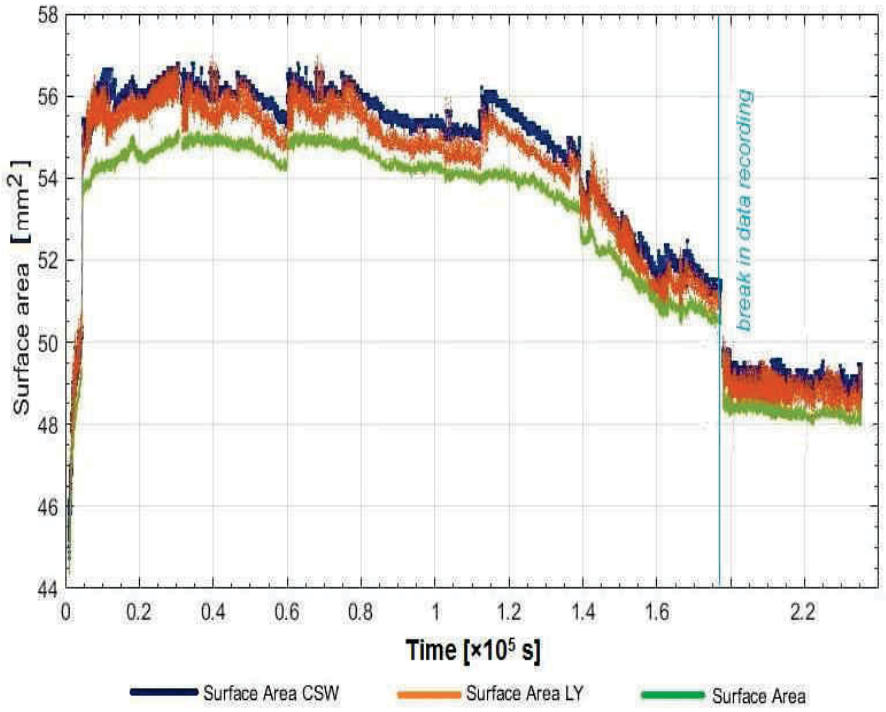

Figure 61: Surface area long-time measurement for “Crude oil A”.
Rotational speed - 3600 min^{-1}

The surface area changed from 44 mm^2 to 56 mm^2, remaining more or less constant during the plateau phase. As illustrated in Figure 61, an abrupt increasing in the surface area in the first minutes of the experiment is observed. A subsequent increase in IFT values and a decrease in surface area were caused by a contraction of the droplet.

Comparative studies have confirmed that the results obtained can be considered as stable experimental results. The data from the experiments show a similar trend; IFT values decrease over time. The comparison of the IFT distribution in the first hours of experiments shows that started values of the IFT are higher for measurements with a large drop volume. It can be seen from Figure 62. The drop formation time in the most cases took around 30-40min. Such an explicit dependence on the rotational speed was not observed.

The measurements performed on a full-size drop of 1.9 μl showed an initial IFT value of 2.4 mN/m. The IFT minimum reached the lowest value of 0.16 mN/m (CSW IFT) and 0.157 mN/m (LY IFT). The drop formation is about 30 min. The surface area changed from 7.6 mm^2 to 11mm^2 during the first 2 hr.

On the basis of the tests carried out, the most optimal volume of drops for measurements of “Crude oil A” should be less than 2μl, since the volume of droplets significantly affects both the IFT distribution and the time required to reach the plateau.

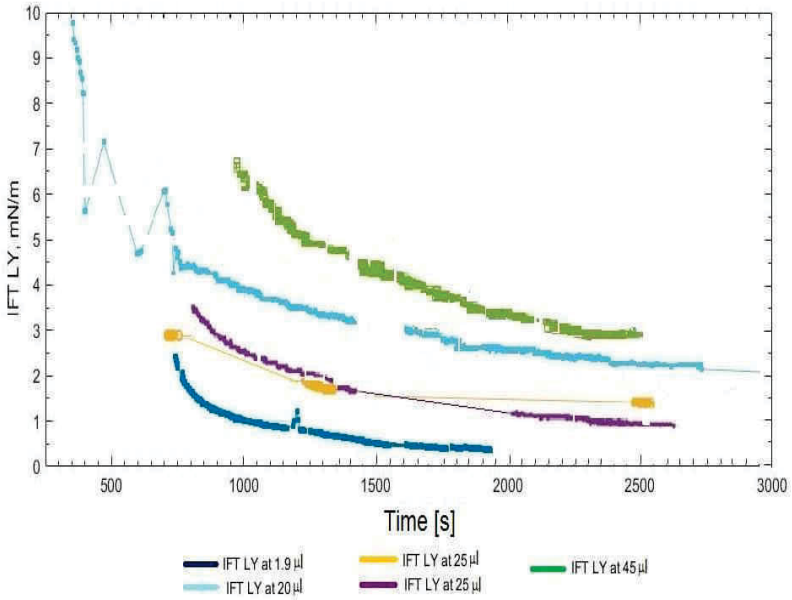

Figure 62: IFT distribution of “Crude oil A”- water for various drop volume

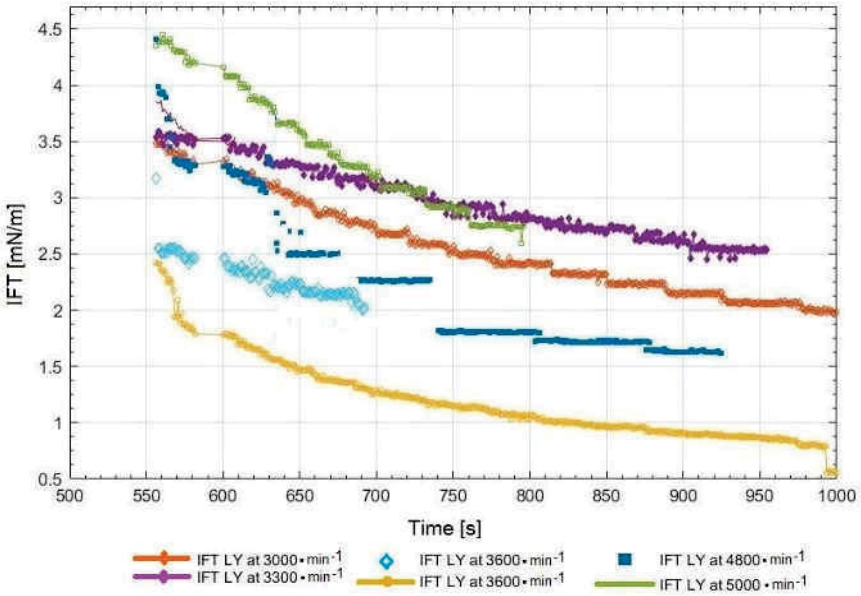

Figure 63: IFT distribution of “Crude oil A”- water for different speeds of rotation

Figure 63 shows the change in the interfacial tension with the drop formation time for measurements carried out with different speeds. It can be seen that the interfacial tension behavior is similar both for low-speed measurements and high-speed measurements; interfacial tension values decrease with time. The interfacial tension is dependent on rate-controlled processes. Relatively high interfacial tension values are observed for a high rotational speed of 5000 min^{-1}, showing a response to quick changes in the size and shape of the interfacial surface area. However, this effect is not observed, for example, for measurements conducted with a rotational speed of 3600 min^{-1}. At the same rotational speed, there is no similarity in IFT values.

Thus, it can be concluded that the behavior of the oil-water system is quite complex and the influence of various factors should not be considered separately.

4.3.2 Oscillating the rotational speed

I conducted test measurements with oscillating rotational speed to analyze the interfacial tension behavior of the “Crude oil A” and the observed non-uniform interfacial tension distribution. Through trial and error, the optimum amplitude and period of the oscillating rotational speed were determined and set at the Rotation Speed Modulation area. The results were recalculated, and the values of the rotational speed were approximated to a sinusoidal curve. The measurements were repeated at different rotational speeds and different droplet volumes. The main conclusion is that the parameters for the oscillating measurements should be chosen based on the physical properties, in particular viscosity, and the selected optimal rotation speed for each oil sample.

.

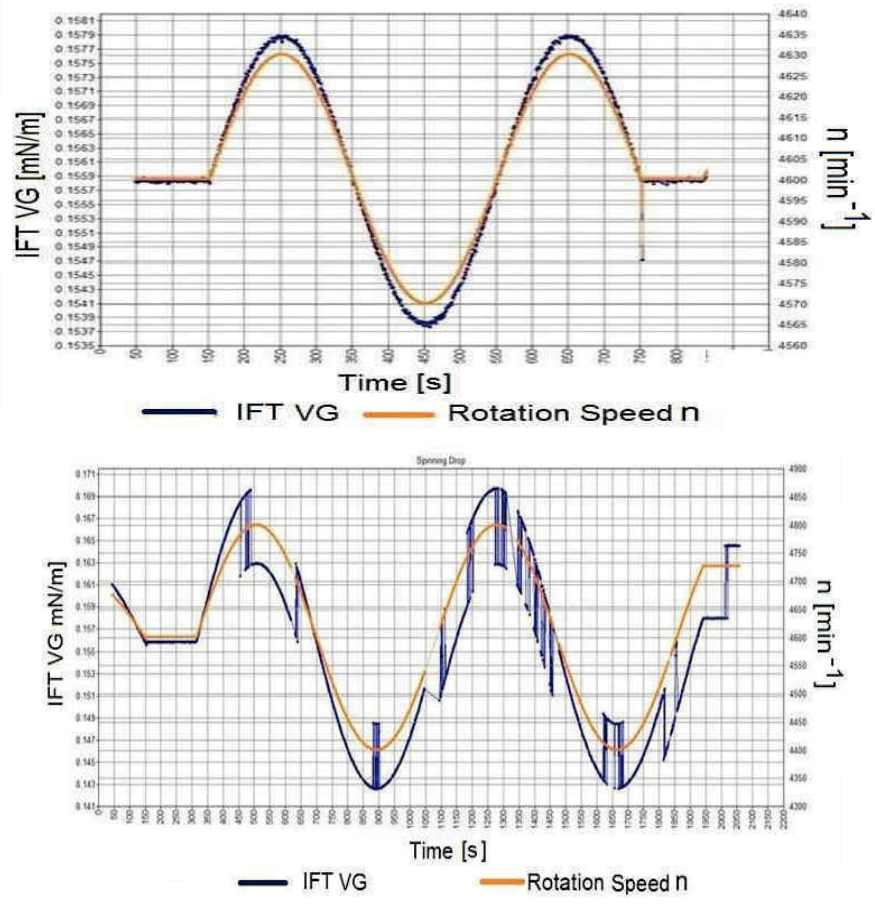

Figure 64: Response of the IFT of “Crude oil A”- water
for a sinusoidal perturbation of a spinning drop

The Figure 64A shows that the interfacial tension changes gradually and imperceptibly without sudden transitions and jumps, whereas in Figure 64B the changes in the interfacial tension distribution occur unevenly. Such an uneven change in interfacial tension was observed not only in dynamic experiments, but also in standard measurements.

The analysis of the recorded movie of oscillating tests helped to understand the observed non-uniform distribution of interfacial tension. It turned out that the fluctuations in the interfacial tension values are related to the motion of the drop. When the droplet is in a stable position, there is no fluctuation of the interfacial tension curve, while even a small droplet movement caused by an instant change in the droplet volume leads to uneven changes in the interfacial tension distribution. Motion occurs due to the elongation or contraction of the oil droplet. As expected, the observed phenomenon was of an artificial origin.
The variations in the measured values of the interfacial tension were within the permissible range in my experiments. However, when we are dealing with a larger variance in the obtained data, it is necessary to take into account the observed error and inaccuracy in the calculations of interfacial tension. The IFT readings should be statistically interpreted and mean IFT values should be taken for each time interval. The choice of the time interval duration can be determined by the required accuracy of the data and the observed IFT distribution.

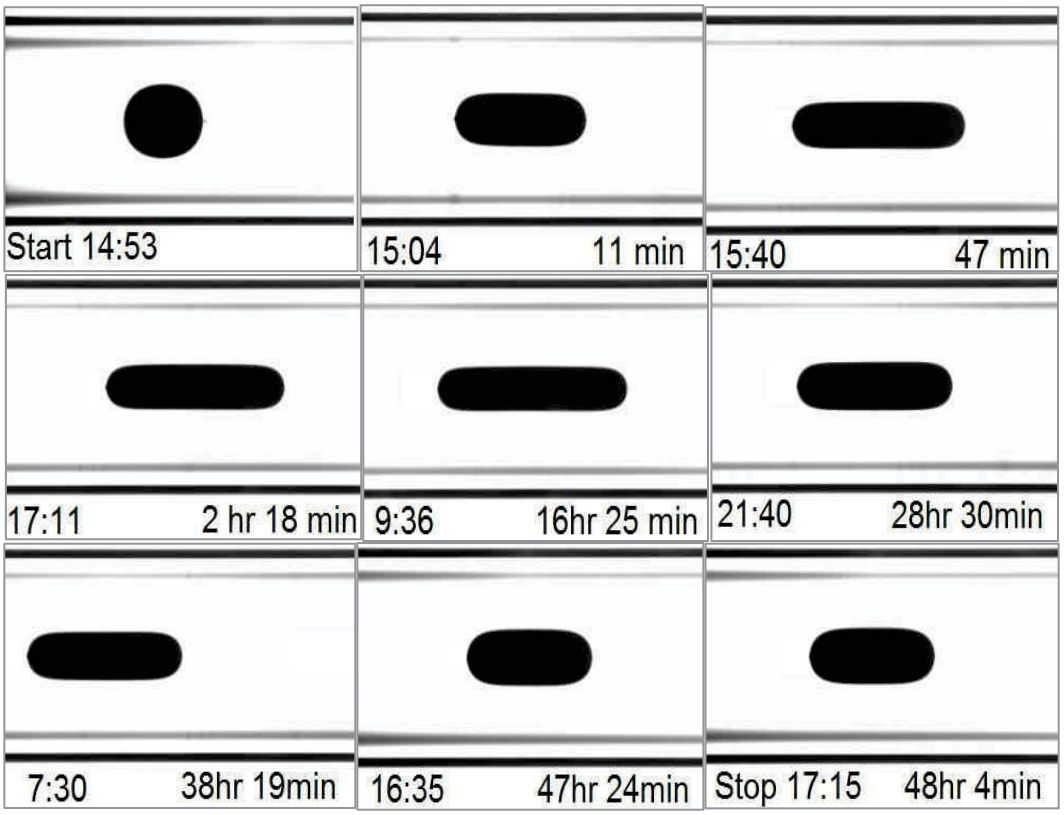

Figure 65: Transformation and motion of the oil droplet over time (starting top left corner). Oil sample - “Crude oil A”. Rotational speed - 3600 min^{-1}

As can be seen in Figures 65, 66, the transformation of droplets in time largely depends on the chosen rotational speed. The time needed to obtain a drop of the required size for measurements is greater for low-speed experiments. And it should be noted that during low-speed tests, the drop returns to its original shape and size after a certain period of time. This must be taken into account when we are discussing whether equilibrium of the oil drop in water was achieved in the experiment.

The Figure 66 shows that during high-speed measurements, the oil drop elongates in size, but does not return to its original size. Both tests were long-term measurements and lasted 3-4 days.

Figure 66: Transformation and motion of the oil droplet over time (starting top left corner). Oil sample -"Crude oil A". Rotational speed - 5000 min^{-1}

For measurements with high rotational speed, the main factor is the drop volume. To ensure the accuracy of measurements, a droplet of small size must be injected in the capillary tube. On the contrary, the rapid elongation of the droplet will not allow measurements to be made on a full-sized drop. Measurements at the ends of the drops, as I have already mentioned, are not desirable.

5 Conclusions

A series of experimental studies was conducted to understand the IFT behavior of three crude oil samples obtained from wells. Elemental compositions, physical and compositional properties of oil samples, except for some properties, were unknown.

Primary focus was stressed upon the study of interfacial tension. Both static and dynamic interfacial tensions were measured with a Spinning Drop Tensiometer, and applied to the crude oil-water interface. Some test experiments were performed to understand the rheological behavior of the available oils. All measurements were carried out at a temperature of 25°C.

Additional preliminary experiments were performed to determine the IFT at the interface between decane and aqueous phase. The main purpose of these measurements was to establish a constant reference IFT value for the system before starting experiments with oil samples and to understand the procedure of measurements themselves.

The average IFT value of decane measured by the instrument was close to the value of 38 mN/m. As I mentioned in Section 3.4.1, the interfacial tension values measured on a full-sized drop are lower than those given in the literature [23], [29], [36].

Higher IFT CSW values were obtained at elevated temperatures and during measurement performed at the spherical ends of the droplet. The IFT values are close to the literary Than value, which is 46 mN/m. But IFT, calculated by Vonnegut method, showed the IFT value of about 34 mN/m. The variation is in an acceptable range for each data set. Although the agreement of my data with the standard value is better, the data obtained are not reliable. As I concluded in Section 3.4, there is a significant inconsistency in the data measured at the spherical ends of the droplet, which can arise from a systematic error in determining the length and the curvature radius of a droplet.

The most likely cause of errors in measured values relative to the actual values of interfacial tension in a decane-distilled water system can be an impurity of liquids, especially in distilled water. As already mentioned in Paragraph 3.4.1, no additional steps have been taken to ensure the purity of liquids, except for the general preparation of the sample for measurement.

Incorrect calibration of the device is considered a secondary factor, which can lead to erroneous results. However, I eliminate the great influence of this factor, since the calibration of the instrument was strictly consistent with the rules and was repeated during the measurements.

In Chapter 4, I reported interfacial tension for three oil samples and gave illustrative examples describing the IFT behavior of these oils. The interfacial tension of oil droplets in the aqueous phase was measured by submitting them to slow and rapid expansion and monitoring the interfacial tension evolution. Experimental results showed that different interfacial behavior can be observed in oils of different types.

The results from the IFT measurements were difficult to interpret in correlation with the crude oil properties.

The “Crude oil A” has a higher TAN value than the other two oils and, as might be expected, should have a higher degree of interfacial activity. According to Buckley and Fan (2007), oils

with a high TAN value should have the lowest interfacial tension [41], [42]. The tests performed proved this assumption. The lowest IFT was observed for “Crude oil A”. Further correlation of interfacial tension with the physicochemical properties of oils and viscosity was not possible due to lack of data.

The highest interfacial tension was observed for the “Crude oil B”. The interfacial tension of this oil to distilled water varies between 12 and 15 mN/m. The average value is 12.40± 0.25 mN/m.

For the “Crude oil C”, the average value is about 5.50±0.23 mN/m. The variance between IFTs measured by different approaches is low. The average values for the “Crude oil A” varies between 0.79±0.19 mN/m and 2.1±0.20 mN/m. For each oil sample, the re-measurement data set is precise, and the values are close to each other.

For all examined oils, the IFT values decreased with time. Comparison of the IFT behavior for three crude oils in distilled water shows that the trends are quite similar for the crudes. Complex interfacial tension curve obtained for the “Crude oil C” can be assumed to be based on the physical properties of this oil. The time plots of the mean IFT value of the oil data are depicted below (Figures 67, 69, 71). The curve lines were drawn for the IFTs measured by three approaches and illustrate the main features from the measurement results.

It should be noted that all measured IFT are true interfacial tensions at a given time after droplet formation. However, only the “plateau” value is considered to be “equilibrium” interfacial tension value. Thus, the IFT values in the plateau phase are of interest.

Because no available experimental data exist on the oil samples, the results are compared with the average IFT value taken from the “equilibrium” interfacial tension values. Each sample was measured in at least three sets with one condition - with more or less the same rotational speed and the droplet volume. Then an average was taken for each oil sample. The averages and calculated uncertainties are presented in Tables A1-3 (Appendix A).

Standard deviations were calculated for dynamic and “equilibrium” part of the IFT curve. To get more accurate values, I calculated the standard deviation for time intervals of 1000 seconds for the dynamic part of the IFT curve and large time intervals for the stable part of the curve.

As known, the improved oil recovery mechanism of reducing IFT is related to the remobilization of residual oil after water flooding. Reduction in interfacial tension significantly accelerates the penetration of non-wetting fluid, increases the capillary numbers and therefore the displacement efficiency.

One of the factors that should be taken into account is a reduction of the initial values of interfacial tension for given crude oils.

To illustrate effects of the initial values of interfacial tension and the rate of the reduction for oil samples, the obtained results were shown as a percentage distribution. Due to lack of data on available oil samples, I assumed the minimum obtained in long-time IFT measurements as a level of stability. This assumption is the simplest ones that can be formulated in the framework of conducted IFT studies to account for the process of displacement.

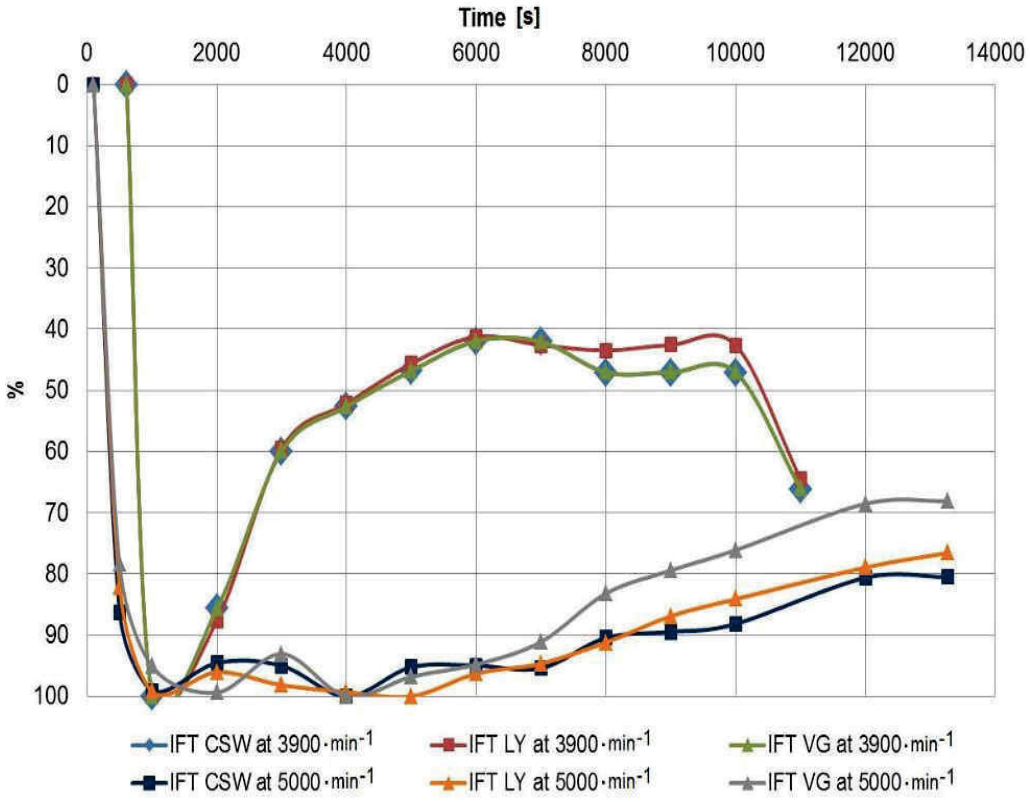

Figure 67: Average IFT vs. time for “Crude oil C” – distilled water system

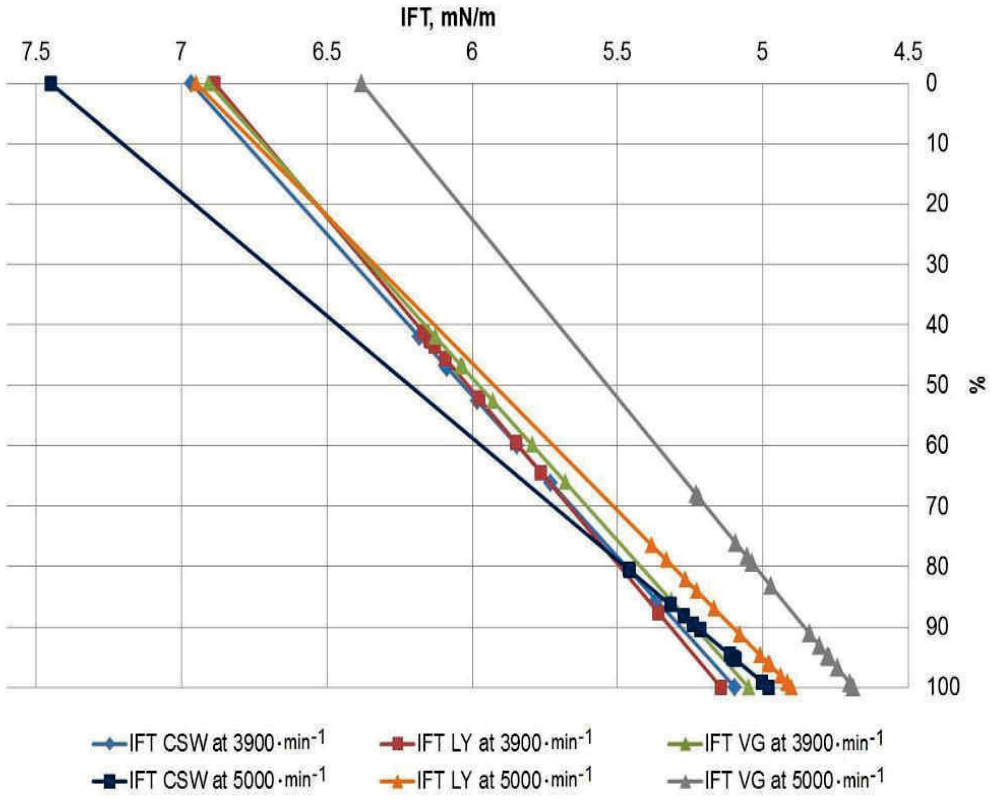

Figure 68: Average IFT of “Crude oil C” – distilled water system

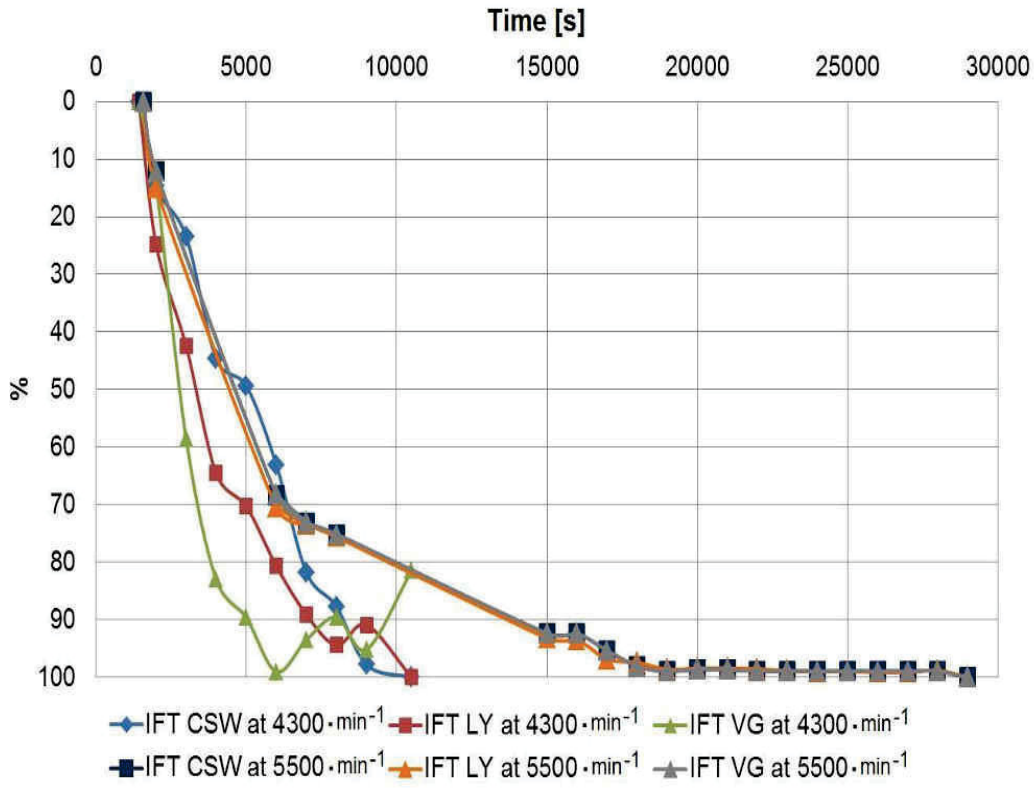

Figure 69: Average IFT vs. time for “Crude oil B” – distilled water system

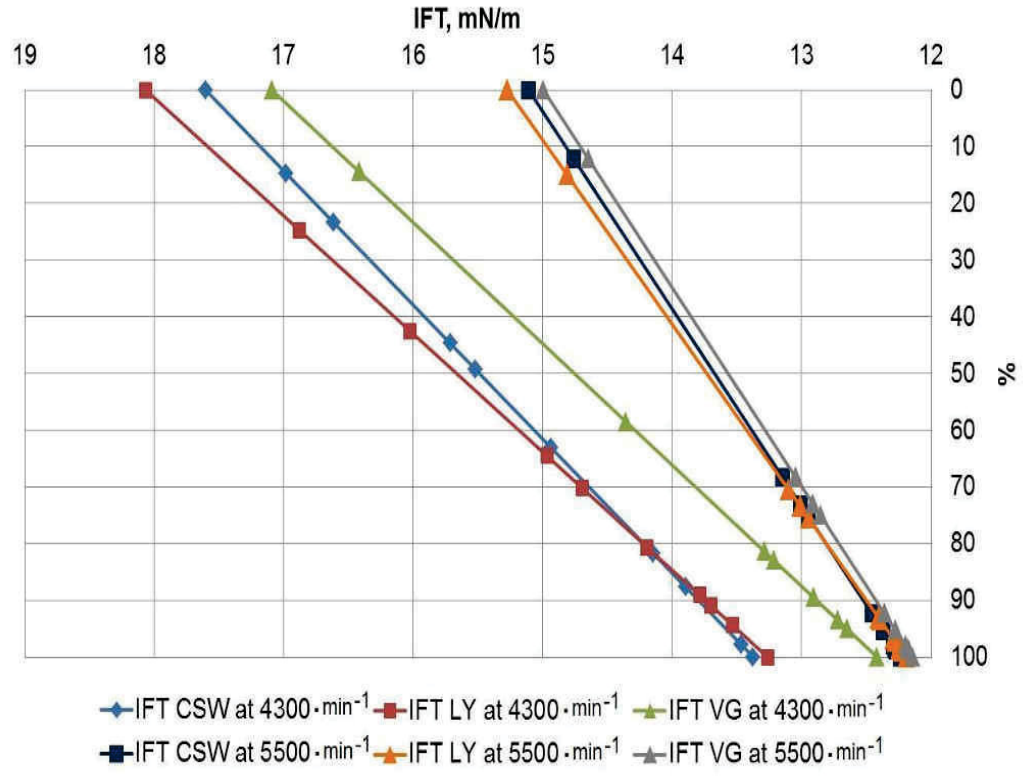

Figure 70: Average IFT for “Crude oil B” – distilled water system

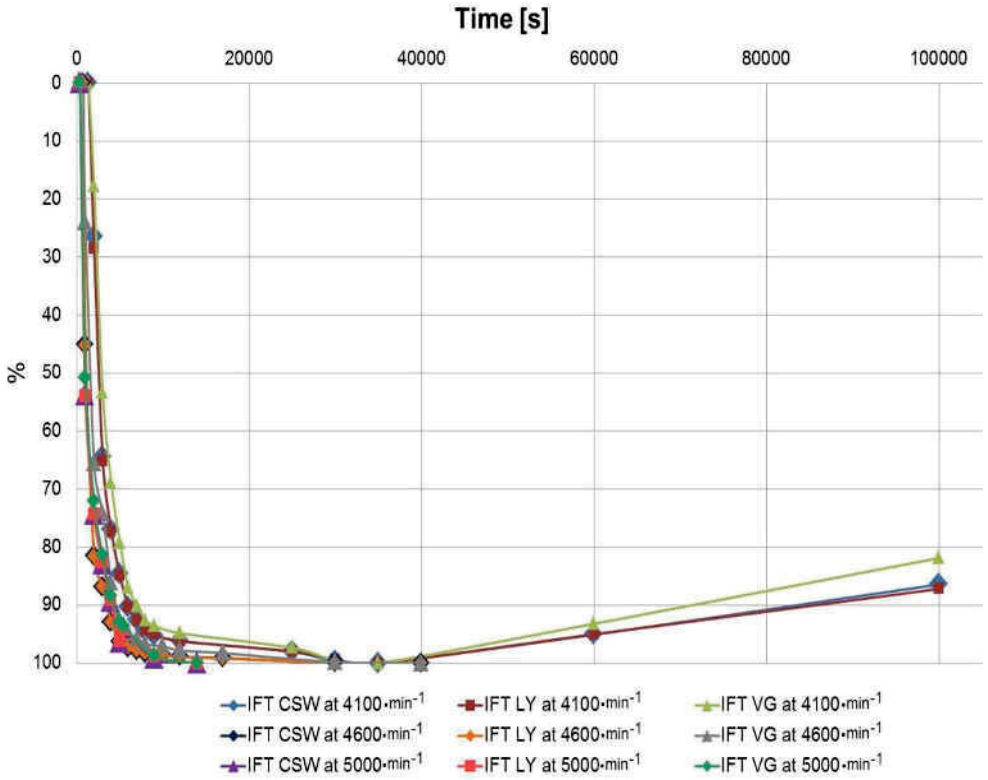

Figure 71: Average IFT vs. time for “Crude oil A” – distilled water system

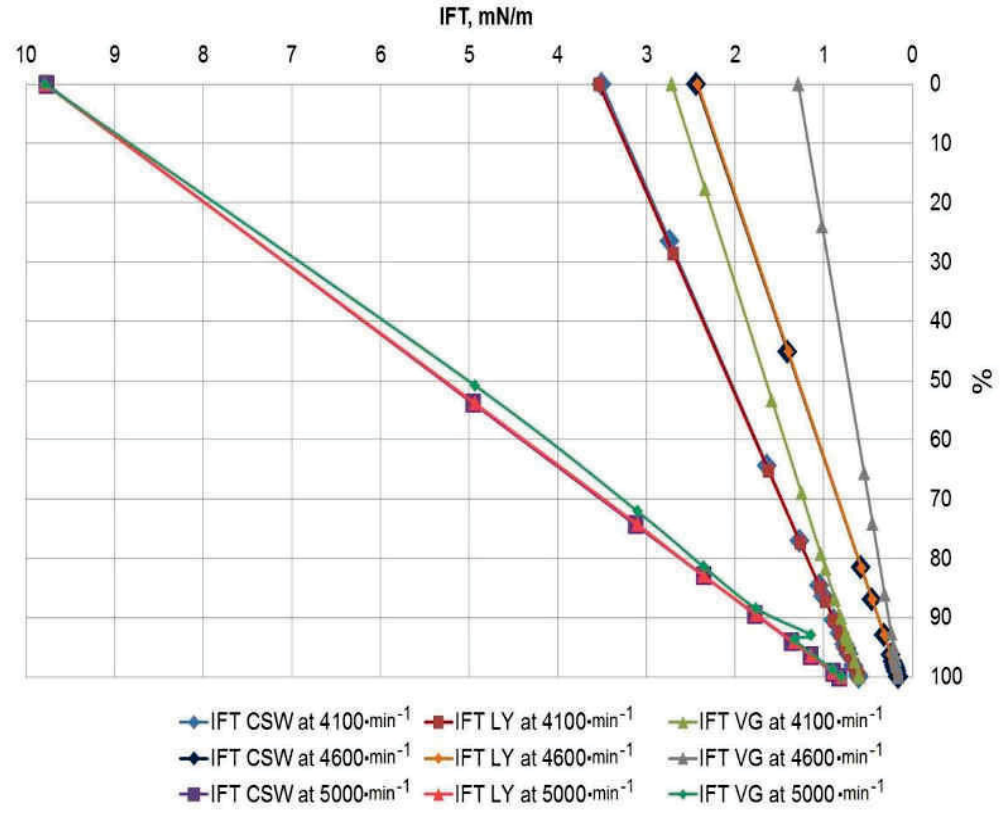

Figure 72: Average IFT for “Crude oil A” – distilled water system

As shown in the figures above, the oil samples studied have different IFT reduction rates.
For “Crude oil C”, there was a different trend for the curves of IFT vs. aging time. Interfacial tension rapidly decreased to a low level of 4.5-5 mN/m in only 10 minutes, as depicted in Figure 67. At a rotational speed of 5000 min^{-1}, the interfacial tension decreased by almost 70-80 % during this time. The IFT range was 2 mN/m (Figure 68). The minimum was reached in 1.5 hour after the start of the rotation and the interfacial tension remained constant for approximately 25-30 minutes. Then, the interfacial tension increased by 20-30 percent within the next 2-3 hours.
At a rotational speed of 3900 min^{-1}, the interfacial tension decreased to the lowest value in 15 min of rotation. Then it began to increase and reached a stable state in 1 hour. The change in the IFT value was about 40 % compared to the initial IFT.
In this case, we are not able to consider IFT minimum in the “Crude oil C”-IFT curve as the actual equilibrium.
Figures 69, 70 show interfacial tension of the “Crude oil B”. During experiment the IFT values of the “Crude oil B” decreased to 12.3-13.5 mN/m. The reduction of interfacial tension by 10-15% in first 25-30 minutes and 70 % in 2-2.5 hours was reached. It took around 5 hours to achieve the constant IFT of 12 mN/m and keep it stable at a rotational speed of 5500 min^{-1}. For an experiment conducted with a rotational speed of 4300 min^{-1}, the equilibrium state was achieved quickly, in 2.9 hours.
For the “Crude oil A”, the initial IFT decreased very quickly and changed by 50-55 % in 1 hour. As can be seen from Figure 71, in the first 40 min the IFT changed by 20 % at a rotational speed of 4100 min^{-1}. After 1 day of rotation it increased by 10-20 %. The minimum values achieved in measurement are 0.6 mN/m and 0.59 mN/m for IFT CSW and IFT VG respectively (Figure 72).
For the rotational speed of 4600 min^{-1}, the IFT changed by 50 % in the first 30 minutes. Then interfacial tension changed slowly by 20 % over 1 hour. The lowest obtained value for the “Crude oil A” of 0.15 mN/m was reached. The initial IFTs in this experiment were 2.4 and 1.29 mN/m for IFT CSW and IFT VG, respectively which is much lower compared to previous tests (Figure 72).
For the rotational speed of 5000 min^{-1}, the initial IFT value was of 8-9 mN/m. It changed rapidly in 10 min of rotation to 40mN/m. Then the interfacial tension gradually decreased and the minimum of 0.8 mN/m was reached also in 1 hour, IFT changed by 50 %.
On the basis of these results, it seems probable that the “Crude oil A” will produce a more stable emulsion due to the long and stable “plateau phase” than either “Crude oil C” or “Crude oil B”.
A number of theoretical points and questions revealed by these studies require further research. Nevertheless, the data obtained during the interfacial tension experiments are accurate and reliable that justifies the practical use of the spinning drop method.
In Table 3, the average IFT values for the examined oils obtained via the spinning drop method are compared with the pendant drop analysis data. As can be seen, the IFT values obtained in spinning drop measurements are lower than the IFT values obtained by the pendant drop method, but the variance is in the acceptable range. This proves that the

spinning drop interfacial tension meter can be used to test IFT values, despite its lower accuracy compared to the pendant drop meter.

Table 4: IFT measured via spinning drop and pendant drop methods

Oil samples	Average IFT, mN/m			
	Spinning drop method			Pendant drop method (P.Arnold)
	IFT CSW	IFT LY	IFT VG	
Crude oil C	5-5.2	4,8-5,2	4.5-5	7
Crude oil B	12.2-13.2	12.2-13.2	12.2-12.4	14.5
Crude oil A	0.6-0.8	0.6-0.8	0.6-0.8	1

The objectives of this thesis were to perform standard IFT measurements and develop the methodology for further investigations. It was found that the rotational speed is not a key factor determining the magnitude of the initial IFT. The initial IFT value is affected by the dosage of the droplet introduced in the capillary tube. Further changes in the behaviour of interfacial tension can be identified with a sharp change in the volume of droplets over time. This knowledge is particularly important for the correlation of data obtained during measurements of interfacial tension.

In addition to the above, test studies were performed to understand the effect of temperature and rheological behaviour of oils. Oscillatory tests for the „Crude oil A" showed that the observed fluctuations (jumps) in the IFT curve have an artificial origin and are related to the motion of the drop.

In addition, a methodology for the preparation of oil samples and instruments for the IFT measurements was developed.

The obtained results are useful for understanding the IFT behaviour of crude oils and can be applied for future research.

6 References

[1] D.W.Green, G.P.Willhite, “Enhanced Oil Recovery,” SPE, 1998, 545 p.

[2] L.W. Lake, "Enhanced Oil Recovery", Prentice Hall, Inc., 1989.

[3] G.A.Pope, “Overview of Chemical EOR,” Center for Petroleum and Geosystems Enginnering, the University of Texas at Austin, October, 2007.

[4] Promod Kumar, K.L.Mittal, Handbook of Microemulsion Science and Technology, New York, N.Y., 1999.

[5] K.L.Lee, Applications and Use of Microemulsions, London: Imperial College , Nov, 2010.

[6] M.J.Broens, “In-situ Microemulsion Formation in Enhanced Oil Recovery,” Delft University of Technology, 2015.

[7] T.F.Tadros, “Emulsion Formation and Stability,” Wiley-VCH Verlag GmbH and Co., KGaA, 2013, p. 76.

[8] J.Sjoblom, “Encyclopedic Handbook of Emulsion Technnology,” New York, Basel , 2001, p. 760 p.

[9] R.Vishnudas, A.Chaudhuri, “A Comprehensive Numerical Study of Immiscible and Miscible Viscous Fingers During Chemical Enhanced Oil Recovery,” no. https://www.researchgate.net/publication/, April 2017.

[10] H.M.Rosano, M.Clausse, Microemulsion systems, New York, N.Y.: CRC Press, 1987.

[11] E.H.Lucassen-Reynders, A.Cagna, J.Lucassen, “Gibbs Elasticity, surface dilational modulus and diffusional relaxation in nonionic surfactant monolayers,” *Colloids and Surfaces ,* vol. Physicochemical and Engineering Aspects 186, pp. 63-72, 2001.

[12] P.Than, L.Preziosi, D.D.Joseph and M.Arney, “Measurement of Interfacial Tension between Immiscible Liquids with the Spinning Rod Tensiometer,” *Journal of Colloid and Interface Science,* vol. 124, no. N 2, p. 556, August 1988.

[13] J.Portwood, “Validating the Effectiveness of Chemical Flooding,” in *E&P*, April, 2016

[14] D.O.Shah, R.S.Schechter, “Improved Oil Recovery by Surfactant and Polymer Flooding,” New York, Academic Press, INC., 1977, p. 578

[15] A. Bailey, “Surface and Interfacial Tension,” in *Thermopedia*, 2010.

[16] K. A.Goebel, “Interfacial Tension of the Water/n-Alkane Interface,” *Langmuir,* vol. 13 (2), pp. 369-372, 1997.

[17] K.C.Powell, A.Chauhan, “Interfacial Tension and Surface Elasticity of Carbon Black (CB) Covered Oil-Water Interface,” vol. 30 (41), University of Florida, Langmuir, 2014, pp. 12287-12296.

[18] Peter S. Liss, R.A.Duce, The Sea Surface and Global Change, Cambridge University, 1997, p.535.

[19] Kruss glossary, https://www.kruss-scientific.com/services/education-theory/glossary/surface-age/.

[20] D.Möbius, R.Miller, V.B.Fainemann, Surfactants: Chemistry, Interfacial Properties, Applications, The Netherlands: Elsevier Science B.V., 2001.

[21] D.Möbius, R.Miller, Drops and Bubbles in Interfacial Research, Canada: Elsevier Science B.V. , 1998.

[22] L. L.Schramm, Emulsions, Foams and Suspensions: Fundamentals and Applications., Canada: Wiley-VCH Verlag GmbH and Co., KGaA, 2005.

[23] H.M.Princen, “Some Aspects of Spinning Drop Tensiometry,” *Colloid and Interaface Science,* no. 169, pp. 241-243, 1995.

[24] J. W.M.Bush, Interfacial Phenomena, MIT Open Course Ware, 2010.

[25] “The spinning drop video tensio-meter (SVT 20N),” http://www.lmsscientific.com/products.php?prod_name=spinning-drop-tensiometer, [Accessed 01 11 2017].

[26] “Optics and Lasers in Engineering,” vol. 46, no. 12, pp. 893-899, December 2008.

[27] S. E.Taylor, “Thermal Destabilization of Bitumen-in-Water Emulsions - A Spinning Drop Tensiometry Study,” *Elsevier Ltd.,* vol. Fuel 90, pp. 3028-3039, 2011.

[28] S.O.Isehunwa, J.Akpabio, “Effect of Temperature and Contamination on the Surface Tension of Niger Delta Crude Oils,” *Australian Journal of Basic and Applied Sciences,* Vols. ISSN 1991-8178, no. 5 (5), pp. 610-616, 2012.

[29] K.Spildo, H. Hoiland, “Interfacial Properties and Partioning of 4-Heptylbenzoic Acid between Decane and Water,” *Journal of Colloid and Interface Science ,* vol. 209, no. 1, pp. 99-108, Jan, 1999.

[30] L.-H. Lee, “Relevance of Film Pressures to Interfacial Tension, Miscibility of Liquids, and

Lewis Acid-Base Approach", Journal of Colloid and Interface Science 214, pp.64-78, 1999.

[32] E.E.Isaac, J.Darol Maunder, Li Jian, "Interfacial Tension of Heavy Oil-Aqueous Systems at Elevated Temperatures," *1988,* no. https://www.researchgate.net/publication /241938601, [Accessed 02.08.2017].

[33] A.Moradian, J.Mostaghimi, "Measurement of Surface Tension, Viscosity, and Density at High Temperatures by Free-Fall Drop Oscillation," *The Minerals, Metals & Material Society and ASM International,* vol. 39B, no. 280, 11 p., 2008.

[34] P.Ramirez-Gonzalez, U.Martines-Cortes, S.Cisneros, "Effect of the Temperature on the Non-Newtonian Behavoir of Heavy Oils," *Energy and Fuels, 2015,* no. ASC Publications, https://www.researchgate.net/publication/273306990 [Accessed 02.08.2017].

[35] O. A.A.Hamouda, "Effect of Temperature, Wettability and Relative Permeability on Oil Recovery from Oil-wet Chalk," *Energies ,* vol. 1, pp. 19-34, 2008.

[36] H.M.Princen, I.Y.Zia, and S.G.Mason, "Measurement of Interfacial Tension from the Shape of a Rotating Drop," *Journal of Colloid and,* no. 23, pp. 99-107, 1967.

[37] J.-L.Salager, "Principle of the Spinning Drop Tensiometer," in *FIRP Booklet E705-A*, Universidad de Los Andes, 2005, pp. 1-6.

[38] "Operating Manual SVT 20 N," in *Spinning Drop Tensiometer*, Dataphysics Instruments GmbH, 2010.

[39] Howard H.Hu, Daniel D.Joseph, "Evolution of a Liquid Drop in a Spinning Drop Tensiometer," *Journal of Colloid and Interface Science,* vol. 162, pp. 331-339, 1994.

[40] D.Georgieva, V.Schmitt, F.Leal-Calderon, D.Langevin, "On the Possible Role of Surface Elasticity in Emulsion Stability," *Langmuir,* vol. 25 (10), pp. 5565-5573, 2009.

[41] R. Vadaraj, C. Brons, "Molecular Origin of Heavy Oil Interfacial Activity," *Fundamental Interfacial Properties of Asphaltenes Derived from Heavy Crude Oils and Their Correlation to Chemical Composition,* Vols. Energy & Fuels, 21 (1), no. Part 1, pp. 195-198, 2007.

[42] J.S.Buckley,T. Fan, "Crude Oil/Brine Interfacial Tensions," *Petrophysics,* vol. 48 (3), pp. 175-185, 2007.

APPENDICES

Appendix A

Table A-1: Measured IFT of “Crude oil C”/Distilled Water system

Liquid pair	Density, g/cm3	Drop Shape	Rotational Speed, min^{-1}	Time, s	Measured IFT, mN/m											
					Mean			Std. Dev.			Mean. Abs. Error			Percentage Error		
					CSW	LY	VG	CSW	LY	VG	CSW	LY	VG	CSW	LY	VG
"Crude oil C"/Distilled Water	871/977	Spherical Ends of Drop, Full-shaped drop	3900 min^{-1}	1000	5,10	5,14	5,05	0,06	0,13	0,06	0,05	0,05	0,05	1,04	0,93	1,04
				2000	5,36	5,36	5,32	0,25	0,28	0,25	0,16	0,16	0,16	2,96	2,96	2,97
				3000	5,85	5,85	5,79	0,57	0,63	0,57	0,10	0,10	0,10	1,69	1,77	1,69
				4000	5,98	5,98	5,93	0,69	0,72	0,68	0,00	0,01	0,00	0,00	0,21	0,00
				5000	6,09	6,09	6,04	0,77	0,80	0,76	0,08	0,08	0,08	1,31	1,31	1,31
				6000	6,18	6,17	6,13	0,83	0,86	0,83	0,02	0,02	0,02	0,30	0,35	0,30
				7000	6,18	6,14	6,13	0,83	0,84	0,82	0,02	0,04	0,02	0,35	0,60	0,35
				8000	6,09	6,13	6,03	0,76	0,83	0,76	0,00	0,03	0,00	0,00	0,43	0,00
				9000	6,09	6,14	6,03	0,77	0,84	0,76	0,00	0,03	0,00	0,00	0,43	0,00
				10000	6,09	6,14	6,03	0,76	0,84	0,76	0,00	0,02	0,00	0,00	0,28	0,00
				11000	5,73	5,76	5,68	0.79	0.84	0.79	0,41	0,40	0,41	7,20	7,01	7,20
			4200 min^{-1}	500	5,32	5,27	5,05	0,19	0,18	0,15	0,38	0,41	0,23	7,20	7,86	4,64
				1000	5,00	4,92	4,77	0,04	0,05	0,12	0,07	0,07	0,06	1,32	1,47	1,34
				2000	5,12	4,98	4,70	0,08	0,04	0,17	0,05	0,05	0,05	0,98	1,00	1,00
				3000	5,10	4,94	4,81	0,02	0,00	0,10	0,00	0,01	0,04	0,07	0,16	0,83
				4000	4,98	4,91	4,69	0,04	0,03	0,19	0,06	0,03	0,17	1,30	0,60	3,68
				5000	5,10	4,90	4,74	0,07	0,03	0,15	0,01	0,02	0,00	0,27	0,38	0,01
				6000	5,10	4,98	4,78	0,07	0,04	0,13	0,03	0,05	0,05	0,59	1,09	0,95
				7000	5,09	5,01	4,84	0,07	0,04	0,08	0,01	0,01	0,00	0,14	0,27	0,01
				8000	5,22	5,08	4,97	0,15	0,09	0,05	0,07	0,05	0,07	1,43	1,02	1,49
				9000	5,24	5,17	5,04	0,17	0,15	0,06	0,01	0,04	0,00	0,21	0,70	0,01
				10000	5,27	5,23	5,09	0,19	0,19	0,09	0,05	0,04	0,05	0,96	0,86	0,97
				12000	5,46	5,33	5,22	0,31	0,25	0,19	3,31	3,24	0,99	60,68	60,81	18,91
				13000	5,46	5,38	5,23	0,06	0,07	0,32	0,30	0,19	0,02	0,57	1,19	0,37
				24500	6,87	6,70	6,38	0,59	0,55	1,05	0,06	0,04	0,19	0,82	0,54	2,98

Table A-2: Measured IFT of “Crude oil B” /Distilled Water system

Liquid pair	Density, g/cm3	Drop shape	Rotational Speed, min^{-1}	Time, s	Measured IFT, mN/m											
					Mean			Std.Dev.			Mean Abs. Error			Percentage Error		
					CSW	LY	VG	CSW	LY	VG	CSW	LY	VG	CSW	LY	VG
“Crude oil B” /Distilled Water	907/977	Full-shape, spherical ends of drop	4300 min^{-1}	2000	16.98	16.88	16.42	2.70	2.71	4.52	0.47	0.32	0.48	2.74	1.90	2.90
				3000	16.61	16.03	14.35	2.44	2.11	3.07	1.13	0.73	0.64	6.82	4.54	4.47
				4000	15.71	14.96	13.21	1.81	1.36	2.26	0.50	0.35	0.48	3.17	2.32	3.61
				5000	15.49	14.67	12.89	1.54	0.99	1.84	0.58	0.47	0.60	3.75	3.17	4.64
				6000	14.93	14.19	12.42	1.25	0.82	1.69	0.20	0.11	0.13	1.31	0.80	1.02
				7000	14.15	13.79	12.72	0.69	0.53	1.91	0.32	0.20	0.28	2.24	1.45	2.22
				8000	13.89	13.53	12.91	0.51	0.35	2.04	0.28	0.13	0.38	2.03	0.96	2.93
				9000	13.47	13.70	12.64	0.21	0.21	2.28	0.08	0.37	0.61	0.62	2.68	4.81
				10000	14.02	13.63	12.66	0.24	0.23	2.22	0.46	0.29	0.54	3.25	2.12	4.29
				10500	13.37	13.26	13.28	0.15	0.16	2.31	0.00	0.00	0.01	0.00	0.01	0.08
		Full-shape drop	5500 min^{-1}	2000	14.76	14.81	14.65	1.89	1.99	1.88	0.13	0.10	0.12	0.85	0.67	0.85
				6000	13.15	13.10	13.05	0.76	0.78	0.75	0.10	0.13	0.10	0.75	1.00	0.75
				7000	13.01	13.01	12.91	0.65	0.72	0.66	0.05	0.03	0.05	0.40	0.23	0.40
				8000	12.95	12.94	12.85	0.61	0.67	0.61	0.10	0.09	0.10	0.75	0.70	0.75
				15000	12.46	12.40	12.36	0.27	0.29	0.27	0.00	0.02	0.00	0.00	0.14	0.00
				16000	12.46	12.39	12.36	0.27	0.28	0.27	0.00	0.04	0.00	0.02	0.29	0.02
				17000	12.37	12.29	12.27	0.21	0.21	0.21	0.00	0.06	0.09	0.76	0.51	0.76
				18000	12.29	12.27	12.20	0.15	0.19	0.15	0.09	0.04	0.04	0.36	0.32	0.36
				19000	12.27	12.23	12.17	0.13	0.17	0.13	0.04	0.04	0.00	0.00	0.29	0.00
				20000	12.28	12.24	12.18	0.14	0.18	0.14	0.00	0.04	0.02	0.16	0.30	0.16
				21000	12,28	12,24	12,18	0,14	0,17	0,14	0,02	0,04	0,02	0,14	0,33	0,14
				22000	12,27	12,24	12,17	0,13	0.17	0,13	0,00	0,03	0,00	0,00	0,25	0,00
				23000	12,27	12,23	12,17	0,13	0,17	0,13	0,00	0,02	0,00	0,00	0,20	0,00
				24000	12,27	12,22	12,17	0,13	0,16	0,13	0,00	0,03	0,00	0,00	0,21	0,00
				25000	12,27	12,23	12,17	0,14	0,16	0,13	0,00	0,03	0,00	0,00	0,22	0,00
				26000	12,27	12,22	12,17	0,14	0,16	0,13	0,00	0,03	0,00	0,00	0,21	0,00
				27000	12,27	12,22	12,17	0,14	0,16	0,13	0,00	0,02	0,00	0,00	0,18	0,00
				28000	12,27	12,23	12,17	0,14	0,17	0,13	0,00	0,03	0,00	0,00	0,22	0,00
				29000	12,24	12,19	12,14	0,11	0,14	0,11	0,05	0,09	0,05	0,43	0,73	0,43

Table A-3: Measured IFT of "Crude oil A"/Distilled Water system

Liquid pair	Density, g/cm3	Drop Shape	Rotational Speed, min^{-1}	Time, s	Measured IFT, mN/m											
					Mean			Std. Dev.			Mean. Abs. Error			Percentage Error		
					CSW	LY	VG	CSW	LY	VG	CSW	LY	VG	CSW	LY	VG
"Crude oil A"/Distilled Water	931/977	Full-shaped Droplet	4100 min^{-1}	2000	2,74	2,70	2,34	1.51	1.49	1.24	0,34	0,34	0,19	12,37	12,71	8,05
				3000	1,64	1,62	1,58	0,73	0,73	0,70	0,10	0,10	0,09	6,29	5,90	5,55
				4000	1,27	1,27	1,25	0,48	0,48	0,47	0,10	0,10	0,10	7,76	7,95	7,71
				5000	1,05	1,05	1,04	0,31	0,32	0,32	0,04	0,04	0,04	3,66	3,82	3,68
				6000	0,89	0,89	0,87	0,20	0,21	0,20	0,03	0,03	0,03	3,03	2,89	3,04
				7000	0,82	0,82	0,81	0,15	0,16	0,15	0,01	0,01	0,01	1,07	1,38	1,08
				8000	0,76	0,77	0,75	0,14	0,14	0,14	0,01	0,01	0,01	1,30	0,97	1,31
				9000	0,74	0,75	0,73	0,10	0,11	0,10	0,00	0,01	0,00	0,34	1,31	0,35
				10000	0,74	0,74	0,73	0,10	0,11	0,10	0,00	0,01	0,00	0,01	0,95	0,01
				12000	0,72	0,71	0,71	0,08	0,09	0,08	0,00	0,02	0,00	0,01	2,42	0,01
				25000	0,66	0,66	0,65	0,04	0,05	0,04	0,02	0,02	0,01	2,27	2,92	2,28
				30000	0,62	0,62	0,61	0,01	0,02	0,01	0,02	0,02	0,01	2,43	2,75	2,45
				35000	0,61	0,60	0,60	0,00	0,01	0,00	0,01	0,01	0,01	1,50	1,16	1,50
			4600 min^{-1}	1000	1,41	1,40	1,02	0,99	0,98	0,72	0,25	0,26	0,09	17,97	18,23	8,55
				2000	0,58	0,57	0,55	0,41	0,41	0,39	0,15	0,15	0,11	25,82	25,68	20,58
				3000	0,46	0,45	0,45	0,32	0,32	0,32	0,05	0,05	0,05	11,24	11,22	10,95
				4000	0,32	0,32	0,31	0,23	0,23	0,22	0,03	0,03	0,03	9,05	9,06	9,31
				5000	0,24	0,24	0,24	0,17	0,17	0,17	0,01	0,01	0,01	3,39	2,98	3,41
				6000	0,22	0,22	0,21	0,15	0,15	0,15	0,00	0,00	0,00	1,63	1,63	1,56
				7000	0,21	0,21	0,20	0,15	0,15	0,14	0,00	0,00	0,00	2,18	2,42	2,22
				8000	0,20	0,19	0,19	0,14	0,14	0,14	0,00	0,00	0,00	1,90	2,36	1,91
				10000	0,19	0,19	0,19	0,14	0,13	0,13	0,00	0,00	0,00	0,67	0,53	0,67
				12000	0,18	0,18	0,18	0,13	0,13	0,13	0,00	0,00	0,00	1,68	1,63	1,69
				17000	0,18	0,18	0,18	0,13	0,13	0,13	0,00	0,00	0,00	0,01	0,53	0,01
				40500	0,16	0,16	0,16	0,11	0,11	0,11	0,00	0,00	0,00	2,32	2,76	2,34
			5000 min^{-1}	1000	4,96	4,94	4,81	2.54	2.59	2.46	1,29	1,29	1,14	26,00	26,06	23,69
				2000	3,12	3,10	3,08	1.26	1.30	1.24	0,32	0,31	0,32	10,20	10,13	10,24
				3000	2,35	2,36	2,32	0,71	0,78	0,71	0,12	0,11	0,12	5,17	4,57	5,19
				4000	1,78	1,77	1,74	0,31	0,36	0,30	0,09	0,09	0,09	5,05	5,22	5,27
				5000	1,15	1,14	1,37	0,03	0,09	0,04	0,41	0,41	0,06	35,48	35,64	4,21
				5500	1,36	1,32	1,32	0,02	0,05	0,00	0,00	0,02	0,00	0,32	1,69	0,02